Algerian Democratic Republic and Populaire

Ministry of Higher Education

and scientific research

Echahid Hamma Lakhder University of El-Oued

Faculty of Technology

Thesis presented for obtaining the

ACADEMIC MASTERS

Domain: Science and Technology

Sector: Mechanical Engineering

Specialty: Energy

Thesis:

«Numerical simulation of the distribution system of diesel engine (13511-64071) under mechanical loading»

Before the jury composed of:

President: Dr. BERKANE Houda

Examiner: Pr. AOUN Yassine

Supervisor: Pr. GHERBI Mohamed Tahar.

Presented by:

SALHI Tedjani

BEGGAS Ayoub

University year: 2023/2024

DEDICATION

In the beginning, all praise is due to Allah who granted us strength, courage, and determination to complete this humble work, hoping it meets your expectations. I dedicate this work to the dearest people in my heart, my mother and father. Thank you for your love, sacrifices, support, encouragement, and faith in me throughout this long journey. I pray that Allah grants your health, well-being, and long life. I also dedicate this work to my brothers and sisters, especially my dear brother and sister, Mohamed and Zohra. Thank you for your support and care for me from childhood to adulthood. I also extend my gratitude to my sister Najat, who has always been my companion and guide during my elementary school years. Finally, not to forget, I thank all my colleagues and dear friends. I wish them success and may Allah guide them to what He loves and is pleased with.

Tedjani

Acknowledgements

Once again, all praise is due to Allah who has granted us health, strength, and determination to achieve many things beyond our ordinary capabilities.
Clearly, we want to start by expressing our gratitude and appreciation to our esteemed supervisor, Pr. Gharbi Mohamed Taher, who was kind enough to supervise and carefully follow our work despite the challenges, and for his patience and humility that made him a role model.
We also extend our thanks to Pr. AOUN Yassine for agreeing to chair the jury for this thesis, as well as to Dr. BERKANE Houda for agreeing to examine this work. We express our heartfelt thanks to all the professors in the Mechanical Engineering Department at the University of El Oued who contributed to our education and training to reach such milestones. To everyone who has contributed to offering help and support, near or far, as encouragement, we hope this conveys our deep gratitude.

Abstract

The distribution system plays an important role in the internal combustion engine, as it regulates the time of opening and closing the valves to allow the fuel and air mixture to enter the engine and the exhaust. The camshaft is considered the basic and direct element responsible for this process because it is responsible for converting the rotary movement of the crankshaft into a reciprocating movement and transmitting it to open and close the valve to supply fuel to the combustion chamber. The study aims to analyze the fatigue characteristics of a diesel engine camshaft (13511-64071) made of gray cast iron when it is under mechanical loads. SolidWorks was used to design the camshaft geometry, and ANSYS Workbench was used to evaluate the camshaft properties by two types of analyses. The first analysis was the model analysis, through which we obtained relatively high frequencies, as the lowest frequency was 395.8 Hz and the highest frequency was 1998.2 Hz. The second analysis was the static structural analysis. In this analysis, we applied a torque of 706.5 Nm to the camshaft. We obtained values for deformations and stresses, where the maximum deformation was 0.0027 mm and the maximum equivalent elastic stress was 6.7368E-6. Then, as an additional suggestion to improve the distribution system, we compared gray cast iron and cast carbon steel.

Keywords: *Mechanical loads. Diesel engine. Camshaft. Elastic stress. Plastic deformation.*

Résumé

Le système de distribution joue un rôle important dans le moteur à combustion interne, car il régule le temps d'ouverture et de fermeture des soupapes pour permettre au mélange de carburant et d'air d'entrer dans le moteur et l'échappement. L'arbre à cames est considéré comme l'élément fondamental et direct responsable. ce processus car il est chargé de convertir le mouvement de rotation du vilebrequin en un mouvement alternatif et de le transmettre pour ouvrir et fermer la vanne pour alimenter en carburant la chambre de L'étude vise à analyser les caractéristiques de fatigue d'un arbre à cames de moteur diesel (13511-64071) en fonte grise lorsqu'il est soumis à des charges mécaniques. SolidWorks a été utilisé pour concevoir la géométrie de l'arbre à cames et ANSYS Workbench a été utilisé pour évaluer les propriétés de l'arbre à cames par deux types d'analyses. La première analyse était l'analyse typique, grâce à laquelle nous avons obtenu des fréquences relativement élevées, puisque la fréquence la plus basse était de 395,8 Hz et la fréquence la plus élevée était de 1998,2 Hz. La deuxième analyse était l'analyse structurelle statique. Dans cette analyse, nous avons appliqué un couple de 706,5 Nm à l'arbre à cames. Nous avons obtenu des valeurs de déformations et de contraintes, où la déformation maximale était de 0,0027 mm et la contrainte élastique équivalente maximale était de 6,7368E-6. Ensuite, comme suggestion supplémentaire pour améliorer le système de distribution, nous avons comparé la fonte grise et l'acier au carbone moulé.

Mots clés: *Charges mécaniques, Moteur diesel, Arbre à cames, Contrainte élastique, Déformation plastique.*

ملخص.

يلعب نظام التوزيع دوراً هاماً في محرك الاحتراق الداخلي، حيث يقوم بتنظيم زمن فتح وإغلاق الصمامات للسماح لخليط الوقود والهواء بالدخول إلى المحرك والعادم ويعتبر عمود الكامات العنصر الأساسي والمسؤول المباشر عن هذه العملية وذلك لأنها لمسؤول عن تحويل الحركة الدورانية للعمود المرفقي الي حركة ترددية ونقلها لفتح وإغلاق صمام لتزويد الوقود لغرفة الاحتراق. أداء عمود الحدبات بشكل رئيسي يعتمد على التصميم المناسب والمواد المستخدمة فيه. لذلك من المهم جدًا اختيار المواد والتصاميم المناسبة لعمود الكامات وذلك لتحسين كفاءة نظام التوزيع خاصة وكفاءة المحرك عامة. تهدف الدراسة إلى تحليل خصائص الكلال لعمود كامات خاص بمحرك ديزل (13511-64071) المصنوع من الحديد الزهر الرمادي عندما يكون تحت أحمال ميكانيكية. تم استخدام SolidWorks لتصميم الشكل الهندسي لعمود الكامات، و ANSYS Workbench لتقييم خصائص عمود الكامات عن طريق نوعين من التحاليل. التحليل الأول هو التحليل النموذجي، حيث حصلنا من خلاله على ترددات مرتفعة نسبيًا، حيث كان أدنى تردد 395.8 هرتز وأعلى تردد 1998.2 هرتز. اما التحليل الثاني فكان التحليل الهيكلي الثابت. في هذا التحليل، قمنا بتطبيق عزم دوران بقيمة 706.5 نيوتن متر على عمود الكامات. حصلنا على قيم للتشوهات والإجهادات، حيث كان أقصى تشوه 0.0027 مم وأقصى إجهاد مرن مكافئ $6,7368^{-6}$ بعدها وكاقتراح إضافي لتحسين نظام التوزيع قمنا بمقارنة بين الحديد الزهر الرمادي والفولاذ الكربوني المصبوب.

الكلمات المفتاحية: الأحمال الميكانيكية، محرك الديزل، عمود الكامات، الإجهاد المرن، التشوه البلاستيكي.

Table of Contents

chapter I: general information about internal combustion engine.

chapter II: distribution system

chapter III: Modelling by Finite element method (FEM).

chapter IV: Numerical simulation of distribution system

List of figures

List of Tables

General introduction

General introduction

Our civilization is distinguished from all other civilizations due to its intensive use of mechanical power. The primary source of power for waging war or making peace was human muscle. Then, animals were trained to assist, and wind and water were harnessed. However, a significant step in this direction was taken when humans discovered the technique of converting energy from one form to another. One of these techniques that accomplishes the task of energy conversion is the internal combustion engine. Among the most famous and widely used types of engines today are internal combustion engines. The expanding gases in the engine convert the chemical energy of the fuel into mechanical energy through combustion. They are predominantly used in the transportation industry.

To ensure the efficient and high-performance operation of an internal combustion engine, whether it is a fuel engine or a diesel engine, there are many systems that play a vital role. Among these systems is the distribution system, which can be defined as all the mechanisms and components responsible for opening and closing the valves that control the flow of air, fuel, and exhaust gases within the engine. This ensures that the valves open and close at the right time, in synchronization with the movements of the piston. The camshaft is considered the key element because it is directly responsible for opening and closing the valves by converting the rotational motion of the crankshaft into reciprocating motion and transmitting it to open and close the valve to supply fuel to the combustion chamber.

We have divided this study into four chapters, each with a specific goal or message to understand the main objective of our study, which is as follows:

In the first chapter, we will first take a look at the most important recent studies related to our study topic. Then, we will provide an overview of internal combustion engines, starting with their engineering, components, operation mechanism, and classifications to their uses.

The second chapter will be dedicated to studying the distribution system to understand its operation mechanism, types, and also the main parts it contains. All of this will serve as a prelude to the last chapter, which includes our study.

In the third chapter, we will understand the general concept and the basic principle of the finite element method and its properties. We will implement the distribution system and study the development of the camshaft using Hamilton's method to see a phenomenon in principle, where the equations of motion are obtained by applying Hamilton's equations to deal with real systems.

The fourth chapter, in its first part, presents the modeling and how to build the camshaft using the 3D modeling software SolidWorks. The second part involves the digital simulation of the crank connecting rod using the finite element code of the ANSYS program and performing two types of numerical simulations: modal analysis to determine natural frequencies and modes, and static analysis to determine stresses, displacement, and deformation.

chapter I: general information about internal combustion engine.

I.1 Introduction

The widespread use of mechanical power is the feature that distinguishes our civilization from all other civilizations. Human muscles were the main source of strength to wage war or bring peace. Next, the wind and flowing water were harnessed, and animals were taught to help. However, man's discovery of the technology of converting energy from one form to another was a major step in this direction. the internal combustion engine is one such technology that performs this energy conversion function. Internal combustion engines are among the most well-known engine types that exist today. Through the process of combustion, the expanding gases in the engine transform chemical energy contained in fuel into mechanical energy. Typically, they are employed in transportation.

In this chapter of our research, we devoted it to studying and knowing the most important general and specific information about internal combustion engines in preparation for the subsequent study.

I.2 Bibliographic research on the distribution of a diesel engine

Distribution system has been one of the few topics that have been studied directly, so we have compiled a significant number of studies surrounding distribution, most of which relate to diesel engines are more thermally and mechanically stressful than diesel engines essence. We will provide some examples of the results of previous work related to thermal and mechanical constraints of a heat engine applied to distribution.

H. Bayrakceken, I. Ucun [1] :

In this study, a camshaft fracture analysis of an automobile engine was performed. Analyzed the camshaft is broken after a short period of use. For the determination of the failure reason, the microstructure and chemical compositions of the camshaft material. Some fractographic studies are carried out to asses the fracture conditions. A stress analysis is also carried out by the finite element technique for the determination of highly stressed regions on the camshaft.

Dave Marmik M, Kothari Kartik D [2]:

The main objective of this research work is to experimentally measure the values of cam stress, strain and total deformation. This research presents a study of the most important contact surfaces of the modern diesel cam – follower system. The factors that affect the camshaft and its performance are material properties, lubrication system, system operation, and mechanical contact stress. It will generate friction and temperature and cause wear. The analysis is done by finite element analysis.

Andoko Andoko, Riduwan Prasetya [3]:

This research studies the analysis of camshaft failure that occurred in a small vehicle after 14 years of use. Its purpose is to simulate a failed camshaft and evaluate stress and fatigue using ANSYS to find the cause of failure. The results obtained showed that failure occurs due to defects in the fractured part with an indication of the fracture location exceeding the maximum fracture probability and fatigue life.

Witek, Lucjan [4]:

This study looked into the exhaust valve fracture issue with diesel engines. Two fatigue cracks in the damaged valve were found to have started during engine operation, according to a visual inspection of the component. The valve, seat, and guide were the components of a finite element model that was created to explain the cause of the valve's early fracture. The exhaust valve's maximum primary stress distributions for various load scenarios were discovered as a consequence of nonlinear analysis.

Bouziane Fersaoui, Mahfoudh Cerdoun [5]:

This work aims to numerically evaluate the real thermomechanical effect of boundary conditions on valves by considering the actual complex environment. The transient finite element model was developed within the ANSYS APDL program. The main results showed that the distribution of stress intensity has developed in areas called the permeable and seated trunk guide to large thermal gradients, causing high thermal stresses that are responsible for thermal cracks.

Lucjan Witek, Paweł Zelek [6]:

This study examined the fatigue and failure of a turbodiesel engine's connecting rod, and a visual examination of the fracture revealed typical fracture indications. After applying the finite element technique (FEM), the goal of this study is to elucidate the reasons for connecting rod damage. The findings indicated that high temperatures and stress levels in the vicinity of the bolt hole are the primary causes of connecting rod failure.

Liu. XF, Wang. Y [7]:

The mechanical and temperature conditions inside a diesel engine's piston were examined in this study. The semi-empirical formula and this piston's operating parameters were applied. Stress and fatigue life were calculated under extreme conditions using the finite element method (FEM). The results indicated that, under various thermo-mechanical coupling conditions, their relationships followed the Arrhenius model, the inverse force and law model, and the generalized Eyring model, respectively.

Tahar-Abbes [8]:

The electrohydrodynamic behavior of a solid skirt piston in a direct injection diesel engine is presented in this paper. It simulates both the secondary action and the impact of piston lubrication. It considers the impact of both mechanical and thermal load. The obtained results demonstrate the significant influence of the design parameter and the thermomechanical effect on the electrohydrodynamic of the piston.

Qing Zhang , Zheng Xing Zuo [9]:

This study is limited to identifying the causes of failures Which occurs to the valve bridges of the cylinder head of a diesel engine in the running position and for that Stress analysis was performed using the finite element method after which the stress was calculated. After analyzing the results, it was concluded that the stress concentration areas are identical to the real failure areas. The maximum von Mises stress occurs at the inner valve seat edge.

Ademar de Azevedo Cardoso. Ederson Claudio Andreatta [10]:
This study focuses on the analysis of thermo-mechanical fatigue (TMF). For exhaust manifold. The work was done in the temperature field Acquired from 1D simulation and adjusted to fit experimental values measured on the vehicle. Low cycle fatigue (LCF) was present evaluation of the exhaust manifold under compression cycles was considered resulting from temperature fluctuations. Thermal and stress analysis Implemented by the Abaqus package. It was an internal code used in fatigue analysis.

Lucjan Witek, Michał Sikora [11]:
Diesel engine crankshaft failure analysis was performed. Visual inspection of the crankshaft fracture showed typical signs of fatigue failure. In order to explain the cause of premature crankshaft damage, the finite element method was used. The analysis results showed that the main cause of premature fatigue is the high cycle stress of the material in the outer region of the crankshaft. In the final part of this work recommendations were formulated to increase the fatigue life of the analyzed crankshaft.

I.3 An overview

A heat engine is any device that can convert the chemical energy contained in fuel into thermal energy in turn, it is used to produce mechanical energy. Engines usually convert thermal energy into mechanical work, which is why they are called heat engines. When fuel is burned in the presence of atmospheric air, a huge amount of thermal energy is released, as the combustion products reach a high temperature. A heat engine converts the emitted thermal energy into Useful work with the help of the working fluid.

I.3.1 Classification of heat engines

This chart details the Classification of heat engines:

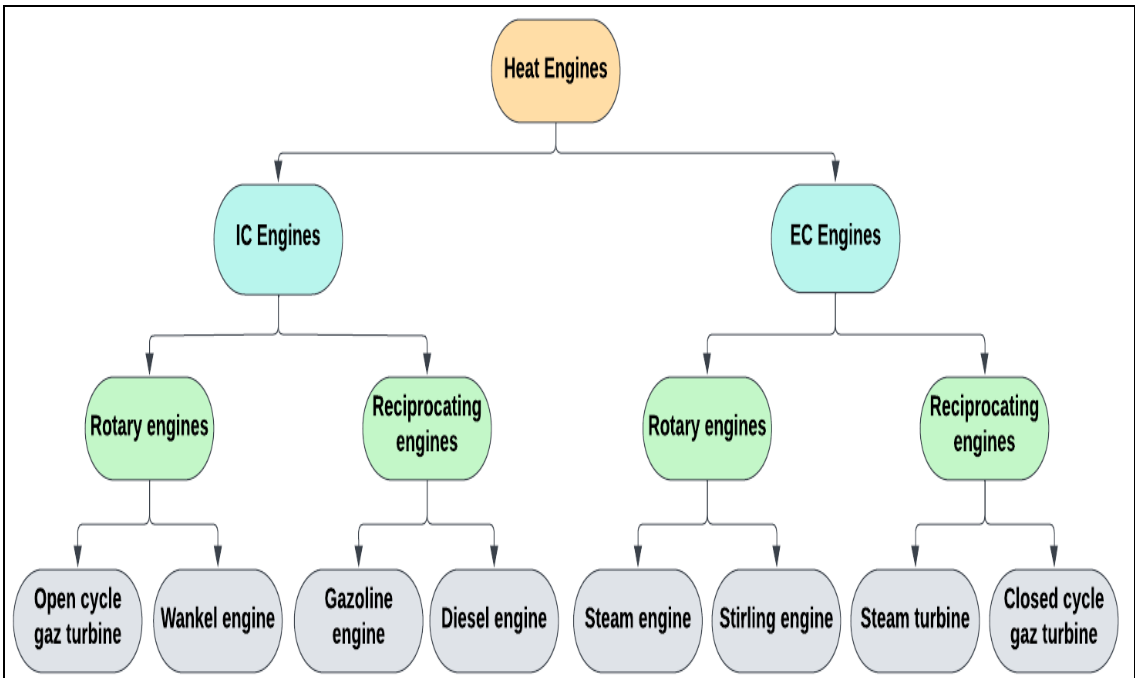

Figure I.1: *Classification of heat engines [12].*

As we see from the diagram shown in ***Figure I.1***, there are two basic types of heat engines:

I.3.1.1 External Combustion Engines (EC Engines)

In external combustion engines, fuel combustion takes place in the presence of air outside the engine cylinder. The thermal energy produced from the fuel is exploited to raise high-pressure steam in a boiler of water. Since steam is the working fluid that enters the cylinder of the steam engine in order to perform mechanical work, in this case the combustion products of the fuel do not enter and therefore do not form a working fluid.

The steam turbine of a steam power plant is another example of an external combustion engine A steam engine can be called an intermittent external combustion engine while a steam turbine can be called a continuous external combustion engine.

I.3.1.2 Internal Combustion Engines (IC Engines)

In internal combustion engines, there are two methods for the combustion process either the fuel is burned inside the engine cylinder, or the combustion products enter the cylinder in the form of a working fluid. In reciprocating engines with a cylinder and piston, the fuel combustion process takes place inside the cylinder. These engines can be called intermittent internal combustion engines, for example. Example: In an open cycle gas turbine plant, the combustion products of the fuel enter the gas turbine and work is obtained in the form of rotation of the turbine shaft.

Intermittent internal combustion engines are the most popular due to their use as first engines in automobiles. These engines are usually reciprocating engines, as the mechanism of operation of the reciprocating engine depends on a piston moving in a cylinder and forming a moving gas-tight seal. Through the connecting rod and crankshaft arrangement, the reciprocating movement of the piston is converted into rotational movement in the crankshaft.

I.3.2 Comparison of I.C. Engines and E.C. Engines

Comparison of IC engine and EC engine is given bellow

Table I.1: *Comparison between I.C. and E.C. Engines [12].*

I.C. Engines	E.C. Engines
1. Combustion of fuel takes place inside the cylinder.	1. Combustion of fuel takes place outside the cylinder.
2. Working fluid may be Petrol, Diesel and Various types of gases.	2. Working fluid is steam.
3. Require less space.	3. Require large space.
4. Capital cost is relatively low.	4. Capital cost is relatively high.
5. Starting of this engine is easy and quick.	5. Starting of this engine requires time.
6. Thermal efficiency is high.	6. Thermal Efficiency is low.
7. Power developed per unit weight of these engines is high.	7. Power Developed per unit weight of these engines is low.
8. Fuel cost is relatively high.	8. Fuel cost is relatively low.

I.4 History of the internal combustion engine

The first patent for an internal combustion engine to be industrially applied dates back to Samuel Brown in the United States. Afterward, the first commercially successful internal combustion engine was created by Étienne Lenoir around 1860. Then, in 1862, the first modern internal combustion engine was developed by Alphonse Beau de Rochas, later improved upon by Nikolaus Otto in 1867. The series of advancements in internal combustion engine technology continued with engineers Gottlieb Daimler and Wilhelm Maybach in 1887, followed by the German engineer Rudolf Diesel creating the first successful diesel engine in 1893. This type of engine is primarily used to propel transportation vehicles such as airplanes, cars, trucks, and boats, as well as various mobile tools like saws and lawnmowers. It is also employed in many stationary installations such as generators and pumps[14].

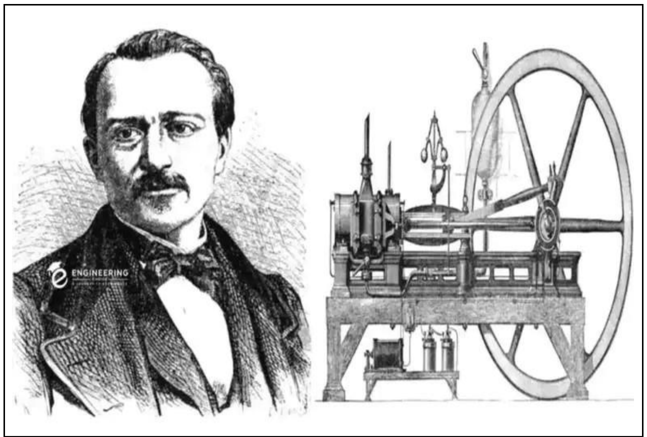

Figure I.2: *Lenoir's first IC engine in 1860 [13].*

I.5 Architecture of an internal combustion engine

Just as we see ***Figure I.3*** the external geometric shape of a type of internal combustion engine, perhaps what is striking in its shape is the simplicity of its design and also the small number of the main components that make it up. And just as we notice that this composition that makes up it has a relationship with each other, whether direct or indirect, for example the relationship that There is a link between the camshaft and the flywheel. Apparently, it seems that the camshaft has a direct relationship with the flywheel, which derives its movement from the crankshaft in an almost direct way. Therefore, we can conclude that the camshaft has an indirect relationship with the crankshaft.

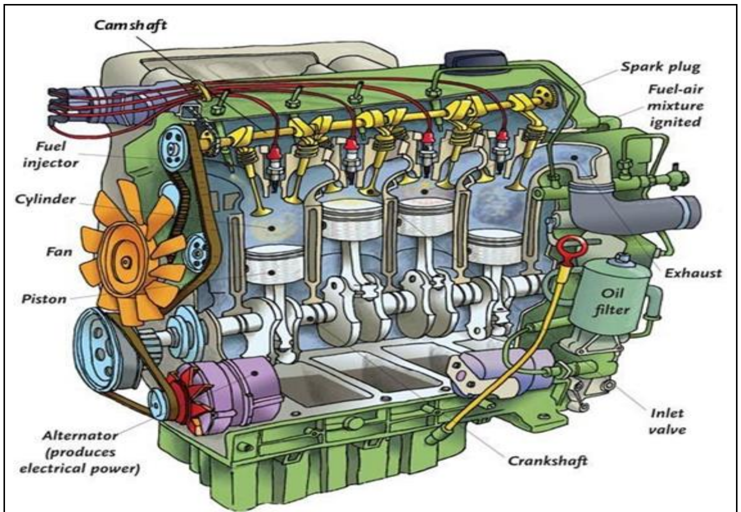

Figure I.3: *The external geometric shape of engine [15].*

When we look closely at the crankshaft, we find that it derives its movement from the combustion chamber. This is a structure in which all of its elements contribute to providing mechanical strength to each other. It is what makes the internal combustion engine one of the best innovations of our time.

I.6 Basic components and of IC engines

I.6.1.1 Fixed components

a) Cylinder block

The cylinder block is the main structure and support for all fixed and moving engine elements and components. They are often composed of cast iron and are manufactured using a mold. The cylinder block must support the cylinder head, crankshaft, cylinders and lower crankcase, which is often connected to the gearbox. This integration forms a unit connected to the car body, ensuring the circulation of water for cooling. The cylinder block must perform several functions, including:

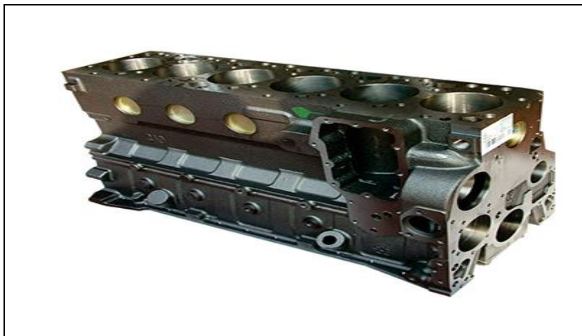

Figure I.4: *Cylinder block of engine [16].*

- Resisting the pressure of gases, which tend to expand and push against the cylinder head.
- Contain cooling water while resisting corrosion.
- Guide the piston.
- A support on which the accessories are fixed.

b) Cylinder head

it is the top of the engine block serves and it is as a housing and mount for other parts of the engine, including the intake and exhaust valves. Usually, cast iron or aluminum is used for its manufacture. It is fixed to the cylinder block with bolts and separated from it by a gasket in the cylinder head. This is because the combustion gases place a large amount of thermal stress on the cylinder head. Passages in the cylinder head allow fuel and air to enter the cylinder, exhaust gases to pass, and coolant to be directed towards the engine block.

Figure I.5: *Cylinder head of engine [12].*

a) Head gasket

It is a metal-plastic gasket that is placed between the engine block, which contains the pistons and cylinders, and the cylinder head, which contains components such as spark plugs and valves. Its goal is to ensure tensile strength. In addition to water resistance to the outside, the gas between the liner and the cylinder head ensures that the combustion chamber in the engine is closed so that the vehicle can build the appropriate pressure required for the engine.

Figure I.6: *Head gasket of engine [17].*

b) Oil Pan (sump)

The oil Pan is an essential part of the engine lubrication system because its function is to store engine oil and provide a reservoir from which oil is drawn to lubricate the various components of the engine. They are usually made of forged steel, aluminum, or die-cast aluminum alloy. It is placed under the engine block and may contain an external or internal strainer and oil filter.

Figure I.7: *Oil Pan of engine [18].*

I.6.1.2 Mobile components

a) The Piston

The piston, a critical component of an internal combustion engine, is the cylindrical component mounted in the cylinder and which forms the walls of the combustion chamber, usually made of aluminum alloy. They fit perfectly into the cylinder, ensuring a gas-tight space with the lubricating rings, and have alternating and rectilinear motion in the cylinder. The main function of the piston is to transfer force from the expanding gases produced during the combustion process to the crankshaft

Figure I.8: *Piston of engine[19].*

b) The valves

The valves can be defined as the components that control the flow of air or mixture into the combustion chamber and also the flow of exhaust gases out of the combustion chamber. Valves are classified into three categories: stem valves, rotary valves, and finally water jacket valves. The most common are stem valves, which are often equipped with all Current internal combustion engines are driven by a camshaft and one or more return springs.

Figure I.9: *Valves of engine[20].*

There are two main types of valves in an engine:

- **Intake Valve:** This valve opens to allow air or air-fuel mixture to enter the combustion chamber during the intake stroke of the engine cycle. It closes during the compression and power strokes to seal the combustion chamber.
- **Exhaust Valve:** This valve opens to allow the exhaust gases produced during combustion to exit the combustion chamber during the exhaust stroke of the engine cycle. It closes during the intake and compression strokes to seal the combustion chamber.

c) The connecting rod

The connecting rod is the mechanical part that ensures the mechanical connection between the piston driven in a straight motion and the crankshaft with rotary motion and also ensures that we transfer gas forces from the piston to the crankshaft. It is usually made of steel.

Figure I.10: *The connecting rod of engine [21].*

It consists of three parts:

- The big end.
- The shank.
- The small end.

d) The crankshaft

The crankshaft plays a crucial role in the operation of the internal combustion engine because it is the element responsible for converting the oscillating movement of the pistons into a rotational movement to drive all engine elements that require rotational movement. It is usually made of high-strength alloy steel or forged steel to withstand the pressures and forces to which it is exposed. During engine operation.

Figure I.11: *The crankshaft of engine [22].*

e) The camshaft

The camshaft is an essential part of an engine's valve system, controlling the opening and closing of the intake and exhaust valves in the event of a misfire. The stainless-steel cam or backbone to the bearing then started the operation of the intake and exhaust valves and began with the movement of the piston in the engine. This was done using lobes or cams, which is an unconventional version along the shaft. He pointed out that the camshaft presses these lobes on the valve head, which leads to the valves opening and closing at times during the engine's combustion cycle.

Figure I.12: *The camshaft of engine [22].*

a) The flywheel

A large, heavy wheel in the shape of a disc that is fixed to the end of the crankshaft is called the flywheel. Its main purpose is to provide rotational inertia, which stores rotational energy and reduces variations in the engine's speed and torque. It also takes in energy from the rotational strokes of the engine. As kinetic energy, it is stored there. Furthermore, it aids in the flywheel's ability to dampen vibrations and sustain the engine's idle speed.

Figure I.13: *The flywheel of engine [23].*

I.7 Terminology of IC engines

refers to the specialized vocabulary or technical terms that are commonly used to describe various components, processes, and phenomena related to internal combustion engines.

1. **Cylinder Bore (d):** refers to the diameter of the cylindrical chamber inside an engine's cylinder block as the piston moves up and down. It is expressed as (d) usually expressed in millimeter (mm) and represents the inner diameter of the cylinder.
2. **Piston Area (A):** The region within a circle, with a diameter equivalent to the cylinder's bore, is termed as the piston area, denoted by the symbol (A) and typically measured in square centimeters (cm^2). This space is commonly determined utilizing the formula for calculating the area of a circle.
3. **Stroke (L):** refers to the distance that the piston travels during a complete cycle of the engine. It is usually indicated by the letter (L) and is expressed in millimeters (mm).
4. **Stroke to Bore Ratio (L/d):** The (L/d) ratio serves as a significant parameter for categorizing engine size.
   - If d < L, it is called under-square engine.
   - If d = L, it is called square engine.
   - If d > L, it is called over-square engine.

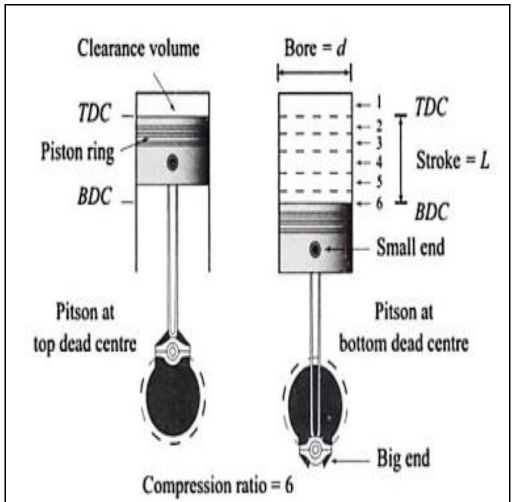

Figure I.14: *IC engine nomenclature [12].*

An engine with an over-square configuration can achieve higher operating speeds due to its larger bore and shorter stroke.

5. **Dead Centre:** In an engine, the term "dead center" refers to the position of the piston at the extreme ends of its stroke within the cylinder. There are two dead centers:
   - **Top Dead Center (TDC):** This is the position where the piston is at its highest point in the cylinder, closest to the cylinder head, at the end of the compression stroke or the beginning of the power stroke.
   - **Bottom Dead Center (BDC):** This is the position where the piston is at its lowest point in the cylinder, farthest away from the cylinder head, at the end of the exhaust stroke or the beginning of the intake stroke.
6. **Displacement or Swept Volume (V_S):** The amount of space moved by the piston during a single stroke is referred to as stroke volume or swept volume. It is quantified in cubic centimeters (cc) and can be calculated as follows: $Vs = A * L = \frac{\pi}{4} d^2 L$

7. **Cubic Capacity or Engine Capacity:** The displacement volume of a cylinder multiplied by number of cylinders in an engine will give the cubic capacity or the engine capacity. For example, if there are (K) cylinders in an engine, then: $Cubic\ capacity = V_S * k$
8. **Clearance Volume (V_C):** Or also alternatively termed as the combustion chamber volume or clearance space, represents the amount of space left in the combustion chamber once the piston reaches its highest point at top dead center (TDC) following the compression stroke. This volume encompasses the area above the piston when it attains its peak position within the cylinder.
9. **Compression Ratio (r):** The ratio of the total cylinder volume to the clearance volume is called the compression ratio (r) of the engine and is given by the following relationship.

$$r = \frac{\text{Total cylinder volume}}{\text{Clearance volume}} = \frac{\mathbf{V_C + V_S}}{\mathbf{V_C}}$$

For gasoline engine (r) varies from 7 to 12 and for Diesel engine (r) varies from 15 to 22.

10. **Piston speed (V_P):** refers to the velocity at which the piston moves within the cylinder during the engine's operation. It is typically measured in units of meters per second (m/s) or feet per minute (ft/min), It is influenced by several factors, including the engine's RPM (revolutions per minute), stroke length and connecting rod length. The formula to calculate piston speed is: $r = \frac{2*L*N}{60}\ [m/sec]$

Where:

L: Stroke length, [m] or [ft].

N: rotational speed [RPM].

I.8 The working principle of an internal combustion engine

An internal combustion engine works by utilizing a sequence of carefully timed explosions within the engine's cylinders to transform the chemical energy stored in fuel into mechanical energy. This is done by finely crushing the fuel and mixing it with air to form a combustible mixture that is fed into the cylinder.

At this stage, the gas is at low pressure. If it is ignited, it will not provide sufficient work. Therefore, it must be compressed to ensure sufficient work is done. After that, the burning mixture relaxes so that the kinetic effort is transformed into rotational movement, through the engine shaft, because of the connecting rod mechanism.

Finally, the burned gases are evacuated before the process is repeated again[24].

I.8.1 Definition of the 4-stroke cycle

The cycle is the set of phases that succeed each other in the engine. The name of (the 4-stroke cycle) goes back to the year 1862 when the French engineer Beau de Rochas, who is considered the founder of the principle of the four-stroke internal combustion engine, registered a patent for the four-stroke cycle, which laid the foundation for modern internal combustion engines[24].

I.8.2 Working of the 4-stroke spark-ignition engine

a) Intake stroke:

During this stroke, the piston moves from top dead center (T.D.C) to bottom dead center (B.D.C), drawing a mixture of fuel and air known as the charge. The intake valve stays open while the exhaust valve stays closed.

b) Compression stroke:

Both the intake and exhaust valves stay closed during this stroke. The piston travels from B.D.C. to T.D.C., compressing the charge to the maximum amount required for clearance. The mixture's temperature and pressure increase during the process. With the aid of a spark plug, the mixture is ignited just before the compression stroke ends. As a result of the fuel's chemical release, the mixture's temperature and pressure rise even more.

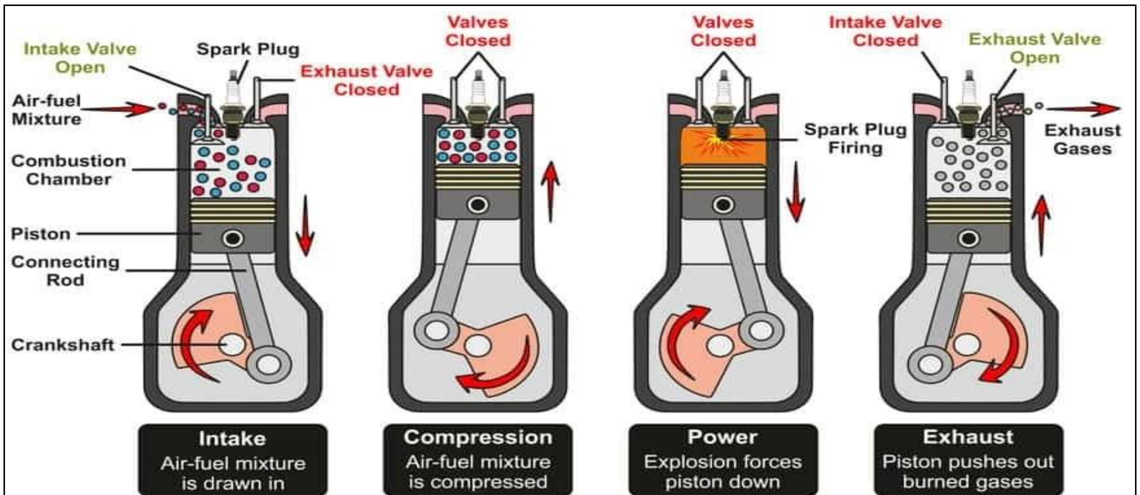

Figure I.15: *The 4-stroke spark-ignition engine [25].*

c) Expansion stroke (power stroke):

High pressure and temperature gases force down the piston to produce motive power during this stroke, keeping the intake and exhaust valve closed and the piston moving from (T.D.C) to (B.D.C).

d) Exhaust stroke:

The exhaust valve is open and the inlet valve is closed during this time stroke. The burned gases in the cylinder are forced out of the cylinder by the piston as it moves from B.D.C. to T.D.C. At the conclusion of the stroke, the exhaust valve closed, leaving residual gases a portion of the burned gases in the clearance space. A new cycle begins when the intake opens once more.

I.8.3 Working of the 4-stroke compression-ignition engine

a) Intake stroke:

The suction or intake valve opens during the suction stroke. The engine cylinder creates suction when the piston travels from TDC to BDC. Fresh air at atmospheric pressure will enter the engine cylinder during this operation. The inlet valve closes at the conclusion of the suction stroke.

b) Compression stroke:

Both of the valves stay closed during this stroke. The piston compresses the air as it travels from BDC to TDC. Pressure and temperature will progressively rise during this process, with temperature between 500^0C and 1500^0C. Fuel is injected into the combustion chamber through the injector at the conclusion of the compression stroke.

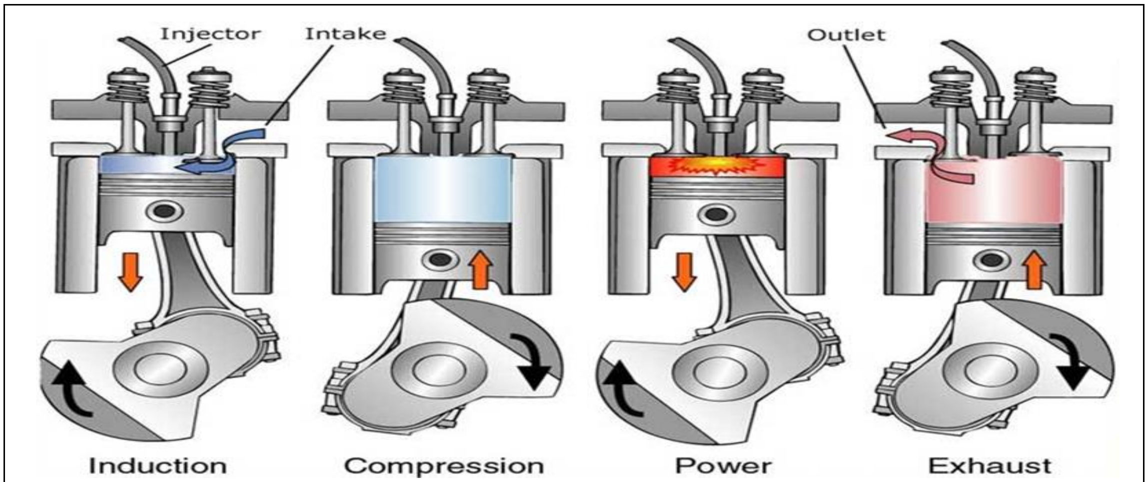

Figure I.16: *The 4-stroke compression-ignition [26].*

c) Expansion stroke (power stroke):

It is not necessary to light the spark plug for the diesel to ignite quickly after injection. burning. Engine time is the fast speed that comes next. When the mixture burns, it dramatically raises the cylinder temperature and pressure, which ranges from 60 to 200 bar, and pushes the piston back (TDC) to (BDC), applying work force to the connecting rod and rotating the crankshaft, or crankshaft that serves as the engine shaft.

d) Exhaust stroke:

The exhaust valve opens. Exhaust gases exit through the exhaust valve under their own pressure. The piston expels the leftover gases as it travels from (BDC) to (TDC). Exhaust valve closes at the end of stroke.

I.9 Internal combustion engine Classification

Internal combustion Engines may be classified according to three Standards as following [27]:

I.9.1 According to the type of ignition

- **Spark ignition engine (gasoline engine)**

- An ignition candle spark starts the burning of the air/fuel combination.
- Controlled ignition system.
- The air/fuel mixture can be done by:
  - Carburetor.
  - Direct fuel injection.

- **Compression ignition engine (diesel engine)**

- Diesel fuel is injected under pressure into very compressed air to start a combustion.
- The combination self-ignites, or ignites on its own will.

I.9.2 According to the number of strokes

- **Four stroke engines**

- **Intake stroke:** the air or the mixture (air-fuel) is introduced into the cylinder.
- **Compression stroke:** Here at this stage the process of compressing the air or mixture takes place.
- **Expansion stroke (power stroke):** quick ignition of the mixture, which causes the gas pressure to suddenly rise and the gas to expand.
- **Exhaust stroke:** Exhaling burning gases.

We observe that only the third stroke provides energy, it is the engine stroke, the three other strokes are resistant.

- **Two stroke engines**

Two-stroke diesel engines or spark ignition engines can be produced, meaning that instead of four combustion cycles per four strokes, there will only be two in these engines. These motors have a poorer efficiency than four-stroke engines, and a two-stroke engine's power is never more than half that of a four-stroke engine of the same displacement.

2 strokes = 2 piston strokes (1 revolution)

- 1st time (from BDC to TDC).
- 2nd time (from TDC and BDC).

I.9.3 According to the type of injection

1. Direct injection.

Direct injection is a typical method found in both diesel and gasoline engines. Indirect injection, whose design varies somewhat, does not follow this pattern. This is rather straightforward: the injector's end opens straight onto the injection chamber. As a result, at the appropriate time (the time on the four beats), it will spray the gasoline directly into this chamber (the cylinder). Because diesel has less fluid than petrol, injecting diesel into a diesel vehicle can be a little trickier. As a result, the injection frequently has a higher pressure. Take note that it is an injector and not a spark plug. Here, the fuel is introduced directly into the combustion chamber while under pressure.

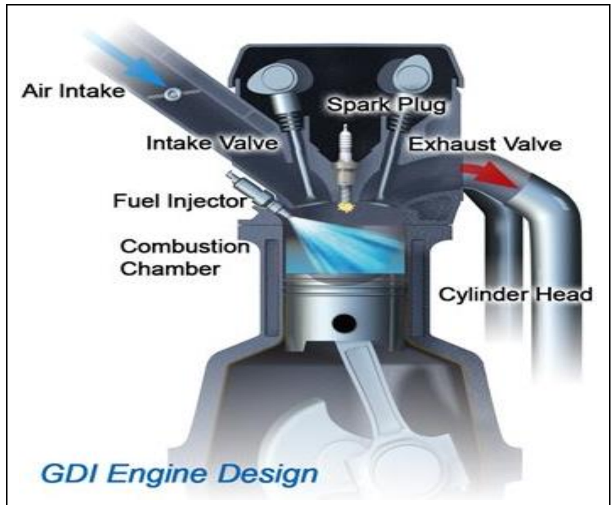

Figure I.17: *The Direct injection [28].*

2. Indirect injection.

actuality only air can pass through a diesel intake valve with gasoline, a mixture of air and fuel can pass through.

As a result, the mixing is carried out in a tiny, independent chamber that is wired to the cylinder rather than somewhere else (in the circuit admission in the case of gasoline). Once more, the mixture will be run through the "air currents" created by the ups and downs of the 4-stroke cycle (as well as by the precise aerodynamics of the engine's interior design).

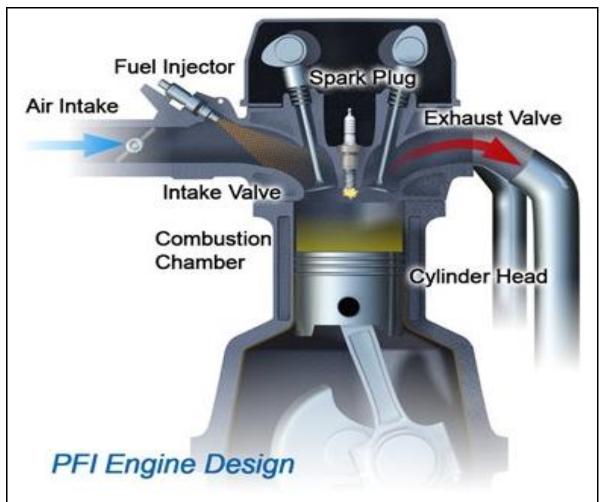

Figure I.18: *The Indirect injection [28].*

Keep in mind that glow plugs are more crucial for indirect injections than for direct ones. In fact, if the engine is obviously not too cold, a direct injection engine will start rather nicely without them. Due to its aerodynamic form, a small chamber attached to the cylinder permits the fuel to be injected as well as mixed with air from the intake. When the piston rises by "crushing" the air, the air circulating in the sphere creates a whirlwind that stirs everything, allowing for a homogeneous mixture and, consequently, better combustion (which boosts performance).

I.10 Application of internal combustion Engines

Perhaps the most important applications of the internal combustion engine, as we know, are land, sea, and air transportation. And also, industrial power plant applications. This table briefly shows the most important applications for both IC engine:

Table I.2: *Some applications of internal combustion engine.*

Domains	Where is it used or exploited
Automobiles	- In order to power vehicles, internal combustion engines (IC engines) are commonly employed in cars, buses, trucks, and motorbikes.
Aircraft	- Small aircraft and helicopters are also propelled by IC engines.
Marine	- Ships, boats, and submarines are among the marine applications for IC engines.
Agriculture	- In agricultural, IC engines are used to power equipment including irrigation pumps, harvesters, and tractors.
Power generation	- In situations like rural locales, building sites, and emergency backup power, where grid electricity is unavailable or unstable, IC engines are employed to generate power.
Construction	- Cranes, bulldozers, and other construction equipment are powered by internal combustion engines.
Military	- IC engines are used in tanks, aircraft, military vehicles.
Small equipment	- IC engines are found in many small appliances, including generators, chainsaws, and lawnmowers.

I.11 Conclusion

In this chapter, we presented general information about the internal combustion engine, first drawing on previous research studies dealing with the same topic as our study, through which we noticed that the current studies focus on developing the properties of the material that makes up the engine parts and also developing its design as a solution to resist stress and failure. In this chapter, we also presented the main components of the engine, which later helped us understand its working mechanism and the combustion process that occurs inside the engine. Then we noticed that the internal combustion engine can be classified in three ways, including the type of spark. Finally, we presented the areas of its use, which were very broad.

chapter II:

distribution system.

II.1 Introduction

One of the crucial and fundamental elements that greatly affects the engine's performance and lifetime is the distribution of fuel and air in the combustion chamber. so named because it is the mechanism in charge of using and distributing power, oversees this intricate operation.

Which includes filling the cylinders with fresh gas, Then the burned gases are evacuated, while being able to maintain the tightness of the cylinder during this compression and combustion stages. Distribution therefore has an important influence on engine performance, and today it is designed partly according to these two constraints. The distribution is subjected to significant stresses, both thermal (it is in contact with the combustion chamber), mechanical (at an engine speed of 6000 rpm the valve is turned 50 times per second).

We shall thoroughly examine the distribution system in this chapter. exposing its parts, workings, and essential function in producing the best possible combustion and energy.

II.2 Definition of the distribution

We can define It as all the mechanisms and components responsible for opening and closing the valves that control the flow of air, fuel, and exhaust gases inside the engine. Which ensures that the valves open and close at the appropriate time and in sync with the piston movements.

It is defined in abbreviation as the system responsible for managing the movement of the intake and exhaust valves.

II.3 Distribution mechanism

As we previously discussed, the distribution's job is to bring the air-fuel combination into the combustion chamber and release the combustion gases outside by timing the opening and closing of the valves. Pear-shaped cams serve as the foundation of its working mechanism. It is fixed to a revolving camshaft that is operated by the crankshaft and by a belt or chain. The engine block houses the camshaft, which is fitted with numerous tiny cams that are positioned correctly on the shaft. Both the metal pushrod, which has a rocker arm resting on the valve stem, and the cams work together to send force to the valves through the pushrod's upper portion ***Figure II.1*** shows the mentioned mechanisms [30].

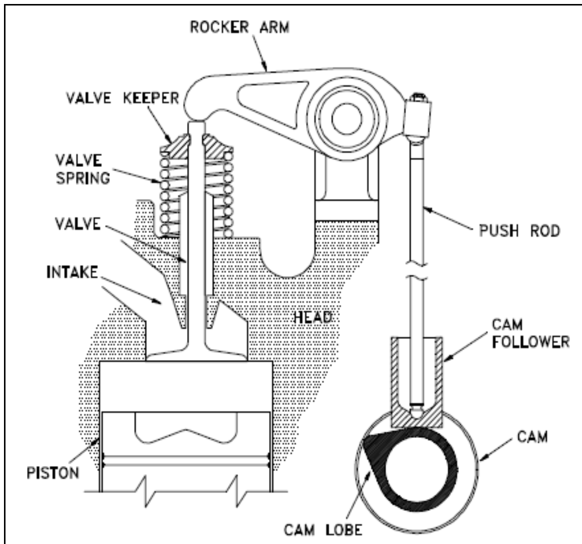

Figure II.1: *Distribution mechanism[29].*

II.4 Distribution types

There are three main types of distribution, which vary depending on the type of belts used.

II.4.1 The distribution by belt

The belts distribution are elements that allow the transfer of kinetic energy and torque between two parallel rotating shafts.

Its use is more common in modern vehicles and industrial equipment. This type has shown its advantage due to the awesome features it has, such as that it does not require lubrication and also does not make any noise when working [32].

Figure II.2: *The* distribution *belts[31].*

II.4.1 Distribution by chain

The chain distribution, as its name indicates, is a group of mechanical parts that transmit engine power to the output shaft. Such as the transmission shaft, it is made up of a chain linking two gears, namely the input gear and the output gear, in order to transmit rotation. The distribution chain is heavier than the belt, having a chain result in higher fuel and energy consumption. From a sound point of view, it is also noisier than the belt, which can be unpleasant for the occupants [32].

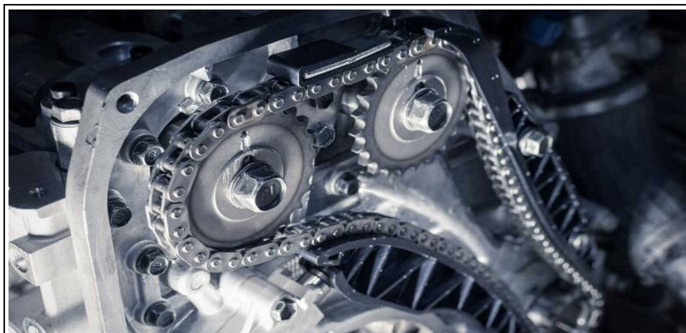

Figure II.3: *The chain distribution[31].*

II.4.2 Distribution by gable cascade

It is a gear that ensures the transmission of motion between the crankshaft and camshafts. What distinguishes it from the previous two types is its very heavy weight, as well as the noise it makes when working. To counter this, the gears have been covered with polymers or even manufactured entirely from synthetic materials, in addition to its complex system. For this reason, it is not widespread and its use is limited only to some diesel engines [32].

Figure II.4: *The gable cascade distribution[31].*

II.5 the distribution components

The internal combustion engine contains multiple distribution elements. Note ***Figure II.5*** shows the basic distribution components. As we can see, timing helps to synchronize. Crankshaft movement with intake and exhaust valves. This is done via a belt or chain, which, as we note. It connects the crankshaft to the camshaft, achieving an equal rotation rate between them after that. As we notice, the movement is transmitted to the camshaft, which in turn performs the distribution process by opening or closing the valves. It performs this process specifically through Pear-shaped cams. As a result, the process of opening the valves is carried out only by pressing them, while the process of closing the valves is done automatically by means of springs.

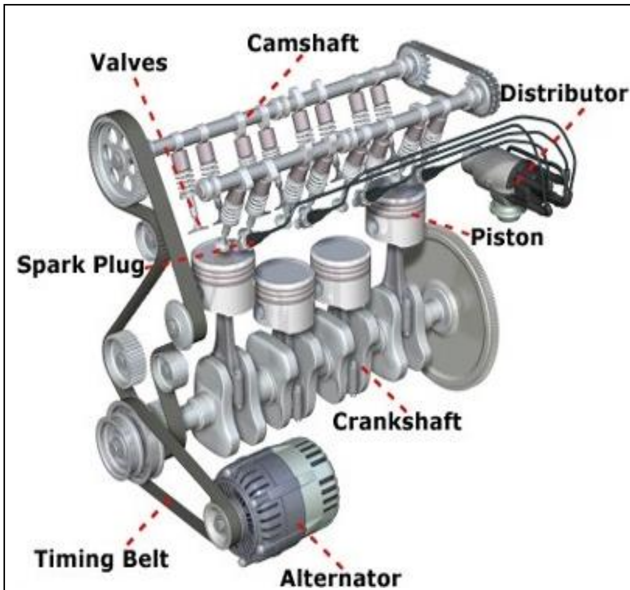

Figure II.5: *Distribution components[33].*

So, as we notice, the degree and time of opening are mainly related to the camshaft and valves, and this is what makes these two components the main components in the distribution system for internal combustion engines.

II.5.1 The camshaft

It is the main element in the engine because it is the most important element in timing control. That's why it's also called a “distribution shaft “. it is responsible for very precise control of valve lift and ensuring this lift for a specific period of time that corresponds to the engine distribution scheme. Due to its important role in the engine, it must be resistant to twisting resulting from spring pressure and wear resulting from friction. It is usually made of cast iron or steel.

Figure II.6: *The camshaft* [22].

II.5.2 The valves components

Engine valves (Intake and exhaust valves) play a vital role in the operation of internal combustion engines ،Because it is the direct controller the flow of fuel or air entering the combustion chamber. This process takes place through the movement transmitted from the camshaft. The various valve system components contribute to ensuring smooth and efficient engine operation, with recent developments helping to improve performance and reduce fuel consumption and emissions.

We mention its elements that have a major role in the composition of the distribution system as follows:

II.5.2.1 The Head and the trip

Two parts are necessary for the valve to operate: the head and the trip. The cylinder head's seat determines whether or not the head allows for gas diffusion and unclogging. The trip, which is joined to the head by a leaf directly, then aids in this dissemination[34].

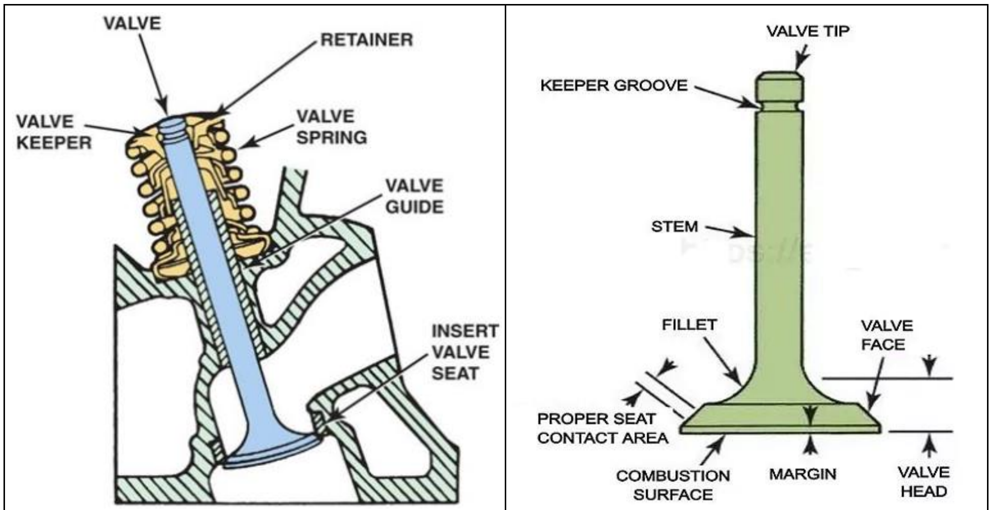

Figure II.7: *Explanatory diagram of a valve[35].*

II.5.2.2 The spring

Every valve has a compressed helical spring positioned between a steel bowl fastened to the valve stem and the machined face of the fixed casing. Resonance can occur when a spring is compressed at a high frequency. "Panic of the valves" is alleged to exist [36].

In order to prevent valve panic, manufacturers specifically use:

- variable pitch springs.
- two opposing springs (opposite helix direction; the diameter of one is only 0.5 mm greater than the external diameter of the other, so that there is friction between them and suffocation of the vibes).

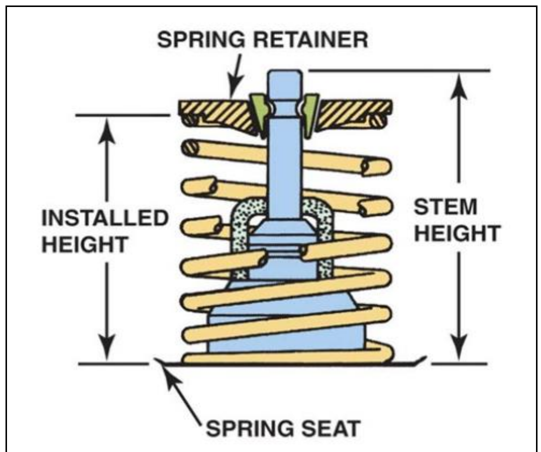

Figure II.8: *Explanatory diagram of a spring[35].*

II.5.3 The tappet

the tappet is placed between the cams and valves. It is considered an intermediary between the rotary movement of the camshaft and the rectilinear movement of the valves, according to the position of the camshaft in relation to the valves. It is necessary to place rocker arms and push rod contributes to reducing friction.

Figure II.9: *The tappet [37].*

In engines with an overhead camshaft, the tappet is reversed and covers the valve return springs lubrication is necessary except when it's gravel [38].

II.5.4 The rocker arm Linguet

Because of the latch's decreased moving mass, installing the camshafts is made easier. This is fundamentally ensured by the following three forms of movement [34]:

Figure II.10: *The rocker arm languet[39].*

1. Rotation, inducing a hydraulic stop.
2. The needle bearing designed to reduce friction with the camshaft.
3. Rotation at level from the second end.

II.5.5 The rocker arms

A rocker arm is a type of rocker lever found in the distribution control's secondary gearbox option. The rocker arm pushes the valve open from one location after receiving the cam's thrust, either directly or through a rod.

Figure II.11: *The rocker arm[39].*

Cast iron is a material that works well for the rubbing portions of the rocker arm. He could be constructed of steel, but the rubbing portions would need to be hardened by heat treatment [38].

II.5.6 Push rod

the pushrod is one of the distribution control components and is a thin metal stick. They are usually made of hardened steel to withstand the forces and pressures they endure while the engine is running. Its function is to transfer movement from the camshaft to the rocker arm by pressing its spherical end on the lower part of the pusher, and its other end is jointed in the form of a bowl using the adjusting screw carried by the rocker arm [38].

Figure II.12: *The push rod[40].*

II.6 The distribution diagram

An engine's intake and exhaust valve opening and shutting are graphically depicted in a distribution diagram. The engine's valves open and close in response to the piston's movement from TDC to BDC. This relationship between the piston and the valves is managed by establishing a graphical representation between them, called a distribution diagram.

The 360-degree figure in the distribution diagram depicts the piston's travel from TDC to BDC during each engine cycle stroke. This movement is expressed in degrees, and the valves' opening and closing are adjusted based on these degrees [41].

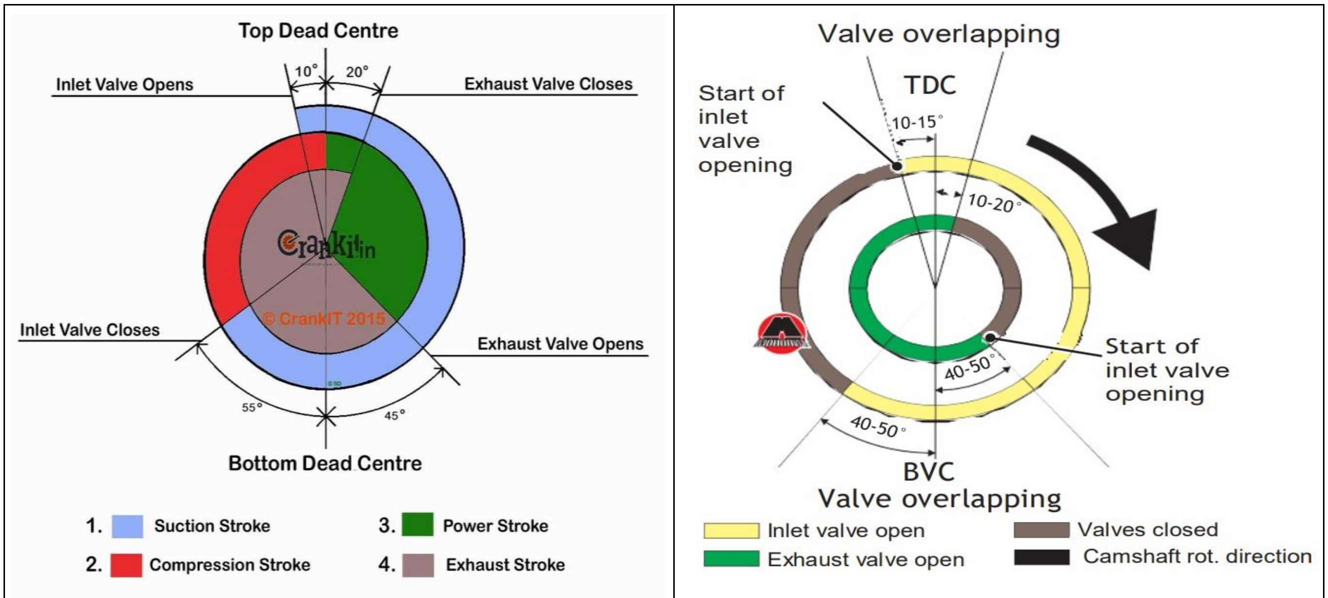

Figure II.13: *The distribution diagram[42].*

- ***Opening and closing of inlet valve:***

- The inlet valve opens 12 to 30° CA ahead of TDC to enable the engine to run quietly at high speeds. The volumetric efficiency rises as a result.
- The inertia movement of fresh charge into the cylinder, or the ram effect, causes the inlet valve to close 10–60° CA after TDC. The real distribution diagram for both low- and high-speed engines is shown in the figure.

- ***Opening and closing of exhaust valve:***

- In order to minimize the effort needed to release the burned gases from the cylinder, the exhaust valve opens 25 to 55° CA before BDC. Since there is more pressure inside the chamber at the end of the expansion stroke, more work needs to be done to get the gases out.
- After TDC, the exhaust valve closes 10 to 30° CA to prevent burned gases from being compressed in the following cycle. The burned gas's kinetic energy can help the gas exhaust as much as possible. Additionally, it improves volumetric efficiency.

- ***Valve overlap:***

- Both the intake and exhaust valves are open during this period. The exhaust gases' high velocity helps draw in the new charge when the intake valve is opened before they have fully exited the cylinder. In order to avoid losing new charge or unscavenged exhaust gas.

II.6.1 Why do we need distribution diagram.

An efficient system must be installed in order to facilitate the numerous processes that are involved in a single engine cycle, which is completed at a rate of approximately 100,000 cycles per minute by a typical engine. These processes range from the intake of the air-fuel mixture to the exhaust of the combustion residual [41].

- ✓ synchronization of the engine cycle phases, from the air-fuel ratios intake to the combustion residuals' exhaust.
- ✓ total seizing of the combustion chamber at the moment the air-fuel mixture ignites since any leaking could be dangerous and damaging to the engine.
- ✓ When the engine needs it (during suction for example feed) it with a mixture of gasoline and air, or air in the case of a diesel engine.
- ✓ Provide the combustion residual an outlet so that the engine can run through its next cycle.
- ✓ The optimal timing of the inlet and outlet valve opening and shutting shields the engine from flaws like detonation or knocking.

II.6.2 The distribution diagram for gasoline engine

Spark ignition engines is another name for gasoline engines. The four-stroke engine's distribution diagram is displayed in the following(***Figure II.14***)[41]:

a) from 10° to 20° before top dead center (TDC), the intake valve opens (IVO), and it closes 30° to 40° after bottom dead center (BDC).

b) The charge compression occurs between 30° and 40° after (BDC) and 20° and 30° before TDC.

c) in the field 20°to 30° is when charge ignition (IGN) occurs prior to TDC.

d) The expansion terminates 30°–50° before BDC, having begun 20°–30° before TDC.

e) The exhaust valve (EVO) closes at 10°–15° after TDC and opens at 30°–50° before BDC.

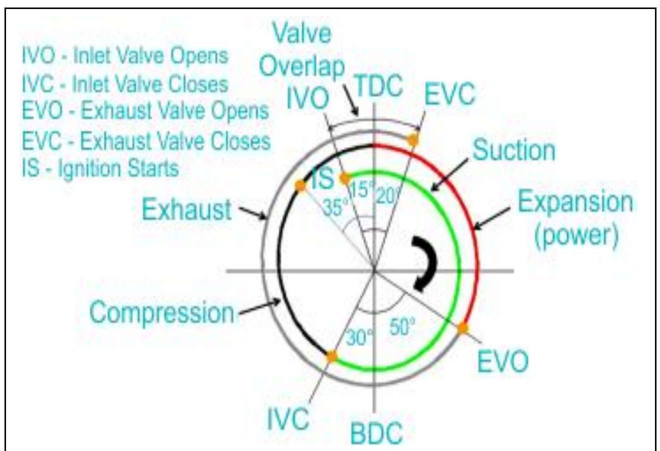

Figure II.14: *The distribution diagram of gasoline engine[43].*

note:

- ➢ A four-stroke internal combustion engine's intake valve stays open for 230°.

II.6.3 The distribution diagram for diesel engine

Compression ignition engines is another name for diesel engines. The four-stroke engine's distribution diagram is displayed in the following (***Figure II.15***)[41].

- **a)** The intake valve closes at 25°–40° after BDC and opens at 10°–20° before TDC.
- **b)** Before TDC, the fuel valve opens at 10°–15°, and then shuts at 15°–20°.
- **c)** At 25°–40° after BDC, the compression begins, and it finishes 10°–15° before TDC.
- **d)** The expansion terminates at 10°–15° before BDC, having begun 10°–15° after TDC.
- **e)** The exhaust valve closes at 10°–15° after TDC and opens at 30°–50° before BDC.

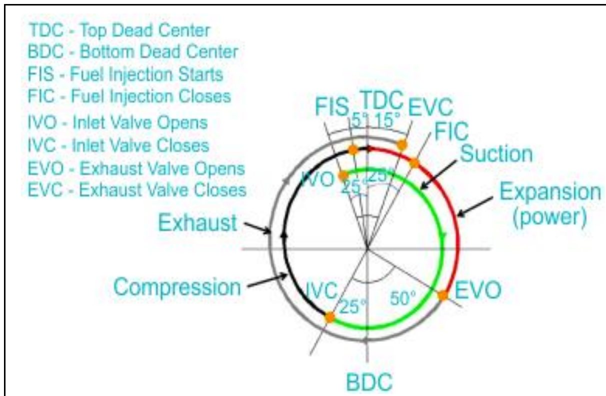

Figure II.15: *The distribution diagram of diesel engine[43].*

II.7 the conception of valves

as previously specified the organs that control the admission and departure of gases into the combustion chamber are the valves. Their head needs to be quite huge in diameter. This dimension is constrained by the combustion chamber's open space, the valve's minimal weight, and its mechanical resistance to deformations and shocks. The conical seat prevents the pushrod from deforming by ensuring ideal sealing during closing and proper centering.

Reach angles are around 90º degrees. Lower temperature intake valves can have an angle of 120º, which protects the valve from well deformations but provides a more significant gas passage section for the same lifting height[44].

II.7.1 The function of valves

The engine valves are protected by the cylinder head. The engine valve's primary job is to permit fluid to enter and exit the cylinder. Fuel is ignited with the aid of air. The piston is propelled forward and downward by the power generated during the combustion of the air-fuel combination. There are two types of engine valves as following[45]:

II.7.1.1 intake valve

To transport gasoline into the engine cylinder, an intake valve is placed. It guarantees that the engine cylinder receives the right amount of gasoline. The gasoline flow into the cylinder ceases when it closes.

Intake valves are most frequently constructed from austenitic stainless steel. This substance is resistant to heat and corrosion. The intake valve is similarly made of alloy steel containing nickel and chromium.

II.7.1.2 Exhaust valve

The discharge valve is another name for the exhaust valve. It is used for exhaust gas discharge. The exhaust valve is typically constructed from silicon steel. An alloy of silicon and chromium is called silicon-chromium steel. The valves used in automobile engines are sometimes referred to as poppet or mushroom valves. A thin edge is prevented by the precise ground surface of the valve head, which provides sufficient space. To match the valve seat angle in the cylinder head, the angular surface is grounded at an angle of either 30° or 45° with respect to the valve head. The valve stem end is where the spring retainer lock groove is situated.

II.7.2 Working principle of valves

The motion of the piston, crankshaft, and camshaft has a significant impact on how the engine valves operate. The intake and exhaust valves opening and closing are controlled by the camshaft. An engine valve functions as follows [45]:

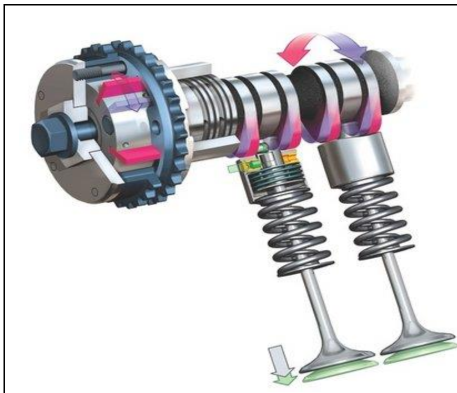

Figure II.16: *Working principle of the intake valve [46].*

- In the intake stroke the piston travels from TDC to BDC. Using a connecting rod, the piston moves the crankshaft during this stroke. the crankshaft further transfers its motion to the camshaft.
- Motion causes the camshaft to press down and open the intake valve. The fluid begins to enter the cylinder when the intake valve opens. This procedure keeps the exhaust valve closed. The fluid is transported in accordance with the specifications, and the piston reciprocates to complete its compression stroke.
- In the compression stroke the camshaft closes the intake valve and pushes it once again.
- The piston completes a compression stroke following compression. Both the intake and exhaust valves stay closed during the compression stroke.
- The piston advances to execute the exhaust stroke once the power stroke is finished. The intake valve stays closed throughout the exhaust stroke, but the exhaust valve is pushed open by the camshaft.

II.7.3 Types of valves

there are three types of valves as following[45]:

II.7.3.1 Poppet valve

Another name for the poppet valve is a mushroom valve. Because of its popping upward and downward action, it is called a poppet valve. The timing and quantity of gas supplied to the engine are controlled by this kind of exhaust valve. The automotive engine is the primary use for the poppet valve.

II.7.3.2 Sleeve valve

The sleeve valve, as its name implies, is a tube or sleeve that is inserted between an IC engine's cylinder wall and piston, allowing it to slide or spin.

II.7.3.3 Rotary valve

There are several varieties of rotary valves. Among the most well-known varieties of rotary valves is the disc-type valve. This valve has a rotating disc with a port on it. The intake manifold and exhaust manifold alternate while the disc turns.

II.7.3.4 Reed valve

The fluid flow in the same direction is opened and closed by the reed valve at varying pressures on opposite sides. That kind of valve is what it is. The rod is mechanical. This rod had a hinge at one end, which covered the channel and limited the direction in which charge or air could go.

II.7.4 Valves construction material

The most frequent materials used to make intake valves are tungsten steel, nickel, or chrome because of their low working temperature. Compared to the intake valve, the exhaust valve is subjected to greater pressure and temperature. Thus, the exhaust valves are made of silicon chromium, nichrome, or cobalt-chromium alloys.

Valve surfaces subject to elevated temperatures can be strengthened by bonding a cobalt-chromium alloy called stellite onto the valve surface through brazing.

Stainless steel alloys, titanium, and tripaloy are other materials utilized in engine valve production. Engine valves' wear characteristics and mechanical quality can also be enhanced by coatings and surface treatments[45].

II.7.5 Causes and problems of valves

a) **Wear and Tear**: Engine valves may become worn down over time as a result of frequent opening and shutting, exposure to high temperatures, and combustion byproducts. Poor sealing and decreased engine efficiency can result from this wear, which can also cause erosion of the valve stem and valve seat.

b) **Carbon Buildup**: On the surfaces of intake and exhaust valves, carbon deposits can build up, especially in engines that burn oil or run under specific circumstances. Overly high carbon accumulation can cause airflow restrictions, interfere with valve seating, and result in rough idling, misfires, and reduced power.

c) **Valve Seat Recession:** The valve seat may erode and recession because to constant contact between the valve face and the valve seat. Poor sealing, compression loss, and higher emissions may come from this.

d) **Valve Burning:** When engines run in harsh environments or with insufficient cooling, valves can overheat and "burn," deforming or even melting the valve surface. If valve burning is not corrected right away, it might result in catastrophic engine failure.

e) **Valve Float:** Insufficient spring pressure or malfunctioning valve train parts can cause the valves to "float," or fail to fully close before the following cycle, at high engine speeds. This may cause piston-to-valve contact, which might result in severely damaged pistons, bent valves, and other engine damage.

II.8 The conception of the camshaft

One mechanical part of an internal combustion engine is the camshaft. He accurately and precisely defines the sequence in which he opens and closes the engine's intake and exhaust valves at the appropriate times. Through the use of channel, belts, or gable cascade, the crankshaft drives the camshaft.

II.8.1 The function of the camshaft

The main function of the camshaft is to open the inlet and exhaust valve of an engine by converting the rotary motion of the crankshaft into a reciprocating motion. Here's a detailed explanation of its function:

1) **Valve Actuation**: As we know, the camshaft contains a number of lobes or cams that are placed to apply pressure either directly on the valves or on the valve lifters. These lobes put pressure on the valve lifters when the camshaft rotates, causing the valves to open.
2) **Timing Control:** A timing belt or chain synchronizes the camshaft's rotation with that of the engine's crankshaft. This guarantees that the valves open and close at the exact appropriate points during the engine's cycle. For the best possible engine performance, efficiency, and emissions management, valve timing is crucial.
3) **Valve Overlap:** The length of time and timing of valve overlap the moment when the intake and exhaust valves are open at the same time are determined by the camshaft design. Engine efficiency is increased by valve overlap, which permits the admission of fresh air-fuel mixture and the scavenging of exhaust gases from the combustion chamber.

II.8.2 The components of the camshaft

Like other car parts, the camshaft comprises various parts, as we see in ***Figure II.17*** there are five components of the camshaft as following [48] :

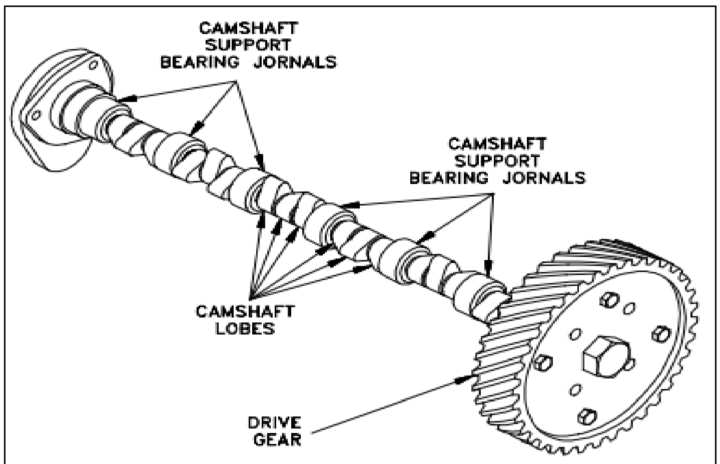

Figure II.17: *The camshaft components [47].*

II.8.2.1 Bearing journals

Maintaining the camshaft's position as it revolves around the engine is the primary goal of the main journal.

II.8.2.2 Cam lobe

The piston's movement is reflected in the camshaft lobes' rotation. This part moves at a different speed depending on the engine speed. The lobes’ primary function is to open and close the intake and output valves.

II.8.2.3 Drive gear

A timing gear or sprocket is installed on the end of the camshaft in engines with overhead camshafts. The camshaft and crankshaft rotate in unison thanks to the meshing of this gear with the timing chain or crankshaft gear.

II.8.2.4 Thrust Plate

A thrust plate is affixed to the end of the camshaft in certain engines in order to regulate end play and stop the camshaft from moving too much in one direction.

II.8.3 Working principle of the camshaft

Movement is transferred from the crankshaft to the camshaft through the timing belt from the crankshaft sprocket. The camshaft then translates the rotational movement into translation movement, which opens the valves [38].

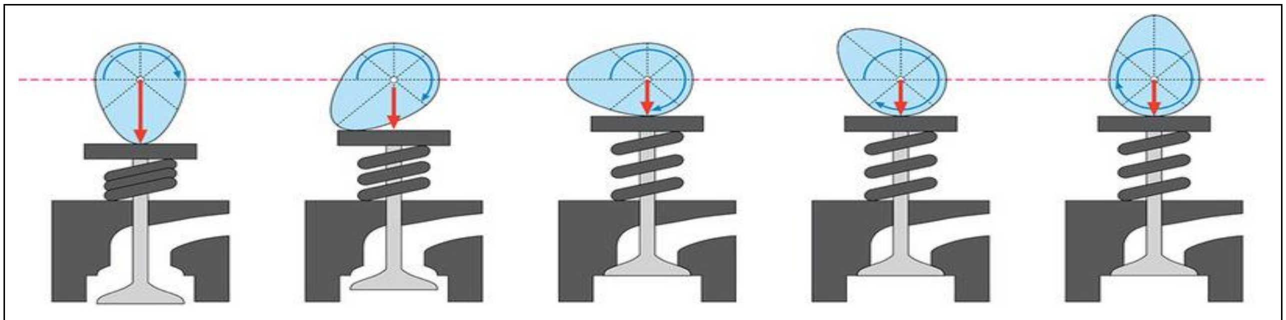

Figure II.18: *The movement of a valve as a cam rotates [49].*

II.8.4 Installation of the camshafts

As we notice from ***Figure II.19***, there are two types of transmission methods: alternative translation straight and continuous translation. As we notice, the camshaft is the first element that transmits the motion to Tappet. As we notice, there are other elements that could be an alternative to this element, such as Roker arm and Push rod, which in turn transmits it to the valves. After the combustion process, the crankshaft transmits rotational motion in four ways, including Belts, Chain, Gable cascade or Mixed .to the camshaft to continue the process.

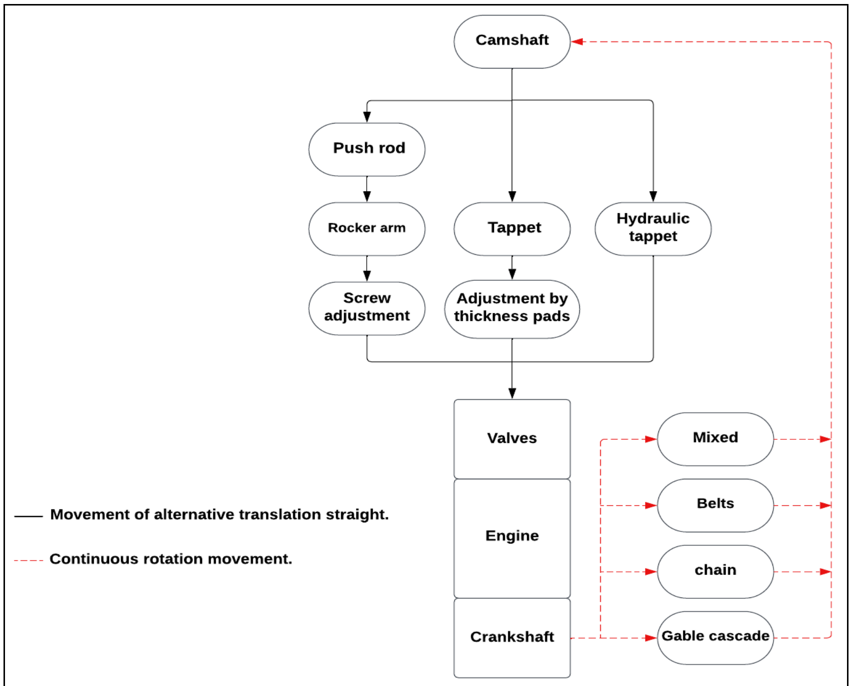

Figure II.19: *Possible installations [50].*

II.8.5 Operation of the camshaft on the valves

The camshaft will begin to spin as soon as the user starts the engine. As the cams revolve, they will gradually exert pressure on the valve stems, which are supported by springs. Depending on the use of the valves connected to the movement, this support effect produced by the camshaft will push the valve tails outside, permitting the entry of air or the outflow of the engine's combustion product. The movement of the springs causes the valve to return to its position once the cam has passed [51].

II.8.6 The types of the camshaft

The camshaft has the following major types[48]:

- Based on lifters used by the camshaft.
- Based on the camshaft driver member shape.

II.8.6.1 Based on lifters used by the camshaft

II.8.6.1.1 Flat Tappet Cam

In actuality, a flat tappet cam is not flat. There is a little crown on the face of these cameras. It is mounted such that the lifter spins on the lobe and the lobe moves in opposition to one another. This cam's lobes are made with a tiny, tapered form.

II.8.6.1.2 Roller Cams

The fuel-air mixture needs are impacted by the roller cam's ability to maintain the valve open at high lift for prolonged periods of time due to its rounded tip. Additionally, the valve might open faster due to the lobe's structure. These camshafts' primary benefits are that they allow for a more aggressive cam profile, reduce internal friction, and promote high speeds. These are quite durable. Put otherwise, its useful life is infinite.

II.8.6.2 Based on the camshaft driver member shape

II.8.6.2.1 Cylindrical Cams

The form of this kind of cam is cylindrical. It is sometimes referred to as a drum cam barrel. There is a groove carved in the cylindrical cam's surface. This groove cut is how the cam follower moves. The cam axis on this camshaft is parallel to the follower member's motion.

II.8.6.2.2 Radial Cams

Another name for a radial cam is a plat or disc cam. Because its axis is perpendicular to the direction in which the follower is moving, it is referred to as a radial cam. The contour plate of this kind of cam is not uniform. This plate is used to translate the motion of the cam to that of the driven member or cam follower.

II.8.6.2.3 Conjugate Cam

It has two rollers. These rollers are connected to the camshaft's follower or driver. In order to reduce noise and achieve silent operations, the rollers often restrict the movements of others.

II.8.6.2.4 Globoid Cam

The design of this cam and a cylindrical cam are quite similar. The primary distinction is that a concave or convex assembly is used to replace the cylindrical cam.

II.8.6.2.5 Spherical Cam

A groove may be found on the curved design of the spherical cam. It is shaped like a sphere. Running through the groove is the follower. The follower's movement is perpendicular to the spherical cam's rotating axis.

II.8.6.2.6 Translating Cam

There is a contour plate with grooves on this cam. As they move over the cam groove surface, the follower parts oscillate.

II.8.6.2.7 Heart-shaped Cam

Because of its asymmetrical heart-shaped design, it is known as a heart-shaped cam. Following the cam edge, the follower moves. It moves continuously and smoothly. The most typical way to deplete this kind of cam is to wind the cable firmly across the solenoid.

II.8.6.2.8 Wedge Cam

This cam's end features a broad basement and a pointed form. There is a sliding motion between the driver and the cam.

II.8.6.2.9 Spiral Cam

It has a groove on the surface and is shaped like a spiral semicircle. According to the camshaft's linear movement in the driver member, the follower of this cam moves perpendicularly[48].

II.8.7 The position of the camshaft

The placement of the camshaft varies per model. The timing shaft of an engine with side valves is situated close to the crankshaft. Right above the valves on the cylinder head is where you'll find an overhead camshaft. The shaft cams need to be taken out while changing the timing belt or crankshaft because of their location. As a result, this kind of operation requires replacing the shaft's SPI seals Cameras [38].

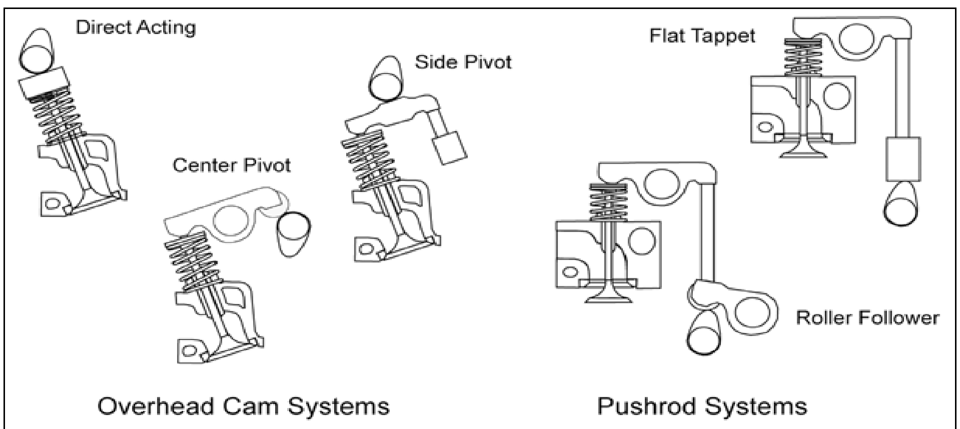

Figure II.20: *Multiple camshaft positions[52].*

II.8.8 The camshaft construction material

The solid material is most often utilized in the camshaft production process. This is due to the high stiffness that these camshafts offer. Because cast iron has greater strength, it is also utilized in the production of camshafts. Since the material is hardened by the chilling process, camshafts constructed of chilled iron can offer exceptional wear resistance. Iron may be combined with other materials to create features that are best suited for specific uses[48].

II.8.9 Causes and problems of camshaft

a) **Wear and Tear:** Because of the continual pressure and friction on their surfaces, camshafts can wear down over time with continuous operation. There might be wear and tear on the camshaft journals or cam lobes, which would lower performance and efficiency.
b) **Camshaft Breakage:** Excessive load or extreme wear can cause camshafts to shatter. This may lead to an abrupt engine shutdown and total camshaft failure.
c) **Camshaft Deformation:** High temperatures or difficult working circumstances might cause camshaft deformation. Deformation can result in alterations to the geometry of the camshaft, which can impact valve timing and result in unstable engine performance.
d) **Improper Installation-Related Breakage:** The camshaft might break or sustain damage if it is fitted incorrectly or if valve parts are fastened incorrectly.
e) **Chemical Corrosion:** some engine fluids, such oils and other chemicals, can corrode the camshafts surface, which will shorten its lifespan and impair performance.

II.9 Conclusion

Finally, after studying this chapter, we have become familiar with the engine distribution system, which, as we discussed, is the system responsible for the movement of the valves. We also touched on its mechanism, which, as we studied, is considered a rather complex mechanism. We then became aware that the type of distribution system is controlled by the nature or type of belt used in the system. Then we studied the main parts of the distribution system, which, as we discussed, are the camshaft and valves, in addition to some intermediate parts. In this part, we also learned about the distribution system diagram, which is a graphical representation of the transmission and change of movement between pistons and valves. Then, at the end of this chapter, given that the camshaft and valves are the basic elements of the distribution system, we conducted a detailed study of each of them.

chapter III: Modelling by Finite element method (FEM).

III.1 Introduction

Finite element method (FEM) is a numerical method used to solve some physics problems. It is a method that makes it possible to determine an approximate solution on a spatial domain, corresponding to certain equations and certain imposed conditions. This method has become an essential component in the arsenal of tools used to design and evaluate industrial goods as modeling aids advance in complexity. This is due to the ease of its implementation and the reliability of the algorithm.

The objective of this chapter is to outline the fundamental concepts of this method, with a focus on the series of tasks involved (including the approach and the associated hypotheses). because this method will serve as the foundation for modeling our project.

III.2 General description of finite element method

In engineering problems, there exist fundamental variables that are not immediately known. However, once these variables are determined, it becomes possible to predict the behavior of the entire structure. These fundamental variables, also known as field variables, vary depending on the specific engineering problem. For instance, in solid mechanics, they manifest as displacements; in fluid mechanics, as velocities; in electrical engineering, as electric and magnetic potentials; and in heat flow problems, as temperatures.

In a continuum, these variables are theoretically infinite. To manage this complexity, the finite element method employs a strategy to reduce the number of unknowns to a finite count. This is achieved by dividing the solution domain into smaller segments, referred to as elements, and expressing the unknown field variables within each element using assumed approximation functions, often referred to as interpolating functions or shape functions. These functions are defined based on the field variables at specified points known as nodes or nodal points. Consequently, in finite element analysis, the unknowns are represented by the field variables at these nodal points. Once these are determined, the field variables at any point within the structure can be obtained using interpolation techniques. Following the selection of elements and nodal unknowns, the subsequent step in finite element analysis involves assembling element properties for each element. For instance, in the context of solid mechanics, this may involve determining the relationship between force and displacement.

III.3 Working principle of FEM

In broad strokes, outlining the operational process of the finite element method involves enumerating the principal stages of its solution methodology[53].

a) **Discretize the continuum:** To begin, the initial stage involves partitioning a solution area into finite elements. Usually, a preprocessor software is utilized to create the finite element mesh. This mesh description comprises various arrays, with key components including nodal coordinates and element connections.

b) **Select interpolation functions:** Interpolation functions serve the purpose of extrapolating field variables across the element. Frequently, polynomials are opted for as interpolation functions. The polynomial's order is contingent upon the quantity of nodes allocated to the element.

c) **Find the element properties:** To formulate the finite element's matrix equation, one must establish a relationship between the unknown function's nodal values and various parameters. Several methods can be employed for this purpose, with the variational approach and the Galerkin method being the most practical options.

d) **Assemble the element equations:** In order to derive the overall equation system encompassing the entire solution domain, it's necessary to compile the equations of all elements. This entails integrating the local element equations for all discretized elements. The assembly process relies on the connectivity between elements. Prior to solving the system, it's essential to enforce boundary conditions, which are not included in the element equations.

e) **Solve the global equation system:** The global equation system in finite element analysis is usually characterized by sparsity, symmetry, and positive definiteness. Both direct and iterative techniques can be employed to solve this system. The sought-after nodal values of the function are obtained as an outcome of the solution process.

f) **Compute additional results:** Often, it's necessary to compute supplementary factors. For instance, in mechanical scenarios, strains and stresses are of significance alongside displacements, which are derived post-solving the overarching equation set.

III.4 Application of the finite element method

The potential uses of the finite element method span across a wide array of fields and are highly diverse. of which we will mention the three most famous fields as following:

1- Civil Engineering: considered as crucial tool in civil engineering for numerically approximating complex structures. As computer-aided engineering (CAE) advances, FEM tools have become more efficient, in design methods and material properties.

2- Aerospace Engineering: Finite element method originated in Aerospace Engineering and has since been used for design optimization in various fields. It addresses structural issues in aircraft components, ensuring structural integrity and passenger safety.

3- Mechanical Engineering: Finite element method is widely used in Mechanical and Aerospace engineering, including crash and thermal analysis. FEA is used by design engineers during product development.

4- Bio-Mechanics: Dental implants have become an integral part of dental practice, replacing missing teeth. Its success depends on its biomechanical behavior, as the pressure distribution differs from that of natural teeth. The distribution of occlusal forces around implants is crucial for bone preservation and this is where the finite element method comes into play.

III.5 FEM in Mechanical Engineering

Finite element method finds extensive application in Mechanical and Aerospace engineering, where it serves various purposes ranging from crash analysis to thermal assessment. Mechanical engineers leverage the full spectrum of Finite Element Method (FEM) capabilities in their work. Particularly, automotive companies widely integrate FEM into their processes, employing it as a pivotal tool in product development. Design engineers utilize FEM to scrutinize their designs at the stage of easily modifiable **CAD** models, ensuring swift incorporation of analysis findings into the design process. [55].

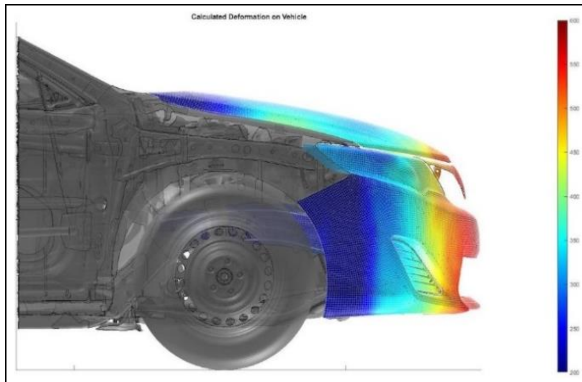

Figure III.1: *FEM simulation of vehicle [54].*

In mechanical engineering, the finite element method finds application across two different mediums.

- The mechanics of solid continuous media.
- The mechanics of continuous fluid media.

In the context of the mechanics of solid continuous media, Problems can be categorized as following:

- **Linear statics**

This form of examination primarily focuses on elastic regions or linear materials. Our aim is to determine the strain **(ε)** and stress **(σ)** of the material under various types of constraints.

- **Linear dynamics**

Linear dynamics examines the behavior of linearly elastic structures under cyclic forces or initial constraints in such analyses, the focus is on determining displacements, and potentially velocities and accelerations, that yield frequencies and natural modes (modal analysis).

- **Nonlinear problems**

There are three classes of nonlinear problems:

1. **Geometric nonlinearities:** This form of examination arises when the impact of travel and distortions becomes significant. Here, the stability of the framework and the stresses are contingent upon unpredictable movements. Such nonlinear behavior is commonly observed in investigations concerning material manipulation, buckling, and post-buckling phenomena.
2. **Behavioral nonlinearities**: When materials exhibit behavior beyond linear elasticity, the stiffness of the structure varies with deformation, leading to nonlinearities in the problem. This form of nonlinearity typically arises in scenarios involving plasticity, viscoelasticity, and damage.
3. **Contact nonlinearities:** If alterations occur in the supports during deformation, the structure's stiffness will be altered, rendering the issue nonlinear. This phenomenon is typical in processes like shaping, such as when stamping a sheet, for instance.

III.6 Classic shapes of elements

There exist various classical shapes representing domains in dimensions of one, two, or three. Each form is distinguished by a designated name indicating its configuration and by the count of geometric vertices it comprises [56].

Table III.1: *Classic shapes of elements[56].*

One-dimensional elements.	 Linear **(2)**	 Quadratic **(3)**	 Cubic **(4)**
Triangular two-dimensional elements.	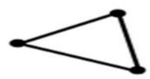 Linear **(3)**	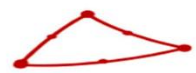 Quadratic **(6)**	 Cubic **(9)**
Quadrangular two-dimensional elements.	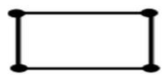 Linear **(4)**	 Quadratic **(8)**	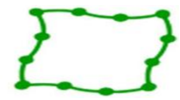 Cubic **(12)**
Tetrahedral three-dimensional elements.	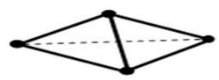 Linear **(4)**	 Quadratic **(10)**	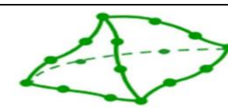 Cubic **(16)**
Three-dimensional hexahedral elements.	 Linear **(8)**	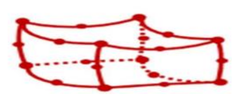 Quadratic **(20)**	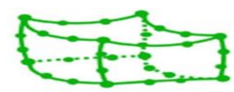 Cubic **(32)**
Three-dimensional Tetrahedron elements.	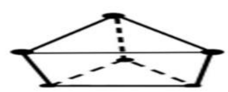 Linear **(6)**	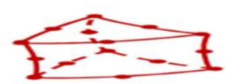 Quadratic **(15)**	 Cubic **(24)**

III.7 Using finite element software

A comprehensive industrial software package should have the ability to tackle a range of large-scale problems, typically involving thousands to hundreds of thousands of variables. These sophisticated programs require substantial preparatory work before being able to effectively address real-world problems. Examples of such software include NASTRAN, ANSYS, ADINA, ABAQUS, CASTEM 2000, CESAR, SAMCEF, among others. The capabilities provided by these programs are extensive[57]:

- Linear or nonlinear analysis of a continuous physical system.
- Static or dynamic analysis.
- Taking into account complex behavioral laws.
- Taking into account various phenomena (elasticity, thermal, electromagnetic, plasticity, flow.) which can be abrupt.
- Optimization issues, etc.

III.8 Flowchart of finite element software

Any finite element calculation software contains the characteristic steps described in ***Figure III.2***

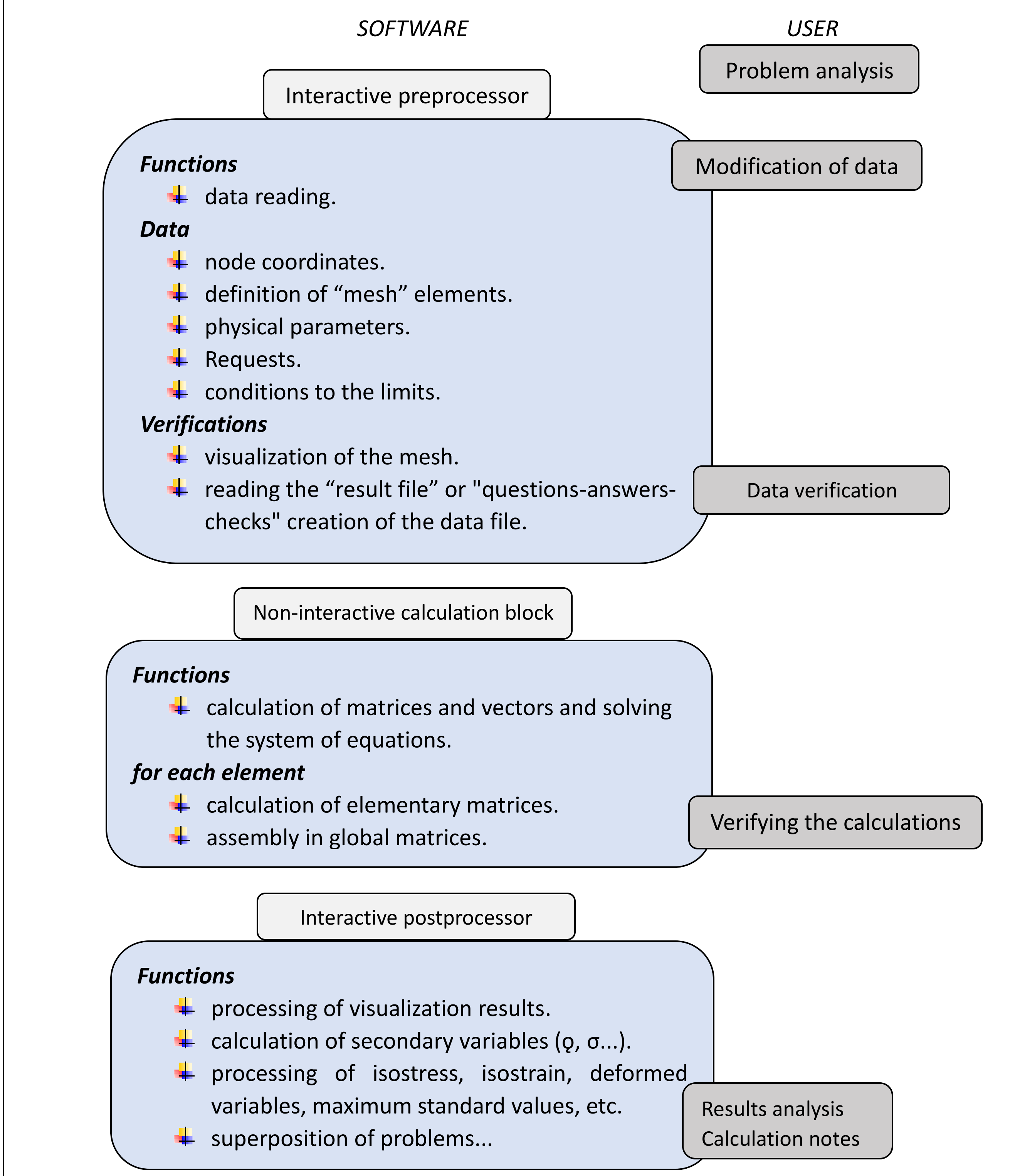

Figure III.2: *Flowchart of finite element software [58].*

III.9 Basic Concept of Finite Element Method

The finite element method (FEM) stands out as a highly versatile and widely utilized approach for analyzing structures across various industrial domains, including aeronautics, automotive. Within the realm of structural analysis, FEM represents a multidisciplinary methodology that integrates insights from diverse fields such as structural mechanics, numerical analysis, and applied computing. Its theoretical foundations draw upon energetic principles of structural mechanics and techniques for spatial function approximation[59].

a) The domain of integration now employs continuous subdomains known as "finite elements" (***Figure III.3***) instead of discrete points, as seen in finite difference methods. These finite elements are finite in number and serve to represent geometric modeling. Through this approach, the method aims to create a model that accurately represents the physical phenomenon in its true form.

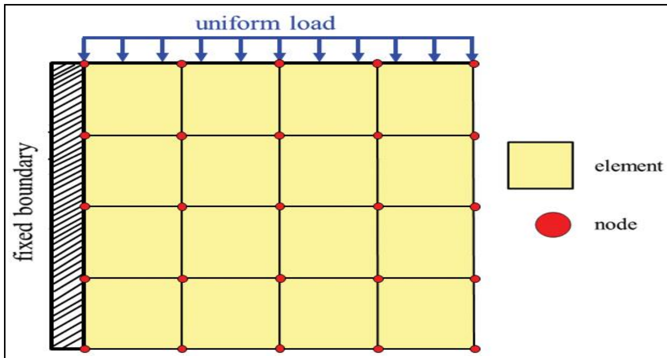

Figure III.3: *Discretization using finite element modeling[60].*

b) The Galerkin-type integral formulation is implemented on specific finite elements rather than the entire integration domain, utilizing standardized shape functions instead of the basic functions of the Galerkin method. This approach unifies the formulation across various problem types. Additionally, the bibliography of related articles is revised and updated. Consequently, the method becomes highly programmable, offering numerous advantages. With these benefits, the method continues to advance and extend into areas previously reliant solely on experimental techniques.

III.9.1 The elementary formulation at the finite element level

For every component within a specific local frame of reference, we select an interpolation function to depict the changes in displacements within that component based on nodal displacements. Following this, we compute the stiffness and mass matrices for each component, along with its force vector. These basic attributes are then converted into parameters for the entire structure.

III.9.2 The overall formulation at the level of the complete structure

This process involves determining the matrix representation of the energy potential for the entire structure, based on the unknown displacements at all nodes. This involves assembling stiffness and mass matrices, as well as force and displacement information for the structure, derived from the elemental properties such as rigidity, mass, and force/displacement vectors for each element.

III.10 Finite element formulation approach

One approach to analyzing lattice or gantry type structures involves initially examining the behavior of individual components (such as bar elements or beams) separately. Then, these components are assembled in a manner ensuring that force equilibrium and movement compatibility are met at each node.

In the following, all the vector and matrix quantities relating to the base element's location are highlighted with a bar.

III.10.1 Discretization of the finite element structure

These are the steps involved in creating the mathematical framework to accurately depict the actual structure. Essentially, this process involves simplifying the structure's geometry from a topological standpoint, reducing one-dimensional elements to their axes, and specifying support conditions and loads. Additionally, from a rheological perspective, it entails selecting the material's constitutive law and identifying the constants that define this law.

III.10.2 Construction of nodal by subdomain

For each element, we choose an interpolation function which represents the variation of displacements $U^{\mathrm{e}}(x, y, z)$inside this element in terms of nodal displacements U^{e}. This model can be conveniently represented by a polynomial expression containing an unknown coefficient for each degree of freedom. Either,

$$U^{e}(x, y, z) = N^{t}\, U^{e} \qquad \text{(III. 1)}$$

where *N* is the interpolation matrix connecting the displacements of a point interior of the element to nodal displacements.

III.10.3 Establishment of the relationship between strain and displacements

This involves finding the matrix B connecting the strain ε of the element to its nodal displacements U^{e}. This relationship is expressed by:

$$\{\varepsilon\} = BU^{e} \qquad \text{(III. 2)}$$

III.10.4 Establishment of the relationship between stresses and strains

For a linear elastic material, the stresses σ are functions linear strains ε. They are expressed by the expression:

$$\{\sigma\} = [D]\{\varepsilon\} \qquad \text{(III. 3)}$$

Where *[D]* is the elasticity matrix.

III.10.5 Calculation of elementary matrices

This step is the most important part of the problem. The displacements U^e at the nodes are determined in such a way that the constraints generated in the element balance the external loading F^e, that is to say that:

$$\overline{kU^e} = \overline{F^e} \qquad (III.4)$$

k^e is the stiffness matrix of the element expressed in the local reference frame. She is deduced from the deformation energy of the element and expressed by:

$$\overline{k^e} = \int_0^V B^T D B \, dv \qquad (III.5)$$

It is also necessary to calculate the mass matrix M^e of each element. This matrix is deduced from the kinetic energy of the element. In the local reference of the element, this matrix is given by the expression:

$$\overline{M^e} = \int_0^V \rho N^T \, N \, dv \qquad (III.6)$$

where ρ is the density of the material constituting the element. Finally, we express the matrices k^e, M^e, U^e and F^e in the global reference defined for the entire structure.

III.10.6 Assembly of elementary matrices

The assembly phase consists of constructing the matrices *K*, *M* and *F* of the complete structure from the elementary matrices k^e, M^e, U^e and F^e, expressed in the global benchmark, of the different elements by summing the energies of deformation and kinetics of each element.

When dealing with a beam structure, it's not feasible to directly combine matrices because they aren't formulated using identical variables. Instead, for every element, it's essential to identify the nodal variables' positions within the displacement vector encompassing all structure nodes. This process involves organizing the elementary matrix terms into a comprehensive matrix, the configuration of which hinges on the sequence used to define global variables.

III.11 Presentation of the problem

(x; y; and z) local landmark

(X, Y and Z) global landmark

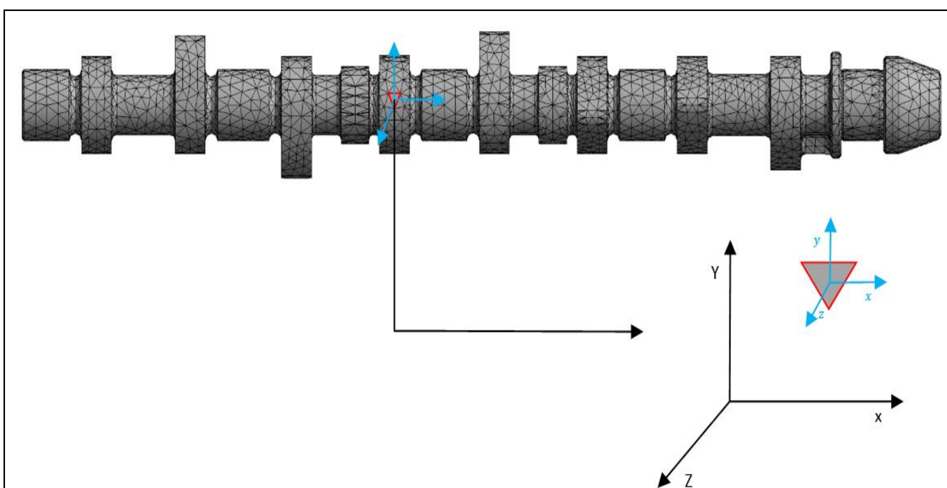

Figure III.4: *Local and global camshaft coordinate system.*

III.12 Working hypotheses

We made a choice Tetrahedron element Contains 3 knot (I.J. K) at six degrees of freedom at each node: three translations in (*Ux. Uy. Uz*) following *x, y, z,* and three rotations (θ_x, θ_y, θ_z) following *x, y, z.*

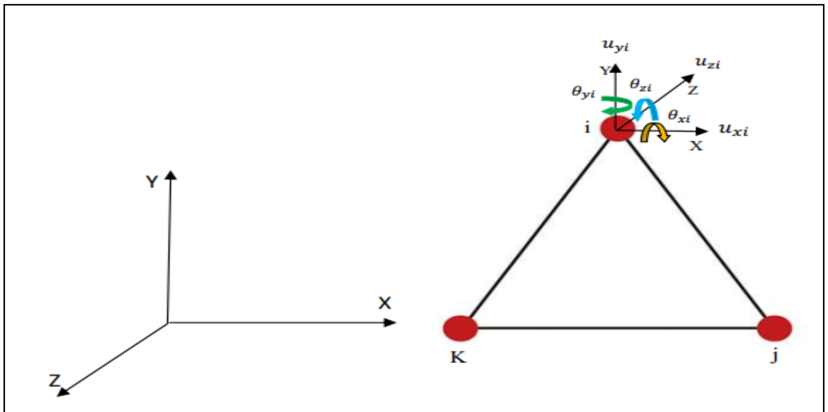

Figure III.5: *Degrees of freedom of camshaft element nodes.*

III.12.1 Shape function

The vector of nodal displacements is:

$$U = \left[\, u_{0xi}\ u_{0yi}\ u_{0zi}\ \theta_{xi}\ \theta_{yi}\ \theta_{zi}\ \ldots\ u_{0xp}\ u_{0yp}\ u_{0zp}\, \theta_{xp}\ \theta_{yp}\ \theta_{zp} \right]^T$$

$$\begin{bmatrix} u_{0x} \\ u_{0y} \\ u_{0z} \\ \theta_x \\ \theta_y \\ \theta_z \end{bmatrix} = \begin{bmatrix} N_i & 0 & 0 & 0 & 0 & 0 & N_j & 0 & 0 & 0 & 0 & 0 \ldots & N_p & 0 & 0 & 0 & 0 & 0 \\ 0 & N_i & 0 & 0 & 0 & 0 & 0 & N_j & 0 & 0 & 0 & 0 \ldots & 0 & N_p & 0 & 0 & 0 & 0 \\ 0 & 0 & N_i & 0 & 0 & 0 & 0 & 0 & N_j & 0 & 0 & 0 \ldots & 0 & 0 & N_p & 0 & 0 & 0 \\ 0 & 0 & 0 & N_i & 0 & 0 & 0 & 0 & 0 & N_j & 0 & 0 \ldots & 0 & 0 & 0 & N_p & 0 & 0 \\ 0 & 0 & 0 & 0 & N_i & 0 & 0 & 0 & 0 & 0 & N_j & 0 \ldots & 0 & 0 & 0 & 0 & N_p & 0 \\ 0 & 0 & 0 & 0 & 0 & N_i & 0 & 0 & 0 & 0 & 0 & N_j \ldots & 0 & 0 & 0 & 0 & 0 & N_p \end{bmatrix} *$$
$$\left[\, u_{0xi}\ u_{0yi}\ u_{0zi}\ \theta_{xi}\ \theta_{yi}\ \theta_{zi}\ \ldots\ u_{0xp}\ u_{0yp}\ u_{0zp}\, \theta_{xp}\ \theta_{yp}\ \theta_{zp} \right]^T \qquad (III.7)$$

With u_{0x} is a movement along the x axis, u_{0y} movement along y, u0z following movement the z axis, and θ_x , θ_y and θ_z rotations around the x, y and z axes respectively.

III.12.2 Determination of interpolation function Ni

The most efficient form for determining Ni is the Lagrange form:

$$u_{0x} = N_i\, u_{0xi} + N_j\, u_{0xj} + N_k\, u_{0xk} + N_l\, u_{0xl} + N_m\, u_{0xm} + N_n u_{0xn} + N_o\, u_{0xo} + N_p\, u_{0xp} \qquad (III.8)$$

$$u_{0y} = N_i\, u_{0yi} + N_j\, u_{0yj} + N_k\, u_{0yk} + N_l\, u_{0yl} + N_m\, u_{0ym} + N_n u_{0yn} + N_o\, u_{0yo} + N_p\, u_{0yp} \qquad (III.9)$$

$$u_{0z} = N_i\, u_{0zi} + N_j\, u_{0zj} + N_k\, u_{0zk} + N_l\, u_{0zl} + N_m\, u_{0zm} + N_n u_{0zn} + N_o\, u_{0zo} + N_p\, u_{0zp} \qquad (III.10)$$

$$\theta_x = \frac{\partial u_{0y}}{\partial z} = N_{i,z}\,\theta_{xi} + N_{j,z}\,\theta_{xj} + N_{k,z}\,\theta_{xk} + N_{l,z}\,\theta_{xl} + N_{m,z}\,\theta_{xm} + N_{n,z}\theta_{xn} + N_{o,z}\,\theta_{xo} + N_{p,z}\,\theta_{xp} \qquad (\text{III}.11)$$

$$\theta_y = \frac{\partial u_{0y}}{\partial y} = N_{i,y}\theta_{yi} + N_{j,y}\,\theta_{yj} + N_{k,y}\,\theta_{yk} + N_{l,y}\,\theta_{yl} + N_{m,y}\,\theta_{ym} + N_{n,y}\theta_{yn} + N_{o,y}\,\theta_{yo} + N_{p,y}\,\theta_{yp} \qquad (\text{III}.12)$$

$$\theta_z = \frac{\partial u_{0y}}{\partial x} = N_{i,x}\theta_{zi} + N_{j,x}\,\theta_{zj} + N_{k,x}\,\theta_{zk} + N_{l,yx}\,\theta_{zl} + N_{m,x}\,\theta_{zm} + N_{n,x}\theta_{zn} + N_{o,x}\,\theta_{zo} + N_{p,x}\,\theta_{zp} \qquad (\text{III}.13)$$

$$\begin{aligned} N_j &= L_{xi'}(x).L_{zi''}(z), & N_j &= L_{ji'}(x).L_{zi''}(z), \\ N_k &= L_{xk'}(x).L_{zi''}(z), & N_l &= L_{xk'}(x).L_{zj''}(z), \\ N_m &= L_{xk'}(x).L_{zk''}(z), & N_n &= L_{xi'}(x).L_{zk''}(z), \\ N_o &= L_{xi'}(x).L_{zk''}(z), & N_p &= L_{xi'}(x).L_{zj''}(z), \end{aligned} \qquad (\text{III}.14)$$

$$\begin{aligned} L_{xi'}(x) &= \tfrac{2x}{l^2}\left(\mathrm{x}-\tfrac{1}{2}\right)(\mathrm{x}-l), & L_{xj'}(x) &= \tfrac{2x}{l^2}\left(\mathrm{x}-\tfrac{1}{2}\right)(\mathrm{x}-l), \\ L_{xk'}(x) &= \tfrac{2x}{l^2}\left(x-\tfrac{1}{2}\right), & L_{zi''}(z) &= \tfrac{2x}{l^2}\left(z-\tfrac{1}{2}\right)(z-l), \\ L_{zj''}(x) &= \tfrac{2z}{l^2}(\mathrm{z}-l), & L_{zk''}(x) &= \tfrac{2z}{l^2}\left(\mathrm{z}-\frac{1}{2}\right), \end{aligned} \qquad (\text{III}.15)$$

The projections on the x axis using "the projections of the nodes on the z axis" and the Lagrange interpolation function

III.12.3 Movement Field

$$\theta_x\,(x,y,z) = -\frac{\partial u_{0y}}{\partial x} \qquad (\text{III}.16)$$

$$\theta_y\,(x,y,z) = -\frac{\partial u_{0y}}{\partial y} \qquad (\text{III}.17)$$

$$\theta_z\,(x,y,z) = -\frac{\partial u_{0y}}{\partial y} \qquad (\text{III}.18)$$

The field of movement is written:

$$u_x\,(x,y,z) = u_{0x}\,(x,z) - y\,\frac{\partial u_{0y}}{\partial x}\,(x,z) \qquad (\text{III}.19)$$

$$u_z\,(x,y,z) = u_{0z}\,(x,z) - y\,\frac{\partial u_{0y}}{\partial z}\,(x,z) \qquad (\text{III}.20)$$

$$u_y\,(x,y,z) = u_{0y}\,(x,z) \qquad (\text{III}.21)$$

III.12.4 The strain

The field of strain is written:

$$\varepsilon_{xx} = \frac{\partial u_{0x}}{\partial x} - y\frac{\partial^2 u_{0y}}{\partial x^2} \quad (III.22)$$

$$\varepsilon_{zz} = \frac{\partial u_{0z}}{\partial z} - y\frac{\partial^2 u_{0y}}{\partial z^2} \quad (III.23)$$

$$\varepsilon_{yy} = 0;\ \varepsilon_{yz} = 0;\ \varepsilon_{yx} = 0 \quad (III.24)$$

$$\varepsilon_{xz} = \left(\frac{\partial u_{0x}}{\partial z} - \frac{\partial u_{0z}}{\partial x}\right) - 2y\frac{\partial^2 u_{0y}}{\partial x \partial z} \quad (III.25)$$

The strain tensor:

$$\varepsilon = \begin{bmatrix} \varepsilon_{xx} & \varepsilon_{xz} & 0 \\ \varepsilon_{xz} & \varepsilon_{zz} & 0 \\ 0 & 0 & 0 \end{bmatrix} \quad (III.26)$$

The strain matrix is reduced to three non-zero components:

$$\varepsilon = \begin{bmatrix} \varepsilon_{xx} \\ \varepsilon_{zz} \\ k_{xz} \end{bmatrix} \quad (III.27)$$

The strain of a plane element is composed of two terms, one membrane and the other inflection like the following:

$$\{\varepsilon\} = \{\varepsilon^m\} + y\{k\} \Rightarrow \begin{Bmatrix} \varepsilon_{\text{xx}} \\ \varepsilon_{\text{zz}} \\ k_{\text{xz}} \end{Bmatrix} + \begin{Bmatrix} k_{\text{x}} \\ k_{\text{z}} \\ k_{\text{xz}} \end{Bmatrix} =$$

$$\begin{bmatrix} \frac{\partial}{\partial x} & 0 \\ 0 & \frac{\partial}{\partial z} \\ \frac{\partial}{\partial x} & \frac{\partial}{\partial z} \end{bmatrix} \begin{bmatrix} N_i & 0 & N_j & 0 & N_k & 0 & N_l & 0 & N_m & 0 & N_n & 0 & N_o & 0 & N_p & 0 \\ 0 & N_i & 0 & N_j & 0 & N_k & 0 & N_l & 0 & N_m & 0 & N_n & 0 & N_o & 0 & N_p \end{bmatrix} *$$

$$\begin{bmatrix} u_{0xi} & u_{0yi} & u_{0zi} & \theta_{xi} & \theta_{yi} & \theta_{zi} & \ldots & u_{0xp} & u_{0yp} & u_{0zp} & \theta_{xp} & \theta_{yp} & \theta_{zp} \end{bmatrix}^T +$$

$$\begin{bmatrix} \frac{\partial^2}{\partial x^2} \\ \frac{\partial^2 u_{0y}}{\partial z^2} \\ \frac{\partial^2}{\partial x \partial z} \end{bmatrix} \begin{bmatrix} N_i & N_j & N_k & N_l & N_m & N_n & N_o & N_p \end{bmatrix} \begin{bmatrix} u_{0yi} \\ u_{yi} \\ \vdots \\ u_{0yp} \end{bmatrix} \quad (III.28)$$

$$= \begin{bmatrix} \frac{\partial N_i}{\partial x} & 0 & \frac{\partial N_j}{\partial x} & \cdots & \frac{\partial N_o}{\partial x} & 0 & \frac{\partial N_p}{\partial x} & 0 \\ 0 & \frac{\partial N_i}{\partial x} & 0 & \cdots & 0 & \frac{\partial N_o}{\partial x} & 0 & \frac{\partial N_p}{\partial x} \\ \frac{\partial N_i}{\partial x} & \frac{\partial N_i}{\partial z} & \frac{\partial N_i}{\partial x} & \cdots & \frac{\partial N_o}{\partial x} & \frac{\partial N_o}{\partial z} & \frac{\partial N_p}{\partial x} & \frac{\partial N_p}{\partial z} \end{bmatrix} *$$

$$\begin{bmatrix} u_{0xi} & u_{0yi} & u_{0z} & \theta_{xi} & \theta_{yi} & \theta_{zi} & \ldots & u_{0xp} & u_{0yp} & u_{0zp} & \theta_{xp} & \theta_{yp} & \theta_{zp} \end{bmatrix}^T +$$

$$y \begin{bmatrix} \frac{\partial^2 N_i}{\partial x^2} & \frac{\partial^2 N_j}{\partial x^2} \cdots & \frac{\partial^2 N_p}{\partial x^2} \\ \frac{\partial^2 N_i}{\partial z^2} & \frac{\partial^2 N_j}{\partial z^2} \cdots & \frac{\partial^2 N_p}{\partial z^2} \\ \frac{\partial^2 N_i}{\partial x \partial z} & \frac{\partial^2 N_j}{\partial x \partial z} \cdots & \frac{\partial^2 N_p}{\partial x \partial z} \end{bmatrix} \begin{bmatrix} u_{0y} \\ u_{yj} \\ \vdots \\ u_{0yp} \end{bmatrix} \quad \text{(III. 29)}$$

$$[B_m] = \begin{bmatrix} \frac{\partial N_i}{\partial x} & 0 & \frac{\partial N_j}{\partial x} & \cdots & \frac{\partial N_o}{\partial x} & 0 & \frac{\partial N_p}{\partial x} & 0 \\ 0 & \frac{\partial N_i}{\partial z} & 0 & \cdots & 0 & \frac{\partial N_o}{\partial z} & 0 & \frac{\partial N_p}{\partial z} \\ \frac{\partial N_i}{\partial x} & \frac{\partial N_i}{\partial z} & \frac{\partial N_j}{\partial x} & \cdots & \frac{\partial N_o}{\partial x} & \frac{\partial N_o}{\partial z} & \frac{\partial N_p}{\partial x} & \frac{\partial N_p}{\partial z} \end{bmatrix} \quad \text{(III. 30)}$$

$$[B_f] = y \begin{bmatrix} \frac{\partial^2 N_i}{\partial x^2} & \frac{\partial^2 N_j}{\partial x^2} & \cdots & \frac{\partial^2 N_p}{\partial x^2} \\ \frac{\partial^2 N_i}{\partial z^2} & \frac{\partial^2 N_j}{\partial z^2} & \cdots & \frac{\partial^2 N_p}{\partial z^2} \\ \frac{\partial^2 N_i}{\partial x \partial z} & \frac{\partial^2 N_j}{\partial x \partial z} & \cdots & \frac{\partial^2 N_p}{\partial x \partial z} \end{bmatrix} \quad \text{(III. 31)}$$

III.12.5 Field of stress

The stress field of a layer of laminates is given by the following relation:

$$\begin{bmatrix} \sigma_{xx} \\ \sigma_{zz} \\ \sigma_{xz} \end{bmatrix}_k = \begin{bmatrix} \varrho'_{11} & \varrho'_{12} & \varrho'_{13} \\ \varrho'_{21} & \varrho'_{22} & \varrho'_{23} \\ \varrho'_{31} & \varrho'_{32} & \varrho'_{33} \end{bmatrix}_k \begin{bmatrix} \varepsilon_{xx}{}^m \\ \varepsilon_{zz}{}^m \\ \varepsilon_{xz}{}^m \end{bmatrix} + y \begin{bmatrix} \varrho'_{11} & \varrho'_{12} & \varrho'_{13} \\ \varrho'_{21} & \varrho'_{22} & \varrho'_{23} \\ \varrho'_{31} & \varrho'_{32} & \varrho'_{33} \end{bmatrix}_k \begin{bmatrix} k_x \\ k_z \\ k_{xz} \end{bmatrix}, \quad \text{(III. 32)}$$

$$\varrho'_{ij} = C'_{ij-} \frac{c'_{i3} \; c'_{j3}}{c'_{33}} \quad \text{(III. 33)}$$

Such that it is the contents of the main horse stiffness

The membrane results, in a laminate given by:

$$N(x,z) = \sum_{k=1}^{n} \int_{nk-1}^{nk} \left[\left(\varrho'_k \varepsilon^m \, (x,z) \; + \; y \varrho'_k k(x,z) \right) \right] dy, \quad \text{(III. 34)}$$

Or by integrating in the thickness:

$$N(x,z) = \left[A_{ij}\right] \varepsilon^m(x,z) + \left[B_{ij}\right] k(x,z) \quad \text{(III. 35)}$$

Where:

$$= \sum_{k=1}^{n} \ (h_k - h_{k-1})\varrho'_k \tag{III.36}$$

$$A_{ij} = \sum_{k=1}^{n} \ (h_k - h_{k-1})(\varrho'_{ij})_k \tag{III.37}$$

And

$$B = \sum_{k=1}^{n} \ \frac{1}{2}(k^2{}_k - k^2{}_{k-1})\varrho'_k \tag{III.38}$$

$$B_{ij} = \frac{1}{2}\sum_{k=1}^{n} \ (h^2{}_k - h^2{}_{k-1})(\varrho'_{ij})_{k'} \tag{III.39}$$

$$B = [B_{ij}] with\ B_{ij} = \frac{1}{2}\sum_{k=1}^{n} \ (h^2{}_k - h^2{}_{k-1})(\varrho'_{ij})_{k'} = \sum_{k=1}^{n} \ (\varrho'_{ij})_k e_k z_k \tag{III.40}$$

The expanded expression of the membrane resultants is therefore written:

$$\begin{bmatrix} N_x \\ N_z \\ N_{xz} \end{bmatrix} = \begin{bmatrix} A_{11} & A_{12} & A_{13} \\ A_{12} & A_{22} & A_{23} \\ A_{13} & A_{32} & A_{33} \end{bmatrix} \begin{bmatrix} \varepsilon\ {}^m_{xx} \\ \varepsilon\ {}^m_{zz} \\ \gamma\ {}^m_{xz} \end{bmatrix} + \begin{bmatrix} B_{11} & B_{12} & B_{13} \\ B_{12} & B_{22} & B_{23} \\ B_{13} & B_{32} & B_{33} \end{bmatrix} \begin{bmatrix} k_x \\ k_z \\ k_{xz} \end{bmatrix} \tag{III.41}$$

Bending and torsion moments:

$$M(x,z) = \sum_{k=1}^{n} \int_{nk-1}^{nk} \left[\left(y\varrho'_k \varepsilon^m\ (x,z)\ +\ y^2 \varrho'_k k(x,z) \right) \right] dy, \tag{III.42}$$

$$M(x,z) = [B_{ij}]\varepsilon^m\ (x,z) + [B_{ij}]k(x,z) \tag{III.43}$$

$$D = \sum_{k=1}^{n} \ \frac{1}{3}\left(h^3{}_k - h^3{}_{k-1}\right)\varrho'_K \tag{III.44}$$

$$D = [D_{ij}] with\ D_{ij} = \sum_{k=1}^{n} \ \frac{1}{3}(h^3{}_k - h^3{}_{k-1})(\varrho'_{ij})_{k'} = \sum_{k=1}^{n} \ \left(e_k z_k^2 + \frac{e_k^3}{12}\right)_k \tag{III.45}$$

The expanded expression of moments is written in the form:

$$\begin{bmatrix} M_x \\ M_z \\ M_{xz} \end{bmatrix} = \begin{bmatrix} B_{11} & B_{12} & B_{13} \\ B_{12} & B_{22} & B_{23} \\ B_{13} & B_{32} & B_{33} \end{bmatrix} \begin{bmatrix} \varepsilon\ {}^m_{xx} \\ \varepsilon\ {}^m_{zz} \\ \gamma\ {}^m_{xz} \end{bmatrix} + \begin{bmatrix} D_{11} & D_{12} & D_{13} \\ D_{12} & D_{22} & D_{23} \\ D_{13} & D_{32} & D_{33} \end{bmatrix} \begin{bmatrix} k_x \\ k_z \\ k_{xz} \end{bmatrix} \tag{III.46}$$

The constitutive equation of a laminated plate is:

$$\begin{bmatrix} N \\ M \end{bmatrix} = \begin{bmatrix} A & B \\ B & D \end{bmatrix} \begin{bmatrix} \varepsilon^m \\ k \end{bmatrix} \tag{III.47}$$

$$\begin{bmatrix} N \\ M \end{bmatrix} = \begin{bmatrix} A & B \\ B & D \end{bmatrix} \begin{bmatrix} B_m & 0 \\ 0 & B_f \end{bmatrix} [q] \tag{III.48}$$

III.12.6 strain energy

The total strain energy of a solid is written in the following form:

$$U_e = \iiint \left(\frac{1}{2} C_{ijkl}\varepsilon_{ij}\varepsilon_{kl} - \sigma_{ij}^m \varepsilon_{ij}\right) dV - \iiint f_i^v \, u_i \; dV - \iiint f_i^s \, u_i \; dS \qquad \text{(III. 49)}$$

Where V and S are respectively the volume and the exterior surface of the element.
This expression can be written in matrix form [61].

$$U_e = \iiint \left(\frac{1}{2} \begin{Bmatrix} \varepsilon^m \\ k \end{Bmatrix}^t \begin{bmatrix} A & B \\ B & D \end{bmatrix} \begin{Bmatrix} \varepsilon^m \\ k \end{Bmatrix} \right) dV - \iiint \{u\}^t \{f^v\} \, dV - \iint \{u\}^t \, \{f^e\} \, dS \qquad \text{(III. 50)}$$

The virtual variation of the displacement field $\{\delta u\}$ gives:

$$\delta U_e = \iiint \left(\frac{1}{2} \begin{Bmatrix} \delta\varepsilon^m \\ \delta k \end{Bmatrix}^t \begin{bmatrix} A & B \\ B & D \end{bmatrix} \begin{Bmatrix} \delta\varepsilon^m \\ \delta k \end{Bmatrix} \right) dV - \iiint \{\delta u\}^t \{f^v\} \, dV - \iint \{\delta u\}^t \, \{f^e\} \, dS \qquad \text{(III. 51)}$$

The discretization of this expression:

$$U_e = \iiint \left(\{\delta q_e\}^t \begin{bmatrix} B_m & 0 \\ 0 & B_f \end{bmatrix}^t \begin{bmatrix} A & B \\ B & D \end{bmatrix} \begin{bmatrix} B_m & 0 \\ 0 & B_f \end{bmatrix} \{q_e\} \right) dV - \iiint \{\delta q_e\}^t \, [N]^t \{f^v\} \, dV \; - \iint [N]^t \, \{f^s\} \; dS \qquad \text{(III. 52)}$$

For any stable system, the stationarity of the potential energy leads to:
$\Pi = 0$ we can simplify the expression above to obtain:

$$\iiint \left(\{\delta q_e\}^t \begin{bmatrix} B_m & 0 \\ 0 & B_f \end{bmatrix}^t \begin{bmatrix} A & B \\ B & D \end{bmatrix} \begin{bmatrix} B_m & 0 \\ 0 & B_f \end{bmatrix} \{q_e\} \right) dV = - \iiint \{\delta q_e\}^t \, [N]^t \{f^v\} \; dV - \iint [N]^t \, \{f^s\} \; dS \qquad \text{(III. 53)}$$

The expression above completely defines the behavior of an element by a system of linear equations in the form:

$$[k_e]\{q_e\} = \{F_e\} \qquad \text{(III. 54)}$$

Where$[k_e]$ is the stiffness matrix of the element, $\{q_e\}$ is the vector of nodal displacements.

So, the elementary stiffness matrix is:

$$[k_e] = \iiint [B_m]^T \, [A][B_m] + [B_m]^T [B][B_f] + [B_f]^T [D][B_f] \, dV \qquad \text{(III. 55)}$$

III.12.7 The kinetic energy

The kinetic energy of the system is written in the following form:

$$T = \frac{1}{2} \iiint \rho V^2 \, dV \qquad \text{(III. 56)}$$

$$E_c = \frac{1}{2} \iiint \rho \left[\left(\frac{\partial u_x}{\partial t}\right)^2 + \left(\frac{\partial u_y}{\partial t}\right)^2 + \left(\frac{\partial u_z}{\partial t}\right)^2 \right] dx \, dy \, dz \qquad \text{(III. 57)}$$

$$T = \frac{1}{2}\iiint \rho[\dot{q}]^t[N]^t\,[N][\dot{q}]\,dV \qquad (\text{III}.58)$$

$$[M_e] = \frac{1}{2}\iiint \rho[N]^t[N]\,dV \qquad (\text{III}.59)$$

$[M]_e$: Elementary mass matrix.

III.12.8 System of equations

Obtaining the system of equations will be done classically by applying the Principle of Hamilton. Hamilton's principle is the basis of the energy study of dynamic systems. The total energy of the system is the sum of the potential energy and the kinetic energy[62].

$$\Pi = U + T \qquad (\text{III}.60)$$

If $\{\delta u\}$ is a kinematically admissible virtual field such that $\{\delta u\}(t_1) = 0$ and $\{\delta u\}(t_2) = 0$, the total energy of the system is stationary, that is mean:

$$\delta\Pi(t) = 0 \qquad (\text{III}.61)$$

$$\delta\int_{t_1}^{t_2}\Pi(t)\,dt = 0 \qquad (\text{III}.62)$$

III.12.9 Finite element discretization

We pose the hypothesis of separation between the spatial and temporal evolution of the fields:

$$u(x,y,z) = \sum_{i=1}^{n_e} N_i\,(x,y)u_i(t) \qquad (\text{III}.63)$$

So

$$\{u\} = [N]\{q_e\} \qquad (\text{III}.64)$$

$$\{\dot{u}\} = [N]\{\dot{q_e}\} \qquad (\text{III}.65)$$

$$\{\ddot{u}\} = [N]\{\ddot{q_e}\} \qquad (\text{III}.66)$$

The discretization of Hamilton's principle gives:

$$\{\delta q_e\}^t\int_v\Big([B_m]^T[A][B_m] + [B_m]^T[B][B_f] + [B_f]^T[B][B_m] + [B_f]^T[D][B_f] + \rho[N]^T[N][\ddot{q}] - [N]^T\{f^u\}\Big)dV - \{\delta q_e\} = 0 \qquad (\text{III}.67)$$

The general system of equations is:

$$[M_e]\{\ddot{q_e}\} + [k_e]\{q_e\} = \{f_e\} \qquad (\text{III}.68)$$

With

$$[M_e] = \int_{Ve}\rho[N]^t\,[N]dV \qquad (\text{III}.69)$$

$$[k_e] = \iiint [B_m]^T\,[A][B_m] + [B_m]^T[B][B_f] + [B_f]^T[B][B_m] + [B_f]^T[D][B_f]dV \qquad (\text{III}.70)$$

$$\{f_e\} = \int_{Ve} \rho[N]^t \left[f^u\right] dV + \int_{Se} \rho[N]^t \left[f^u\right] dV \quad \text{(III.71)}$$

$[M_e]$ is the mass matrix of the element, $[k_e]$ is the stiffness matrix and $\{f_e\}$ is the vector nodal forces in the local reference frame.

The matrices$[M_e]_g\,[k_e]_g$the vectors $\left\{f_e\right\}_g et\ \{q_e\}_g$in the global frame are:

$$[k_e^m]_g = [T_e^m]^t [k_e^m]_l [T_e^m]$$

$$[M]_g = [T_e^m]^t [M_e^m]_l [T_e^m]$$

$$\{q_e^m\}_g = [T_e^m]^t \{q_e^m\}_l$$

$$\{F_e^m\}_g = [T_e^m]^t \{F_e^m\}_l$$

With g indicating the global benchmark. The passage matrix is written:

$$[T] = \begin{bmatrix} [t^m] & 0 & 0 \\ 0 & [t^m] & 0 \\ 0 & 0 & [t^m] \end{bmatrix}$$

With

$$[t^m] = \begin{bmatrix} \cos(x, \mathrm{x}) & \cos(x, Y) & \cos(x, \mathrm{Z}) \\ \cos(z, \mathrm{x}) & \cos(z, Y) & \cos(z, \mathrm{Z}) \end{bmatrix}$$

III.12.10 solution Equations

To solve the equation of motion we use the superposition method. The basic principle is that the response of the blade is the combination of different modes clean of vibration. The contribution of each mode is given by a factor direct amplitude.

$$\{q\} = Y_1\{\Phi_1\} + Y_2\{\Phi_2\} + \cdots + Y_n\{\Phi_n\} \quad \text{(III.72)}$$

With Y_i amplitude of the mode and $\{\Phi_i\}$the eigenvector of the same mode. We can write:

$$\{q\} = [\boldsymbol{\Phi}]\{Y\} \quad \text{(III.73)}$$

With

$$\{\boldsymbol{\Phi}\} = [\{\Phi_1\}\{\Phi_2\} \ldots \ldots \ldots \{\Phi_n\}]$$

$$\{Y\}^t = [Y_1\ Y_2\ \ldots \ldots \ldots\ Y_n] \quad \text{(III.74)}$$

The equation of motion of the blade:

$$[M]\{\ddot{q}\} + [k]\{q\} = \{F\} \quad \text{(III.75)}$$

also, it can be written in this form:

$$[M]\Phi\{\ddot{Y}\} + [k][\Phi]\{Y\} = \{F\} \quad \text{(III.76)}$$

This expression is multiplied by the eigenvector of mode i

$$\{\Phi_i\}^t[M][\Phi]\{\ddot{Y}\} + \{\Phi_i\}^t[M][\Phi]\{Y\} = \{\Phi_i\}^t\{F\} \qquad (III.77)$$

Or

$$\widehat{m}_i\ddot{Y}_l + \widehat{k}_iY_l = F_i \qquad (III.78)$$

$$\widehat{m}_i = \{\Phi_i\}^t[M][\Phi_i]$$

$$k_i = \{\Phi_i\}^t[k][\Phi_i] \qquad (III.79)$$

It is therefore sufficient to solve separation each of these equations to determine the amplitude associated $Y_i(t)$

III.12.11 Resolution procedure

The procedure is as follows:

1. evaluated the matrix and $[M]$ and $[k]$.
2. evaluate the natural frequencies of the system: $|[M] - \omega^2[k]| = 0$
   We deduce and $\{\Phi_i\}$.
3. for each mode i.
   a) Calculate $\widehat{m}_i \ and \ f_i$.
   b) solve the mode equation: $\ddot{y}_l + \omega^2 y_i = f_i \,/\, \widehat{m}_i$.
4. Determine the structural response

$$\{ q(t)\} = [\Phi]\{Y(t)\}$$

III.13 Conclusion

This chapter demonstrates the modeling of the camshaft model using the finite element approach. This method is the most appropriate to model real systems or solid structures because it is more precise and allows us to study all of the camshaft's vibration modes. It is also modular because each camshaft mode has unique characteristics. and its description in 3D. The distribution of the mesh is also crucial and depends on the nature of the problem's dimensions. As a result, the user has the ability to add or delete elements at will and adjust stiffness, damping, and external forces at each node.

chapter IV：

Numerical simulation of distribution system

IV.1 introduction

the numerical simulation within the engine is among the most dependable methods for studying the diverse occurrences throughout the combustion process. Its transformative impact on the design, testing, and enhancement of automobiles cannot be overstated. This innovation has ushered in a new era wherein engineers can utilize virtual environments to simulate and scrutinize intricate systems, components, and procedures. Such simulations offer numerous advantages throughout the development stage, encompassing enhanced design, the selection of suitable materials for components, and the assessment of durability.

In this chapter, we simulated the camshaft for a diesel engine (**13511-64071**) which is made with **Gray Cast Iron**, this chapter is divided into two stages in which we used two modeling software. The first stage, in which we modeled the camshaft using the **SolidWorks** software. As for the second stage, we analyzed the camshaft model using the **ANSYS** software. This two software are considered among the most famous calculation programs that rely on the finite element method. Our investigation involved two distinct types of analysis at the ANSYS software level:

- Modal analysis.
- static analysis.

IV.2 Presentation of SolidWorks software

IV.2.1 Definition of SolidWorks

SolidWorks is a powerful computer-aided design (CAD) software used for creating 3D models, simulations, and technical drawings. It's widely utilized by engineers, designers, and architects to design and visualize products and structures before they are manufactured or built. It offers a user-friendly interface with a wide range of tools for modeling, assembly design, sheet metal design, rendering, and simulation. It's known for its parametric modeling capabilities. SolidWorks is commonly used in industries such as aerospace, automotive, manufacturing, and consumer goods.

IV.2.2 Geometric construction of the distribution system

As we mentioned in the second chapter, the two most important parts of the distribution system are the camshaft and the valves along with their parts such as the spring. We will limit the engineering construction process only to the camshaft, taking its necessary dimensions into account. We chose the camshaft to perform the numerical simulation on it because it is the primary controller for opening and closing the valves and it also directly affects the performance and efficiency of the distribution.

IV.2.3 System of units used

We will work in the system of units **“**millimeter, gram, second**”**.

IV.2.4 Camshaft construction

Before to starting the engineering construction of the camshaft, the process will be segmented into several sequential stages. These stages outline the methodology employed in the program for camshaft creation, and they are delineated as follows:

IV.2.4.1 The first camshaft support (Bearing Journal)

a) <u>Construction the 2D Bearing Journal shape:</u>

- We will create a circle with a diameter of 28 mm ***Figure IV.1*** shows the operation we performed on the program.

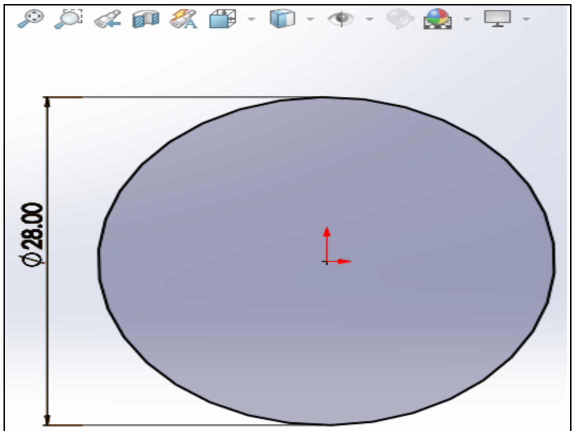

Figure IV.1: *Step of construction a 2D shape of the Bearing Journal.*

b) <u>Construction the 3D Bearing Journal shape:</u>

- We will now create a 28 mm thick volumetric model of the previously defined face around it from the Z axis Figure IV.2 shows the shapes obtained after adding the thickness value.

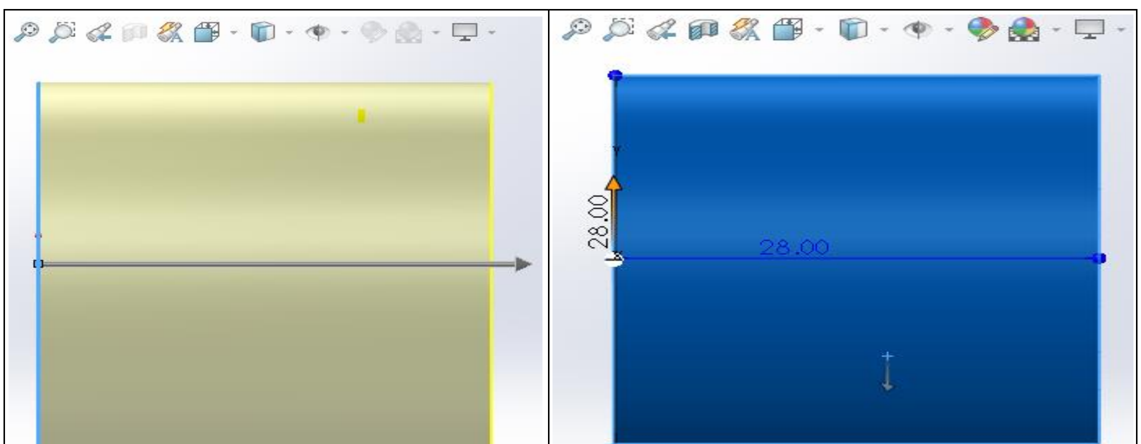

Figure IV.2: *Step of construction a 3D shape of the piston.*

IV.2.4.2 The first cam lobe

a) Construction the 2D cam lobe shape:

- To Construct the 2D cam lobe shape, we will draw three circles help to draw the shape of the cam lobe. where the first circle (Base circle) will have the same center as the landmark, with a diameter of 38 mm. The second circle will have a diameter of 10 mm and its center will be 23.5 mm away from the center of the landmark. As for the last circle, its diameter will be 80 mm. After that, the center of the landmark will not be specified because it is not among the conditions for Construct the cam lobe, The result obtained by drawing three circles is shown in ***Figure IV.3***:

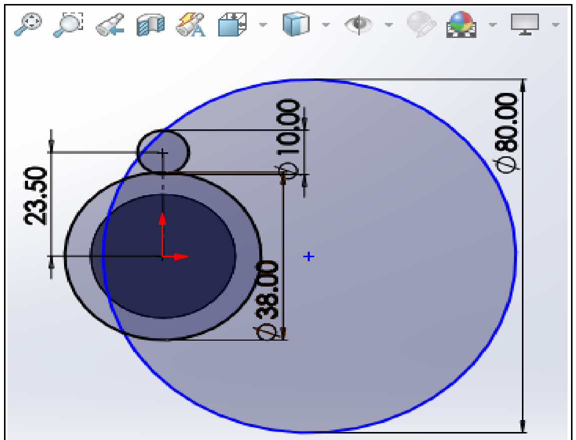

Figure IV.3: *Draw the three circles formed for cam lobe shape.*

- After creating the circles, we will make the circle with a diameter of 80 mm in a tangential relationship with the Base circle. Then we will do the same process with the circle with a diameter of 10 mm, where we will put it in a tangential relationship with the circle with a diameter of 80 mm ***Figure IV.4*** shows the process undertaken at this stage.

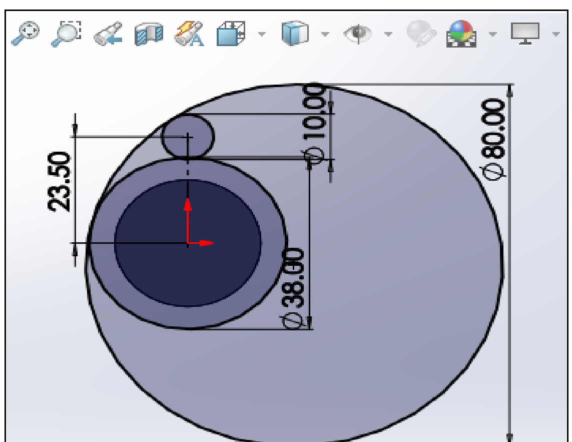

Figure IV.4: *The three circles after making them tangent to each other.*

- After making the circles tangential to each other, we will now cut the excess edges of the circle with a diameter of 80 mm .Then we will create an analogue for the remaining arc of the circle with a diameter of 80 mm. Then we cut the excess edges of the Base circle These processes are explained in ***Figure IV.5*** :

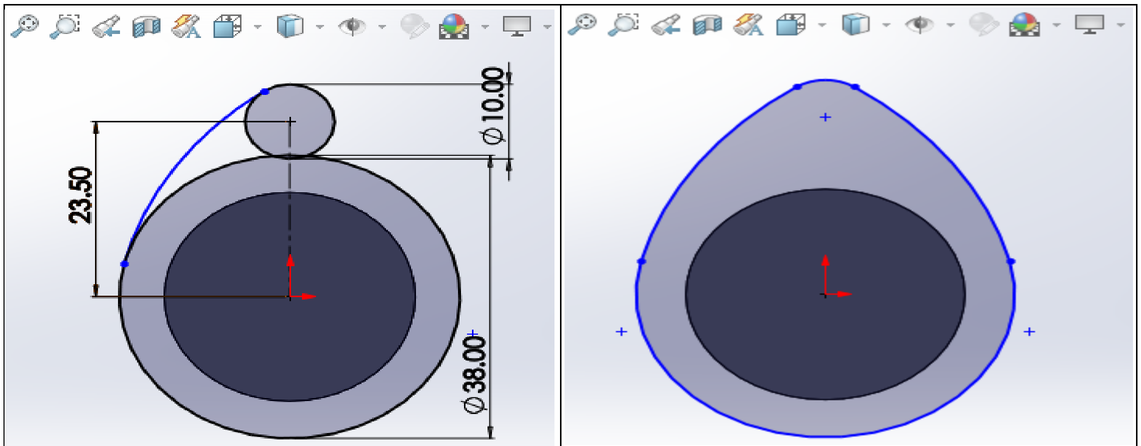

Figure IV.5: *The process of cutting and constructing the remaining arch's symmetry.*

b) Construction the 3D cam lobe shape:

- Now that we have completed the basic shape of the cam lobe, we will now create a 14 mm thick volumetric model of the previously defined face around it. From Z axis.

- After that, we will draw the connecting piece between the first and the second cam lob, which has a diameter of 23 mm and a thickness of 30 mm, which we placed directly because the steps for drawing it are the same as those we adopted to draw the Bearing Journal, which shows the resulting shape .***Figure IV.6*** shows the initial and final shapes obtained.

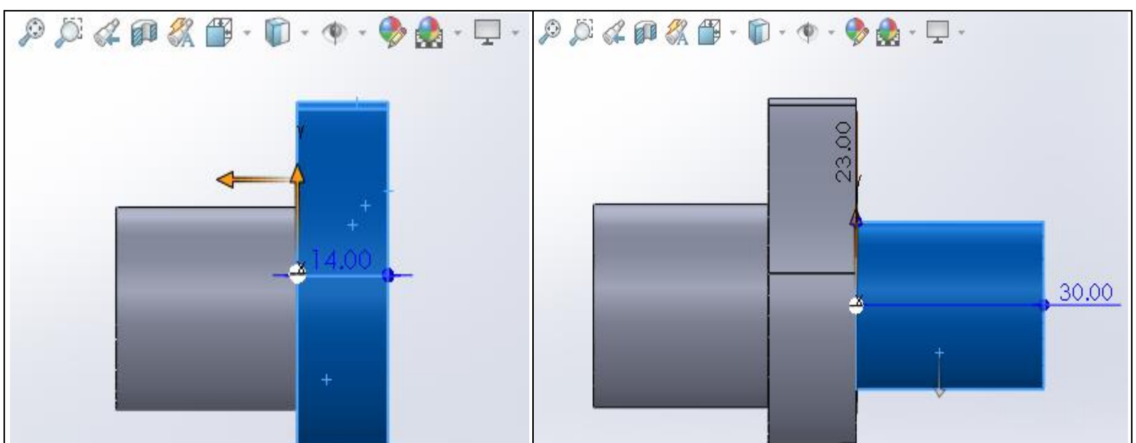

Figure IV.6: *Step of construction a 3D shape of the cam lobe and the connecting piece.*

IV.2.4.3 The second cam lobe

a) Construction the 2D cam lobe shape:

- because all the cam lobes have the same dimensions and differ only in degrees of deviation and also the deviation in relation to the center of the landmark, then we can rely on (convert entities) feature present in the program, which enables us to re-take the first cam lobe without having to redraw it.
- We will make the second cam deviate 110° (degrees) in the positive direction (counterclockwise) from the position of the first cam. ***Figure IV.7*** shows this procedure.

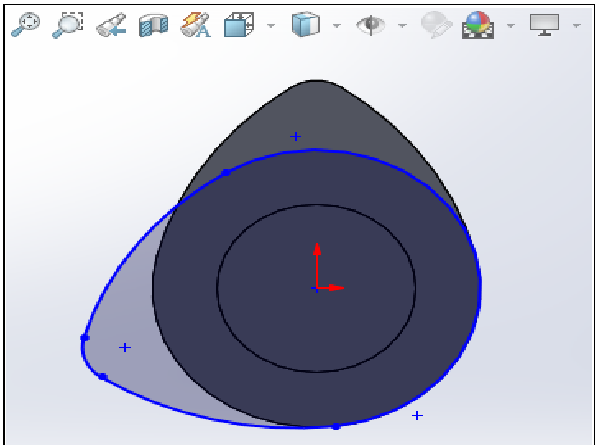

Figure IV.7: *Step of construction a 2D shape of the second cam lobe.*

b) Construction the 3D cam lobe shape:

- After we have drawn the second cam lobe, we will now create a volumetric model of the cam with a thickness of 14 mm on Z axis.
- And after creating the second cam lobe, in order to speed up the process, we will create the second Bearing Journal, which has the same diameter as the first one, 28 mm, and a residual thickness of 36 mm ***Figure IV.8*** shows the initial and final shapes obtained

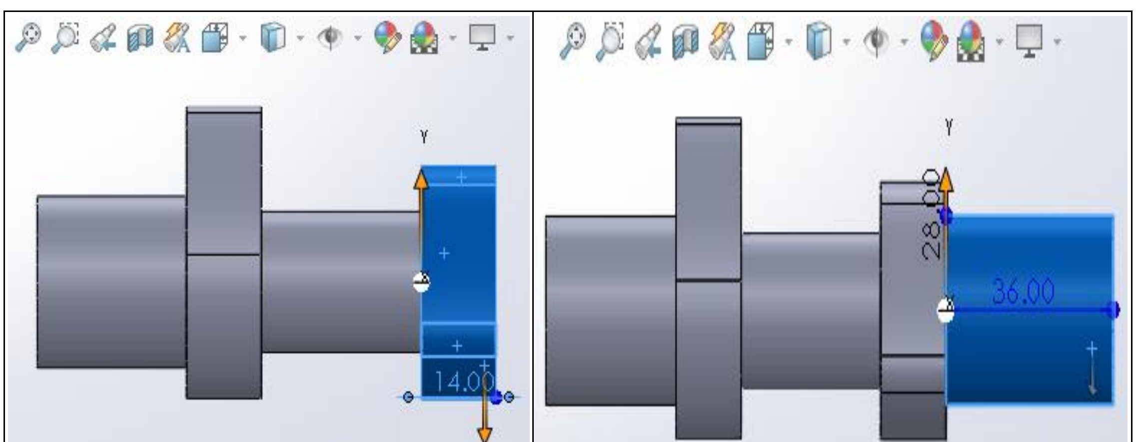

Figure IV.8: *Step of construction a 3D shape of the second cam lobe and Bearing Journal.*

IV.2.4.4 The third cam lobe

a) Construction the 2D cam lobe shape:

- To draw the third cam, we will use the same feature as before (convert entities), but this time the deviation will be -90° degrees (same as clockwise) from the first cam.

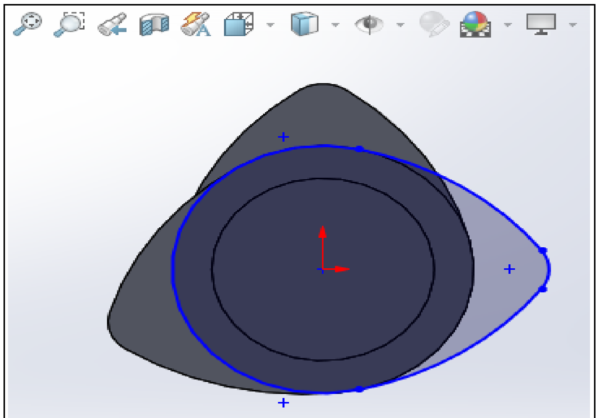

Figure IV.9: *Step of construction a 2D shape of the third cam lobe.*

b) Construction the 3D cam lobe shape:

- After we have drawn the second cam lobe, we will now create a volumetric model of the cam with a thickness of 14 mm on Z axis.
- And after that, we will draw the connecting piece between the third cam lob and the third Bearing Journal, which has a diameter of 23 mm and a thickness of 14 mm, and its center will be at a height of 5 mm from the center.
- After that shortcut, we will create the third Bearing Journal with a diameter of 30 mm and its center at a height of 6.5 mm from the center of the landmark and a thickness of 13 mm. Immediately after that, we will make another piece that connects to the following cam, with a diameter of 23 mm and a thickness of 5 mm.

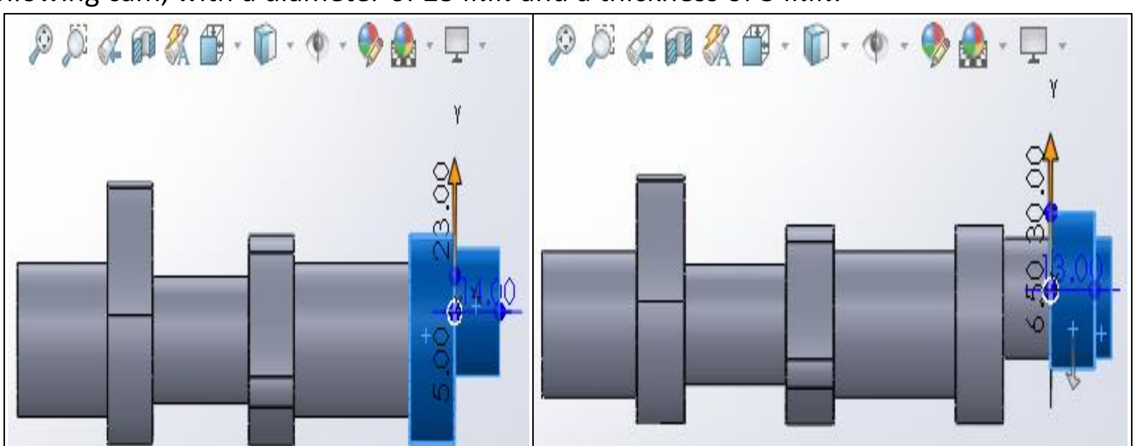

Figure IV.10: *Step of construction a 3D shape of the third cam lobe and Bearing Journal.*

IV.2.4.5 The fourth cam lobe

a) Construction the 2D cam lobe shape:

- To draw the fourth cam, we will use the same feature as before (convert entities), but this time the deviation will be 25° degrees (counterclockwise) from the first cam.

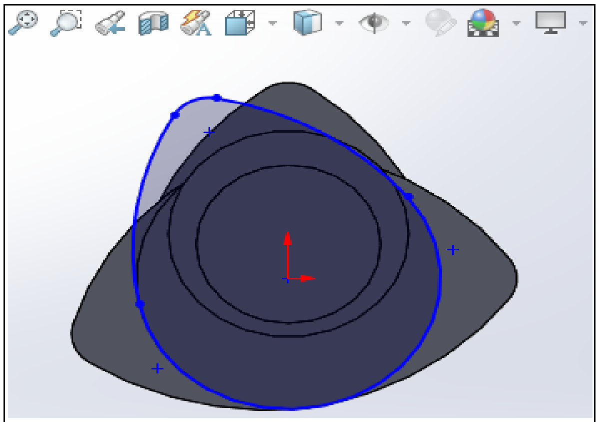

Figure IV.11: *Step of construction a 2D shape of the fourth cam lobe.*

b) Construction the 3D cam lobe shape:

- After we have drawn the fourth cam lobe, we will now create a volumetric model of the cam with a thickness of 14 mm on Z axis.
- And after, we will create the fourth Bearing Journal, which has diameter, 28 mm, and a residual thickness of 33 mm ***Figure IV.12*** shows the initial and final shapes obtained.

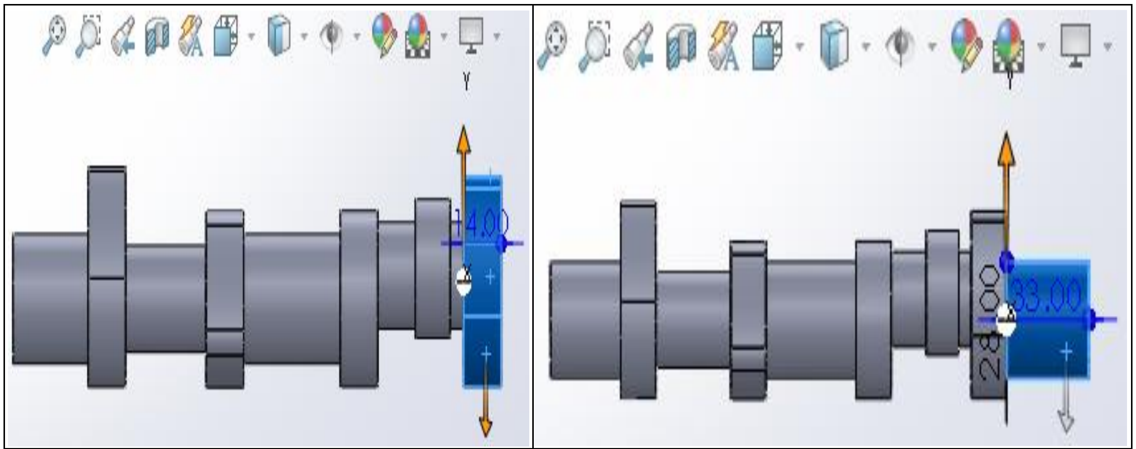

Figure IV.12: *Step of construction a 3D shape of the fourth cam lobe and Bearing Journal.*

IV.2.4.6 The fifth cam lobe

a) Construction the 2D cam lobe shape:

- To draw the fifth cam, we will use the same feature as before (convert entities), but this time the deviation will be 90° degrees (counterclockwise) from the first cam.

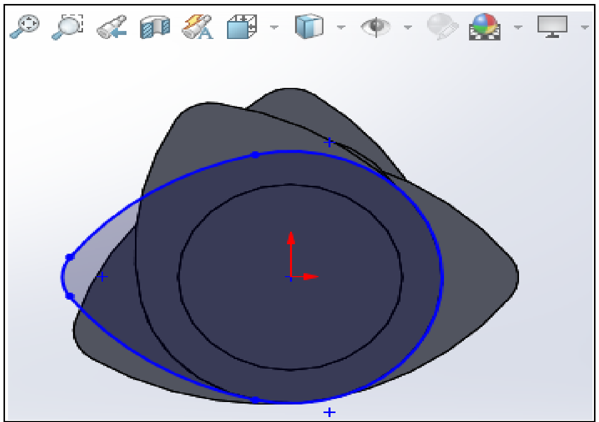

Figure IV.13: *Step of construction a 2D shape of the fifth cam lobe.*

b) Construction the 3D cam lobe shape:

- After we have drawn the fourth cam lobe, we will now create a volumetric model of the cam with a thickness of 14 mm on Z axis.
- And after that, we will draw the connecting piece between the fifth cam lob and the fifth Bearing Journal, which has a diameter of 23 mm and a thickness of 14 mm, and Its center will be 5 mm lower than the center of the landmark.
- After that we will create the fifth Bearing Journal with a diameter of 30 mm and Its center is 6.5 mm lower than the center of the landmark and a thickness of 13 mm. Immediately after that, we will make another piece that connects to the following cam, with a diameter of 23 mm and a thickness of 5 mm ***Figure IV.14*** shows this procedure.

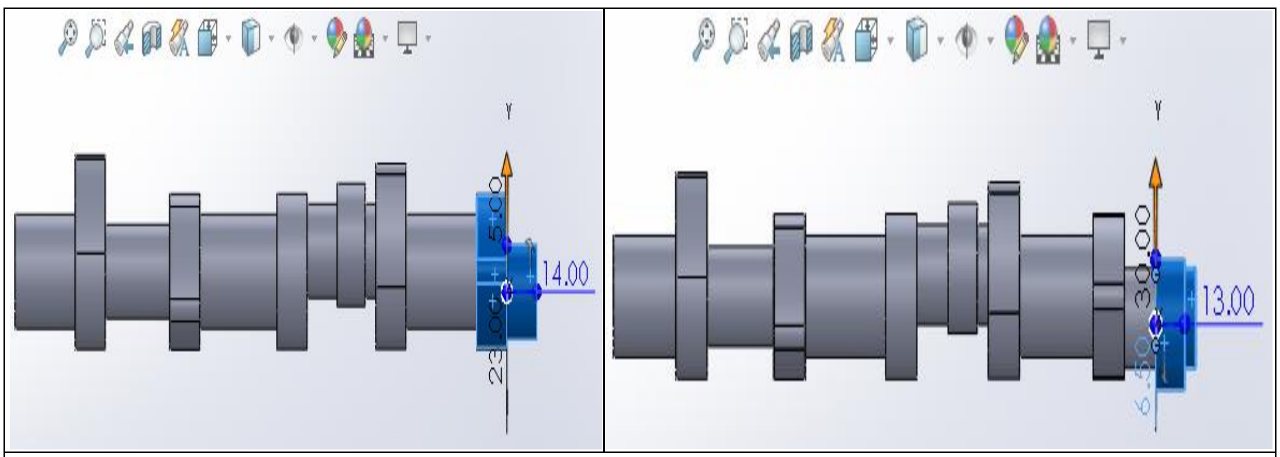

Figure IV.14 : *Step of construction a 3D shape of the fifth cam lobe and Bearing Journal.*

IV.2.4.7 the sixth cam lobe

a) **Construction the 2D cam lobe shape:**

- To draw the sixth cam, we will use the same feature as before (convert entities), but this time the deviation will be 190° degrees (counterclockwise) from the first cam.

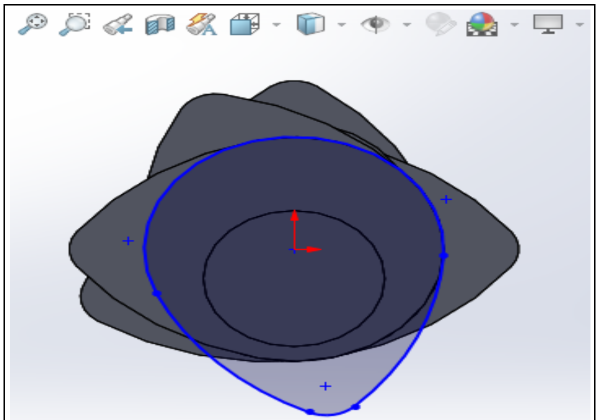

Figure IV.15: *Step of construction a 2D shape of the sixth cam lobe.*

b) **Construction the 3D cam lobe shape:**

- After we have drawn the sixth cam lobe, we will now create a volumetric model of the cam with a thickness of 14 mm on Z axis.
- And after creating the sixth cam lobe, we will also create the sixth Bearing Journal, which has the same diameter as the first one, 28 mm, and a residual thickness of 33 mm ***Figure IV.16*** shows the initial and final shapes obtained.

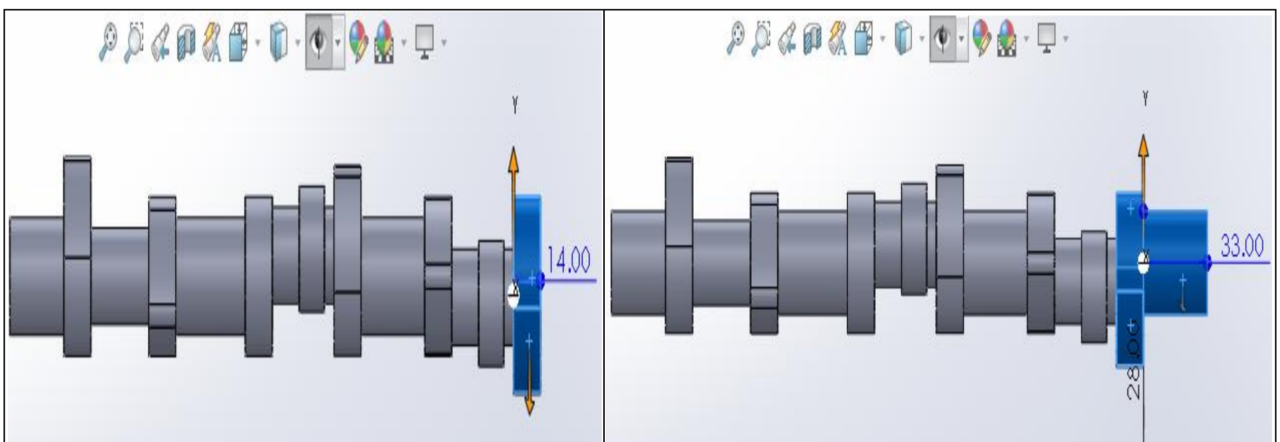

Figure IV.16: *Step of construction a 3D shape of the sixth cam lobe and Bearing Journal.*

IV.2.4.8 The seventh cam lob

a) Construction the 2D cam lobe shape:

- To draw the sixth cam, we will use the same feature as before (convert entities), but this time the deviation will be 180° degrees (counterclockwise) from the first cam.

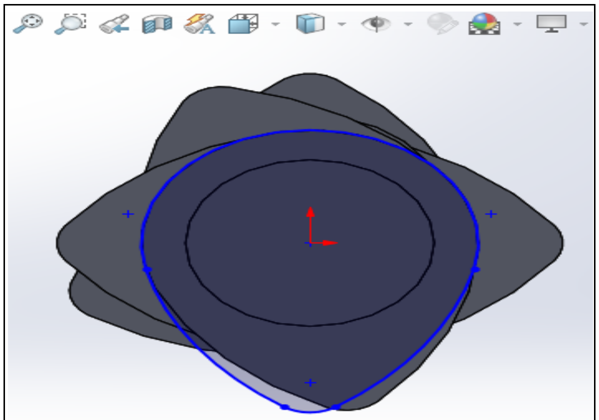

Figure IV.17: *Step of construction a 2D shape of the seventh cam lobe.*

b) Construction the 3D cam lobe shape:

- Now that we have completed the basic shape of the cam lobe, we will now create a 14 mm thick volumetric model of the previously defined face around it from Z axis.

- After that, we will draw the connecting piece between the seventh and the eighth cam lob, which has a diameter of 24 mm and a thickness of 30 mm, which we placed directly because the steps for drawing it are the same as those, we adopted to draw the Bearing Journal, which shows the resulting shape. ***Figure IV.18*** shows the initial and final shapes obtained.

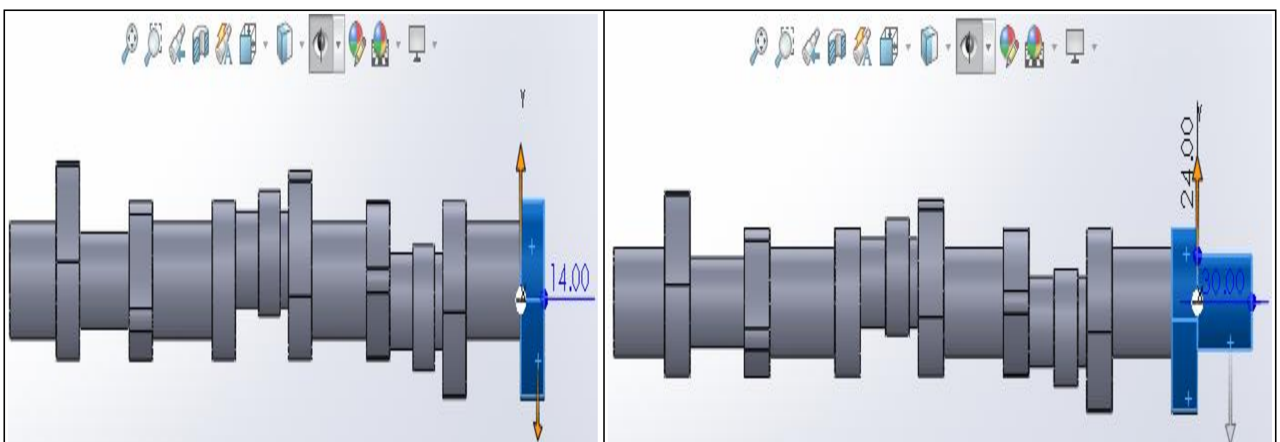

Figure IV.18: *Step of construction a 3D shape of the seventh cam lobe and Bearing Journal.*

IV.2.4.9 The eighth cam lobe

a) Construction the 2D cam lobe shape:

- To draw the sixth cam, we will use the same feature as before (convert entities), but this time the deviation will be -60° degrees (same as clockwise) from the first cam.

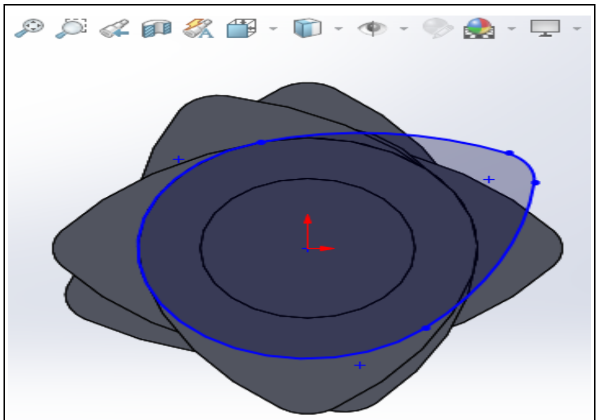

Figure IV.19: *Step of construction a 2D shape of the eighth cam lobe.*

b) Construction the 3D cam lobe shape:

- After we have drawn the eighth cam lobe, we will now create a volumetric model of the cam with a thickness of 14 mm on Z axis.
- And after that, we will draw a connecting piece between the fifth cam lob and the fifth Bearing Journal, which has a diameter of 23 mm and a thickness of 14 mm. also, this piece contains a rectangular piece that has a height of 9 mm and a width of 6 mm and it deflected at an angle of -60° degrees.
- In order to speed up the process, we will complete the last three parts, which are: the Rear bearing, 41.30 mm in diameter and 5 mm thick, and two bearing journals behind each other, the first with a 28 mm diameter and thickness 20 mm, and the second with a 38 mm diameter and 27 mm thickness ***Figure IV.20*** shows final shapes obtained.

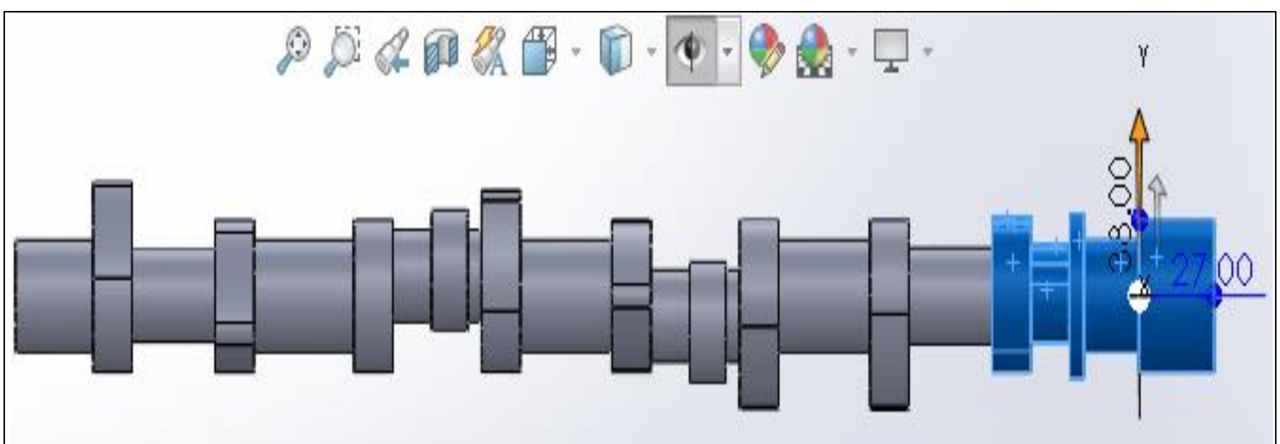

Figure IV.20: *Step of construction a 3D shape of the seventh cam lobe and the Bearing Journals.*

IV.2.4.10 the Final geometric shape of the cam shaft

Three additional operations were carried out to complete the final shape of the camshaft, as described below:

- ✓ A cavity process between the sides of the Bearing Journals numbers one, two, four and six through a circle with a radius of 3 mm. We also hollowed out the seventh Bearing Journal on the right side with a rectangle 2 mm long and 0.5 mm wide, and on the left side also with a length of 1 mm and 0.5 mm width. All of this we did using a feature “Revolved cut”.
- ✓ The second operation that we performed was Operation of “Fillet” between each of the sides of the first and last connecting piece with a value of 2.5 mm. We also performed the same operation between the third and fourth cam and also between the fifth and sixth cam, but with a value of 2 mm.
- ✓ The last process we performed was “the chamfer” process for the right side of the last Bearing Journal, where we chamfered 6 mm from the diameter of the right side and 20 mm from the length of it. After that, we chamfered the right and left sides with 1 mm, and also for each of the left sides of the first last Bearing Journal and also between the two sides of the Rear bearing.

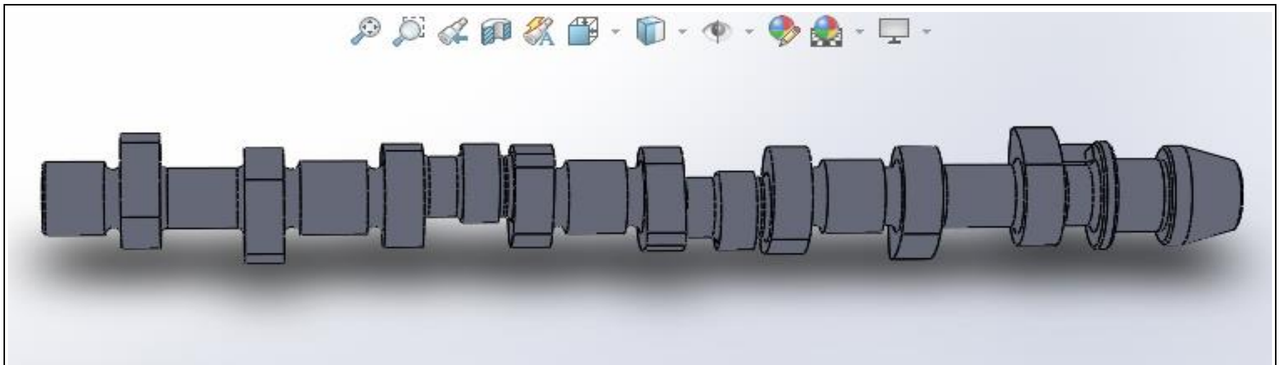

Figure IV.21: *The Final geometric shape of the cam shaft.*

We can summarize all the specifications of the camshaft in ***Table IV.1*** *bellow:*

Table IV.1: *the specifications of the camshaft.*

Properties	Dimensions
Cam thickness ($\boldsymbol{mm}$)	14
Cam height ($\boldsymbol{mm}$)	47.50
Camshaft diameter ($\boldsymbol{mm}$)	28
Base circle height ($\boldsymbol{mm}$)	38
Journal diameter type one ($\boldsymbol{mm}$)	28
Journal diameter type two ($\boldsymbol{mm}$)	30
Total lift of Cam ($\boldsymbol{mm}$)	9.5
Length of Camshaft ($\boldsymbol{mm}$)	432

IV.3 Result and discussion

IV.3.1 Definition of ANSYS software

ANSYS is short for "Analysis System" it is a suite of engineering simulation software developed by ANSYS Inc. Used for finite element analysis (FEA) and computational fluid dynamics (CFD) it allows engineers and designers in various industries to simulate how their product will perform in real-world conditions before it is actually built or manufactured by analyzing a wide range of problems related to mechanical product design and civil structure design using techniques Numerical.

IV.3.2 Modal and static structural analysis

Modal analysis and static structural analysis are two FEA approaches that we will used in the research to evaluate the camshaft's fatigue properties. They were performed using ANSYS Workbench. first will use Modal analysis to identify the camshaft's natural frequency and mode shapes and then we will use Static structural analysis to determine the camshaft's properties, comprising total deformation, strain and stress values.

Before starting Modal and static structural analysis, we will explain the first three steps repeated in both analyses, and with the same conditions, we begin them as follows:

1. **Add the Mechanical properties of material used**

As we mentioned the material the camshaft is made of is gray cast iron, now we will add its mechanical properties to the "Engineering Data" instruction. It shown in ***Table IV.2*** below:

Table IV.2: *Mechanical properties of Gray Cast Iron from Ansys.*

Properties	Values
Young's Modulus (GPa)	110
Poisson's Ratio	0.28
Density (kg/m^3)	7200
Ultimate Tensile Strength (MPa)	240

2. **Import the geometry**

Because we have created a single geometric shape for the camshaft that is unified for both analyses, we will import it from where we constructed it, "SolidWorks software" ***Figure IV.22*** shows the geometric shape of the camshaft after importing it to ANSES.

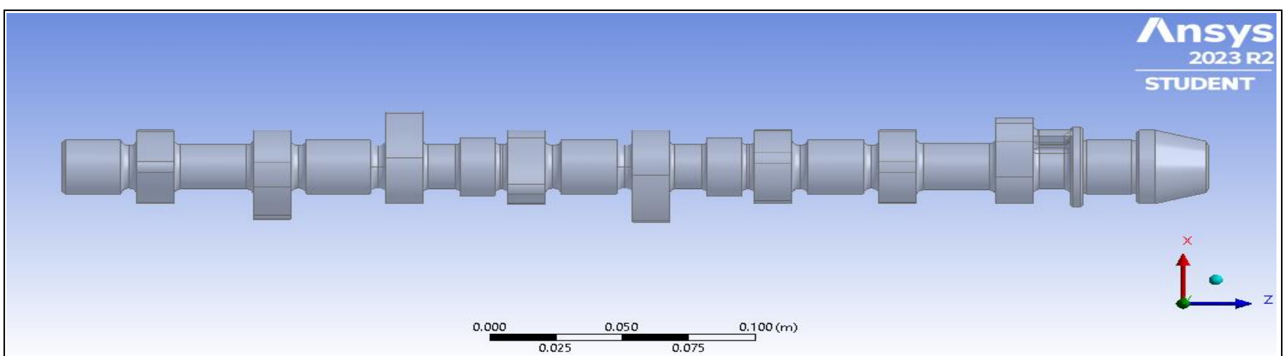

Figure IV.22: *The geometric of the camshaft after importing it to ANSYS.*

3. choosing a mesh to the geometry

Mesh creation is also another common term between the two analyzes that describes the process of separating the analytical chain into a series of discrete parts or finite elements. We will conduct an independent study of the mesh to ensure that the **tetrahedron** method is the optimal shape and size of the mesh by comparing it to **hexahedron** method. As is known, the finer mesh is used, the more accurate the result will become.

Table IV.3 summarized the skewness and orthogonal quality of both mesh methods and compared them to the mesh metric spectrum presented in ***Figure IV.23*** [63].

Table IV.3: *Comparison between tetrahedrons and hexahedrons mesh method.*

Mesh Method	Skewness	Orthogonal Quality
Tetrahedron	0.4916	0.6476
Hexahedron	0.6742	0.4579

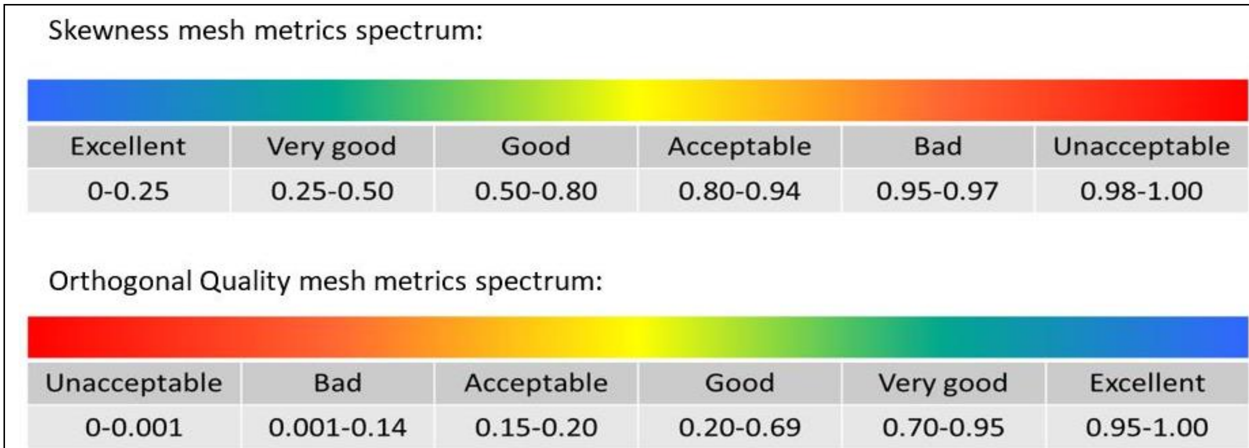

Figure IV.23: *Mesh metric spectrum of the skewness and orthogonal quality[63].*

The orthogonal quality is directly related to how the opposite surfaces' angles are similar to the ideal angle, whereas skewness refers to the contrast between the shape of the cell and the shape of an equilateral cell of identical volume.

Based on the data obtained in ***Table IV.3***, and as we note, the values of the first criterion (the skewness) for choosing the mesh method, we find that the value of the criterion in the Tetrahedron method is equal to 0.4916, while in the Hexahedron method it is equal to 0.6742, based on (the skewness mesh metric spectrum), the Tetrahedron method is better than the Hexahedron method due to Because its value is closer to zero. Also, looking at the second criterion (the orthogonal Quality), we find that the Tetrahedron method took a value estimated at 0.6476, while the Hexahedron method took a lower value estimated at 0.4579, based on (the orthogonal quality mesh metric spectrum), the Tetrahedron method is better than the Hexahedron method in this criterion as well. Because its value is closer to one. Considering the results obtained based on these two criteria, the Tetrahedron method is more suitable for our geometric shape.

After we have confirmed the reason for taking Tetrahedron mesh method, we will now choose the appropriate size for the mesh, and to obtain the appropriate size for the mesh. To obtain this, we have adopted three criteria, which are the quality of the mesh, the number of mesh elements, and also the number of mesh nodes. Therefore, we will study independently of our camshaft by choosing random sizes provided that they were consecutive and close in values. We took the first value for the first sample, **3.5** $\boldsymbol{mm}$, based on the calculation time. ***Table IV.4*** shows the details.

Table IV.4: *Mesh independence study for the camshaft.*

Mesh Element Size (mm)	*Mesh Nodes number*	*Mesh Elements number*	*Mesh Quality*
3.5	113610	73257	0.79345
4	81077	51047	0.77121
4.5	61856	37740	0.75076
5	49677	29359	0.71695
5.5	40095	23066	0.68866
6	34122	19084	0.65282
6.5	29882	16188	0.61734
7	26576	14037	0.56792
7.5	24191	12480	0.53417
5	22498	11392	0.50674

According to the results obtained, as we observe there is a large discrepancy between the number of nodes and also the number of elements between the chosen sizes. As for the quality of the network, all sizes are close. After comparing the sizes of the elements with each other, we found that the optimal size for the mesh element size is **3.5** $\boldsymbol{mm}$ with a number of nodes of 113610 a number of elements of 73257 and a very good mesh quality estimated at 0.79345.

Now, after specifying the mesh method, which is tetrahedron, and also after taking the appropriate mesh element size, which was 3.5 mm, now we take a look at our geometric shape after adding the mesh that shown in ***Figure IV.24***.

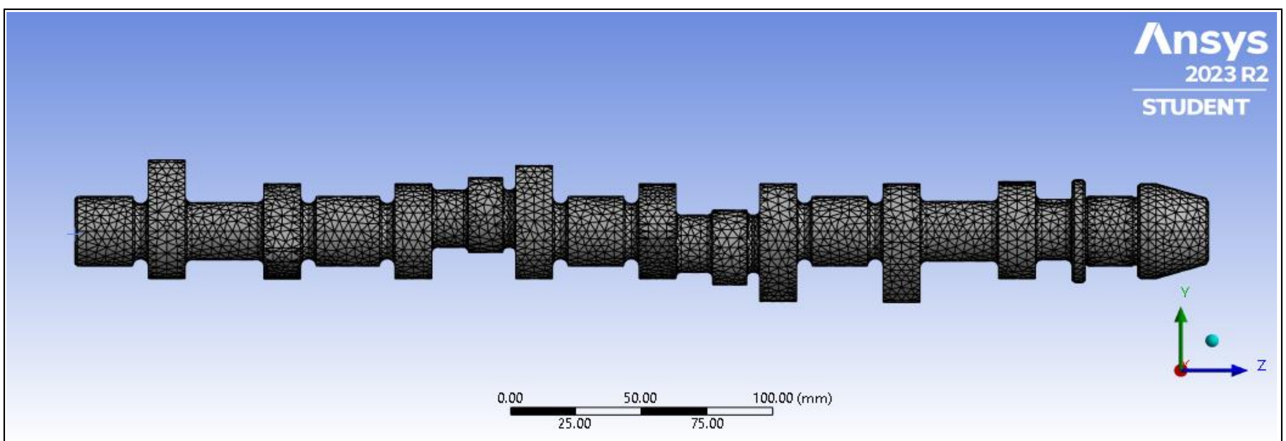

Figure IV.24: *The chosen mesh for camshaft simulation.*

IV.3.2.1 Modal analysis

Model analysis is a technique for identifying the inherent dynamism of a system Properties in the form of natural frequencies, damping factors, and mode shapes. this We will use this method to calculate the natural frequency affecting the camshaft under no-load conditions and also know the frequencies susceptible to vibration in the system to illustrate the mode shapes and how a component distorts in response to natural frequencies.

To obtain the natural frequencies and mode shapes, we must complete an additional step, which is called “Boundary conditions”. We can know what this step is only through its name, as it is the step to which we will add the special boundary conditions. In geometric form, we would like to do Modal analysis, these limit conditions are represented only by adding “Fixed supports” from both sides of the camshaft. The arrows that we can observe in ***Figure IV.25*** on both sides of the camshaft express these two fasteners.

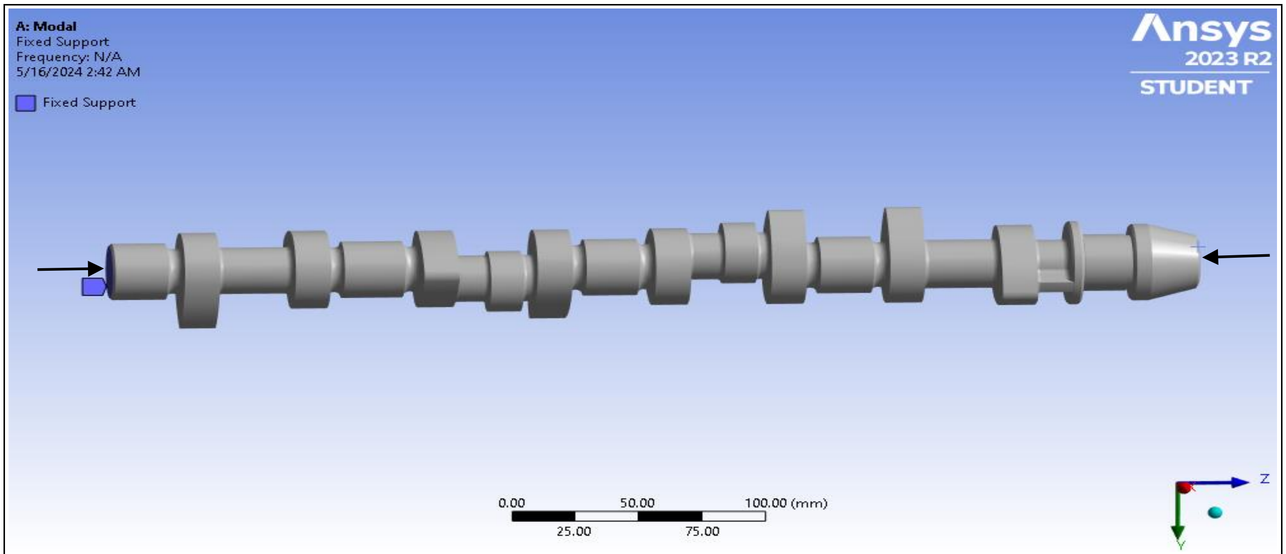

Figure IV.25: *Fixed support on camshaft for modal analysis.*

IV.3.2.1.1 Natural frequencies of the camshaft

We have made 6 modes to our model, where each time we get the value of natural frequency of the mode, The frequencies of the camshaft are presented in ***Table IV.5*** below:

Table IV.5: *Natural frequency of the camshaft through simulation.*

Mode	***Natural frequency (Hz)***	***Type of Mode***
1	395.8	Bending
2	400.96	Bending
3	1060	Bending
4	1075.7	Bending
5	1703	Torsion
6	1998.2	Bending + Torsion

Comment and analysis:

As we can see from ***Table IV.5***, the frequency values for the first and second models are very close (395.8 *Hz* and 400.96 *Hz*). This indicates the presence of the same type of mode between them, which we discovered is Bending. Then, as we notice, the frequency values for the third and fourth modes are also close (1060 *Hz* and 1075.7 *Hz*). This also indicates the presence of the same type of mode, which we discovered is also Bending. As for the fifth and sixth modes, we find that there is a discrepancy in the frequency values (1703 *Hz* and 1998.2 *Hz*). This It indicates that there is more than one type of mode we discovered that it is Bending and torsion.

If we look closely at the values of the six natural frequencies obtained, we find that they are high values and increase significantly from one mode to another. This indicates that the structure has high rigidity, high resistance to deformation, and also good structural engineering. This reduces the risk of resonant vibration problems.

IV.3.2.1.2 mode shapes

In modal analysis, the purpose of mode shapes is to understand the structure of the deformation modes at natural frequencies. Every mode form indicates how it vibrates or distorts when exposed to a certain natural frequency, and it correlates to that frequency. ***Figure IV.26*** shows the total deformation of the modes (or the deformation distribution).

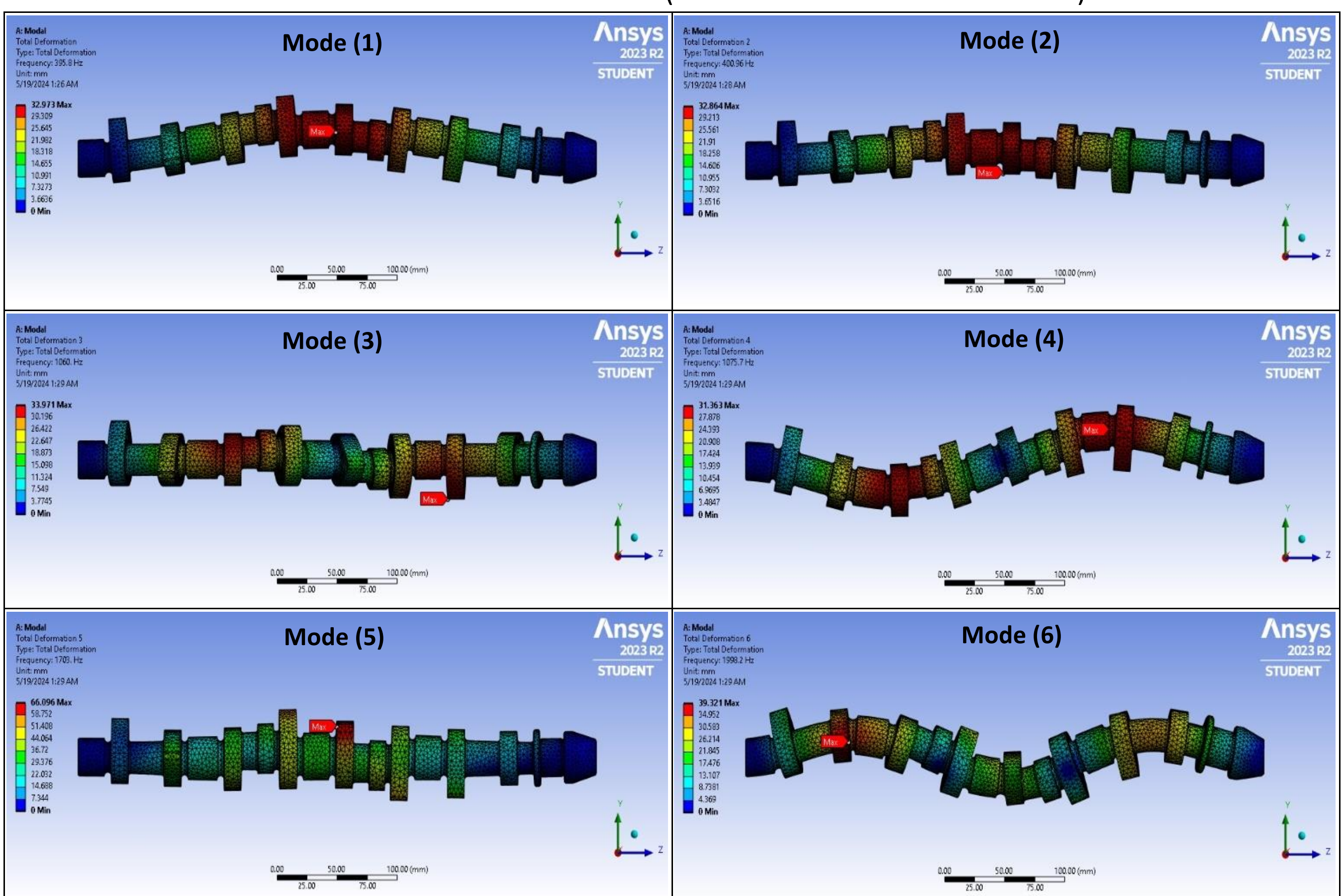

Figure IV.26: *The total deformation of the shape modes.*

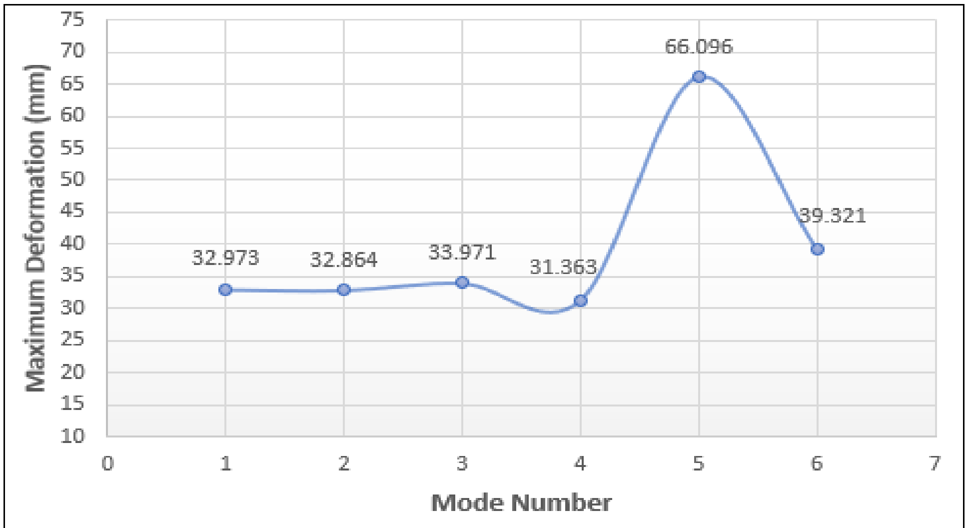

Figure IV.27: *Maximum deformation as a function of mode number.*

Figure IV.27 represents a Curve of the change in the maximum deformation value at each mode. As we notice, the first and second modes have a very close maximum deformation value 32.973 mm and 32.864 mm, and this is due to the closeness in the frequency value between them. As for the third mode, the deformation value increased slightly 33.971 mm. Considering between the third and fourth mode, the deformation value witnessed a decrease from 33.971 mm in the third mode to 31.363 mm in the fourth mode. After that, the deformation value witnessed a significant increase, reaching 66.096 mm in the stage between the fourth and fifth mode, and this is due to the high frequency value and also the type of mode there (Torsion). In the last stage, the deformation value witnessed a significant decrease, reaching 39.321 mm in the sixth mode. This decrease is due to Change in mode type (Bending and Torsion).

IV.3.2.2 Static structural analysis

Static structure analysis is another **FEA** method used to evaluate the design and structure of systems by determining displacements, pressures, and deformations in addition to the forces in structures or components resulting from loads. All this while neglecting the effects of inertia and damping. Implementing this approach has been critical in predicting camshaft performance in terms of fatigue. We will determine and evaluate the total deformation, Equivalent Elastic strain, Equivalent Von-Mises's stress for a camshaft designed using this analytical method.

Before doing this analysis and determining the values of the total deformation and von-Mises stress...etc., we will add the same step that we added in the modal analysis, but in this analysis, we will change the boundary condition that we used in the modal analysis of fixed support, where we will place a **fixed support** stabilizer on **One side** of our camshaft and we will also add **moment** as an additional boundary condition which is valued a **706.5 Nm.**

As we can see, ***Figure IV.28*** shows the first and the second boundary conditions used in static structural analysis. Which is a fixed support on the right side of the camshaft and a moment force applied value of 706.5 Nm**.**

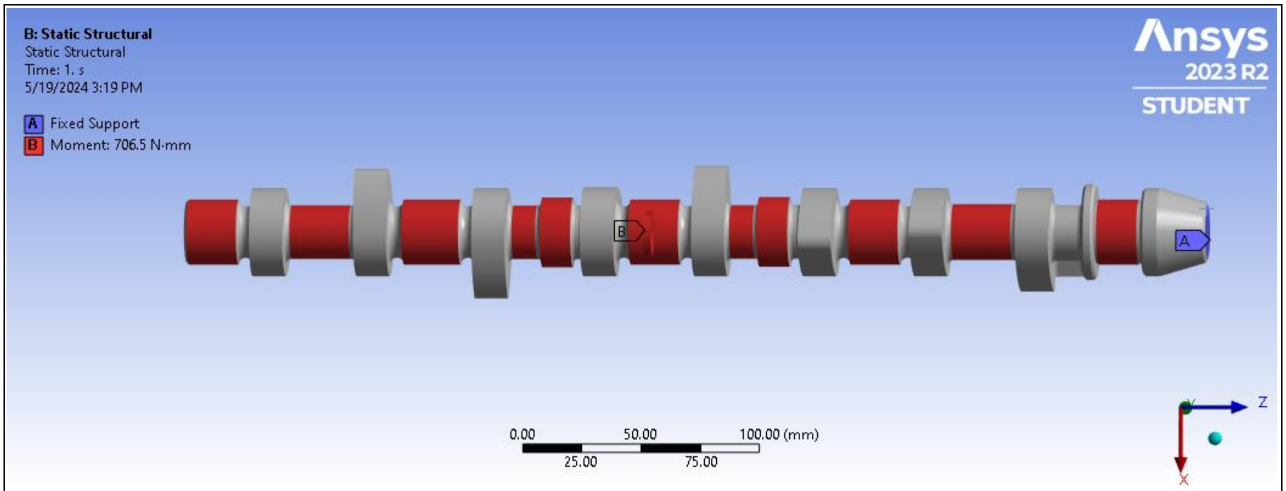

Figure IV.28: *Boundary conditions for camshaft under static structural analysis. (a) fixed support, and (b) moment applied.*

IV.3.2.2.1 The Total deformation of the camshaft

We will show directional deformation and total deformation

- **Directional deformation**

a. <u>The directional deformation along the X axis:</u>

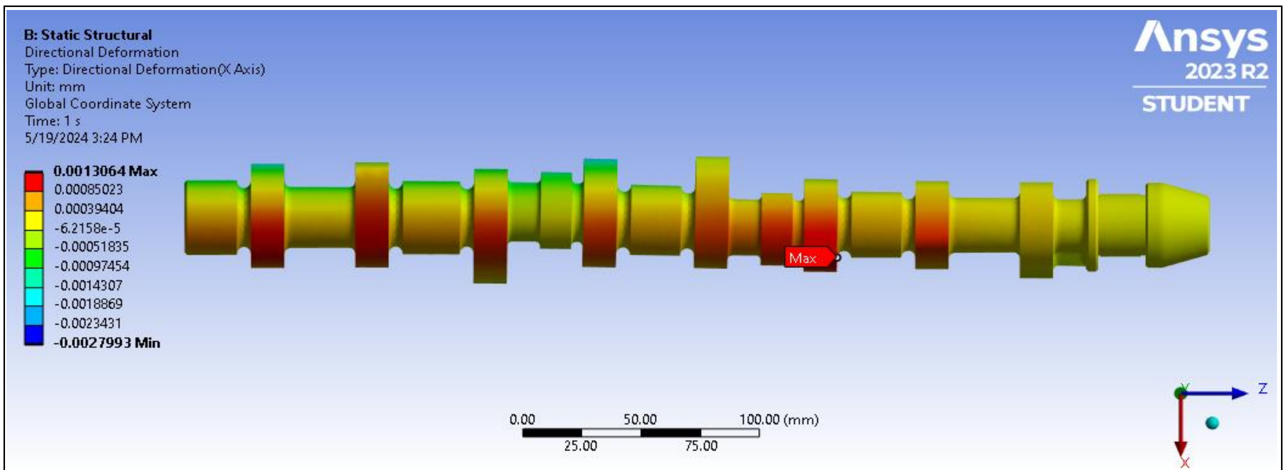

Figure IV.29: *The directional deformation along the X axis.*

As we can see from **Figure IV.29**, the maximum value of the directional deformation on the X axis is estimated at 0.001364 mm.

b. <u>The directional deformation along the Y axis:</u>

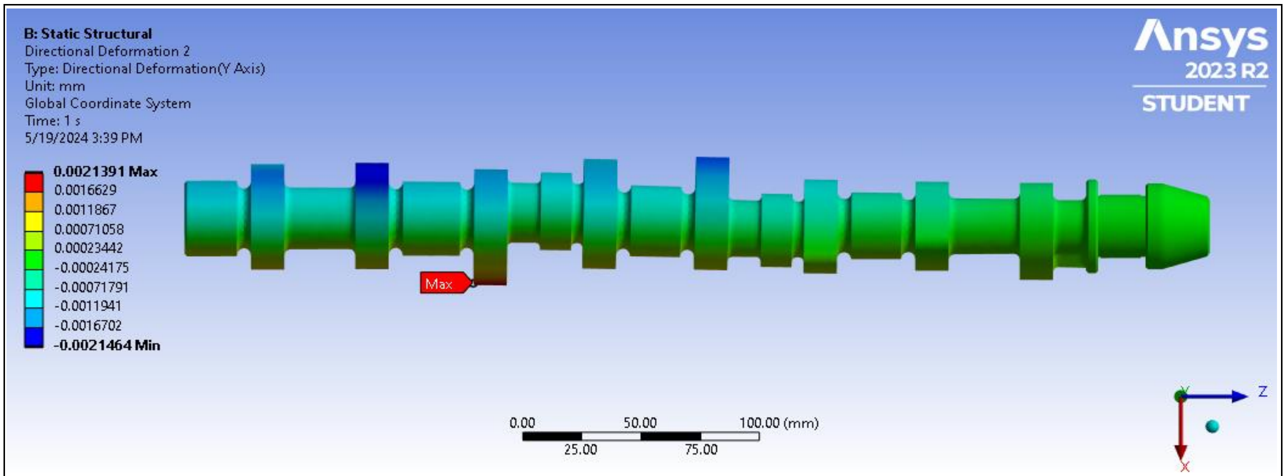

Figure IV.30: *The directional deformation along the Y axis.*

The maximum value of directional deformation, as we observe on poplar ***Figure IV.30***, is estimated at 0.0021391 mm

c. <u>The directional deformation along the Z axis:</u>

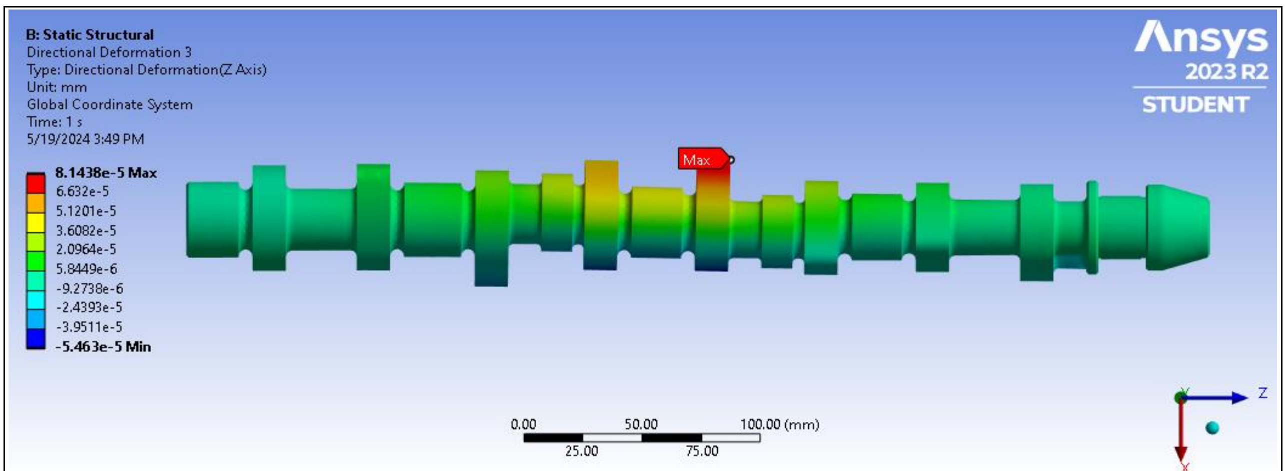

Figure IV.31: *The directional deformation along the Z axis.*

As we note, the maximum value of the directional deformation along the Z axis is estimated at $8.14*10^{-5}\,mm$.

<u>Comments on the results obtained:</u>

The results obtained indicate that the deformations on the three axes (X, Y, Z) are very small and are all within the range of micrometers ($10*^{-3}$ mm) and this indicates that the camshaft is exposed to a small deflection under the influence of the applied moment (706.5 Nm) and also that the camshaft maintains the integrity of its structure.

❖ **Total deformation**

Now that we have obtained and commented on the results of the maximum directional deformations, we will see the distribution of the total deformation on the camshaft and also know its maximum value, ***Figure IV.32*** which shows the total deformation of the camshaft.

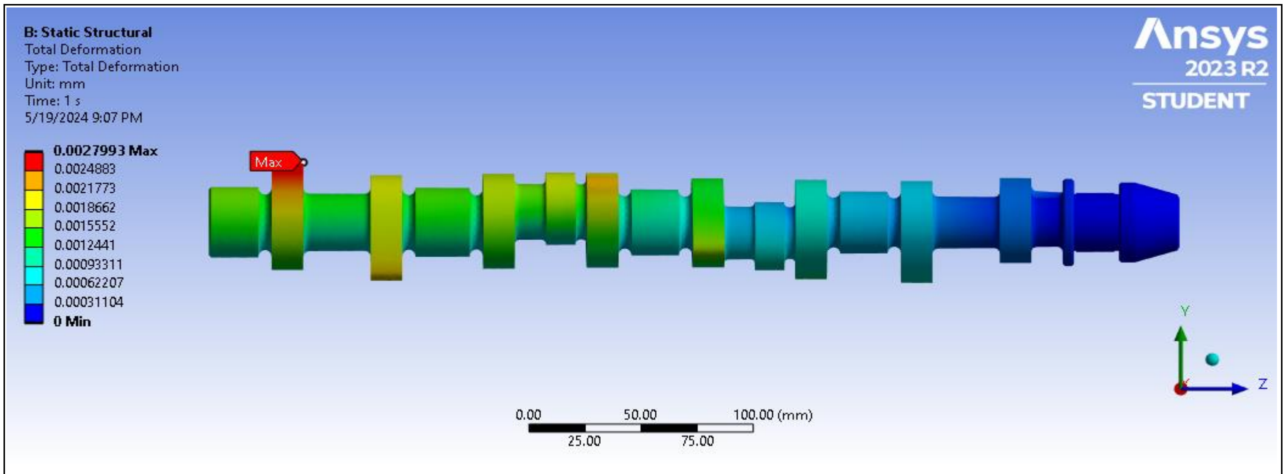

Figure IV.32: *The total deformation of the camshaft.*

<u>Comments on the results obtained:</u>

As we observed from ***Figure IV.32***, the largest value of total deformation is estimated at 0.0027993 mm, which is a very small value and is a positive result as it confirms that the camshaft is well designed to bear the applied loads and that Gray Cast Iron is a suitable material for it ,and also confirms that it can work reliably under conditions of mechanical load.

IV.3.2.2.2 Equivalent Elastic Strain

The distribution of the equivalent elastic strain is also an additional analysis that gives us a more comprehensive assessment of the performance of the camshaft. ***Figure IV.33*** It shows the distribution of the equivalent elastic strain on the camshaft.

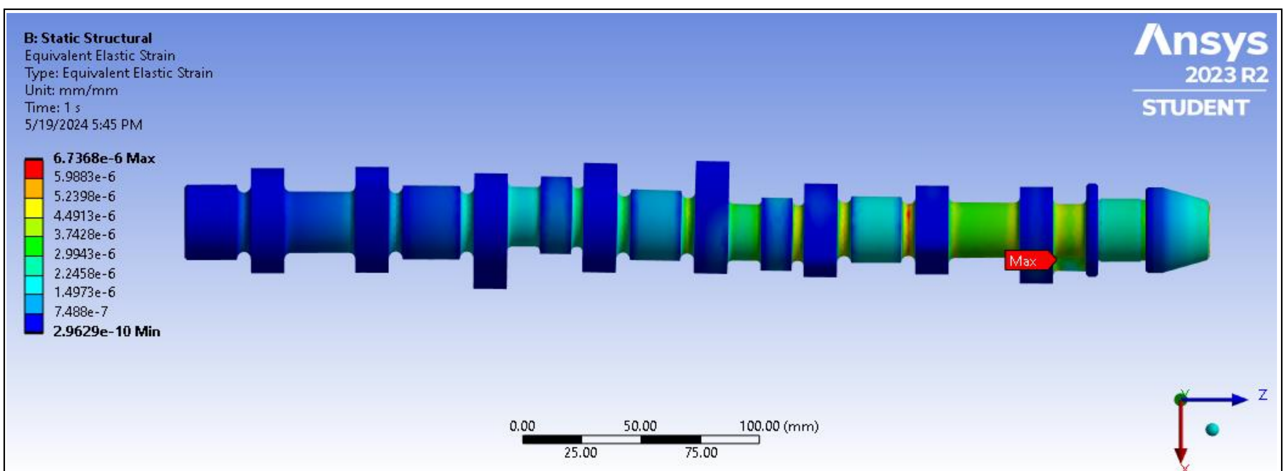

Figure IV.33: *Equivalent Elastic Strain of the camshaft.*

Comments on the results obtained:

As we can see, the maximum value of the equivalent elastic strain reaches ($6.7368*10^{-6}$), which is a very small value. It indicates that the elastic deformations in Gray Cast Iron are very small under the influence of load, which means that the material operates within its elastic range. The maximum value obtained also confirms that the camshaft is able to bear loads without falling into the range of “plastic deformation”. This means that the material retains its elastic properties and returns to its original shape after removing the load.

IV.3.2.2.3 Maximum principal elastic strain

The maximum principal elastic strain represents the maximum and minimum strains that occur at a point in the principal directions. These values give an indication of the deformation to which the material is subjected due to the applied loads. ***Figure IV.34*** show the distribution of the maximum principal elastic strain on the camshaft.

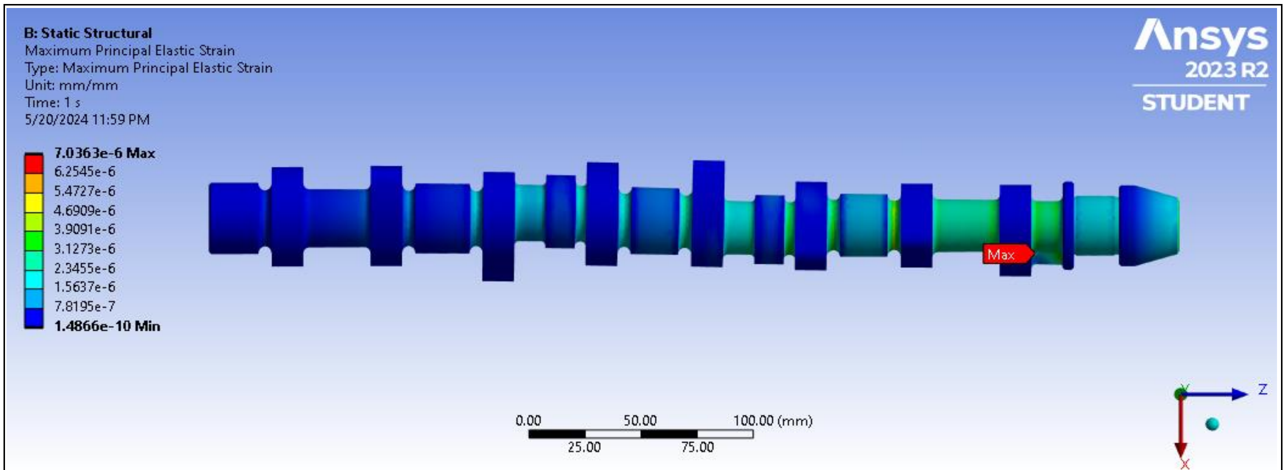

Figure IV.34: *The maximum principal elastic strain of the camshaft.*

Comments on the results obtained:

As shown in ***Figure IV.34***, the maximum value of the maximum principal elastic strain is equal to $7.03363*10^{-6}$, which is a relatively small strain value. It indicates that the material deforms slightly under load conditions, and this value is considered normal in analyzes of the static structure. As can be seen, the minimum strain to which the material is exposed reaches $1.4866*10^{-7}$, which is a very small value that expresses areas in the camshaft that are exposed to very few deformations. The maximum principal strains values indicate that the strain distribution across the material is relatively uniform and there are no areas of high strain concentration that could be alarming. These results also confirm once again that the Gray Cast Iron camshaft remains within its elastic limits when subjected to mechanical loads.

IV.3.2.2.4 Equivalent Von-Mises's stress

Equivalent Von-Mises's stress is also an effective indicator for evaluating and predicting material yield ***Figure IV.35*** showing the distribution of the equivalent Von-Mises on the camshaft.

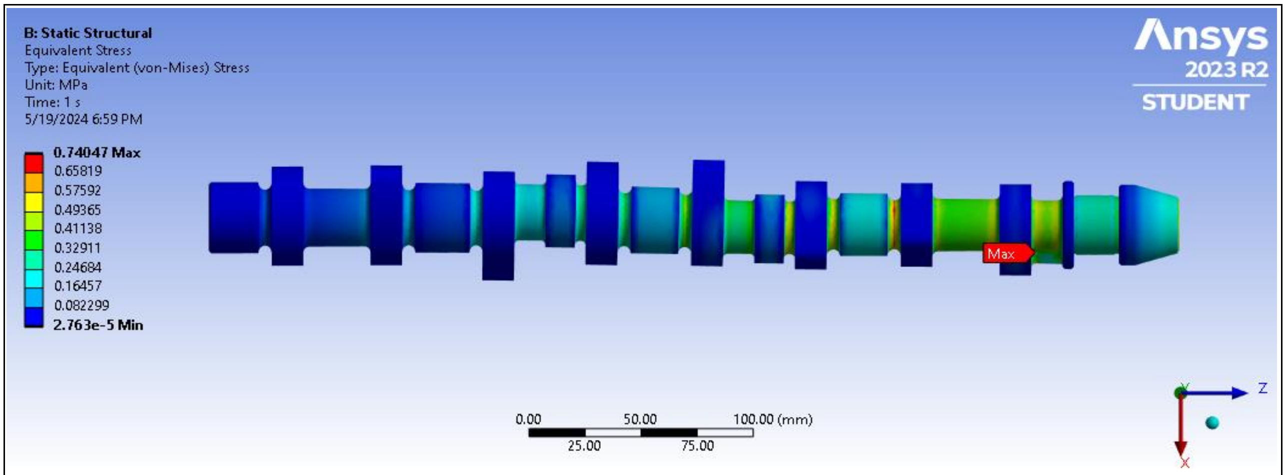

Figure IV.35: *Equivalent Von-Mises's stress of the camshaft.*

<u>Comments on the results obtained:</u>

As we can see from ***Figure IV.35***, the maximum value of the equivalent Von-Mises's stress is 0.74047 MPa, which is a very low value compared to the permissible stress limits for most metal materials used in the manufacture of camshafts. This decrease indicates that gray cast iron is not at risk of collapse or permanent deformation under loads, and also to the camshaft design is proportional to Gray Cast Iron. All of these indicators confirm what we previously concluded: that the camshaft will operate efficiently and reliably under mechanical loads.

IV.3.2.2.5 Maximum principal stress

Principal stress refers to stresses that act in certain directions where the shear values are zero. These values are important for understanding the performance of the material under loading conditions. ***Figure IV.36*** show the distribution of the maximum principal stress on the camshaft.

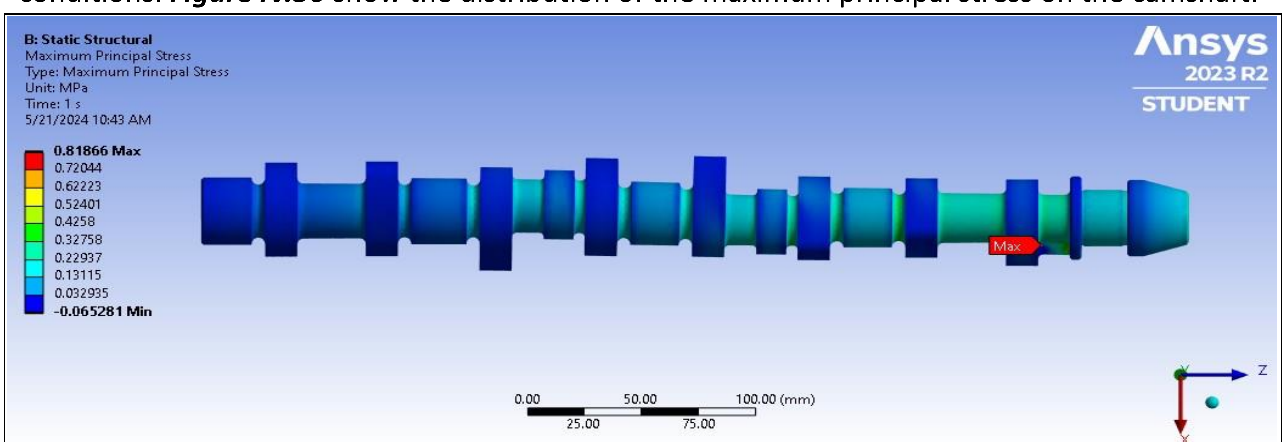

Figure IV.36: *The maximum principal stress of the camshaft.*

Comments on the results obtained:

By Looking at ***Figure IV.36***, the maximum value of the maximum principal stress reaches 0.81866 MPa, which represents the highest stress in the material and is considered relatively low, which indicates that the material bears the loads without approaching the limits of yielding or breaking. Also, as we note, the lowest value of the stress is estimated at -0.66581 MPa, and is negative as an expression. It is a pressure stress. This value indicates that the stress areas in the material are not severe and remain within safety limits. Once again, these results confirm that Gray Cast iron camshaft operates safely under loading conditions.

IV.3.2.2.6 Strain energy

Strain energy is a measure of the energy stored in the material as a result of deformation under loads and is an important indicator for understanding how energy is distributed in the material. ***Figure IV.37*** shows this for our camshaft.

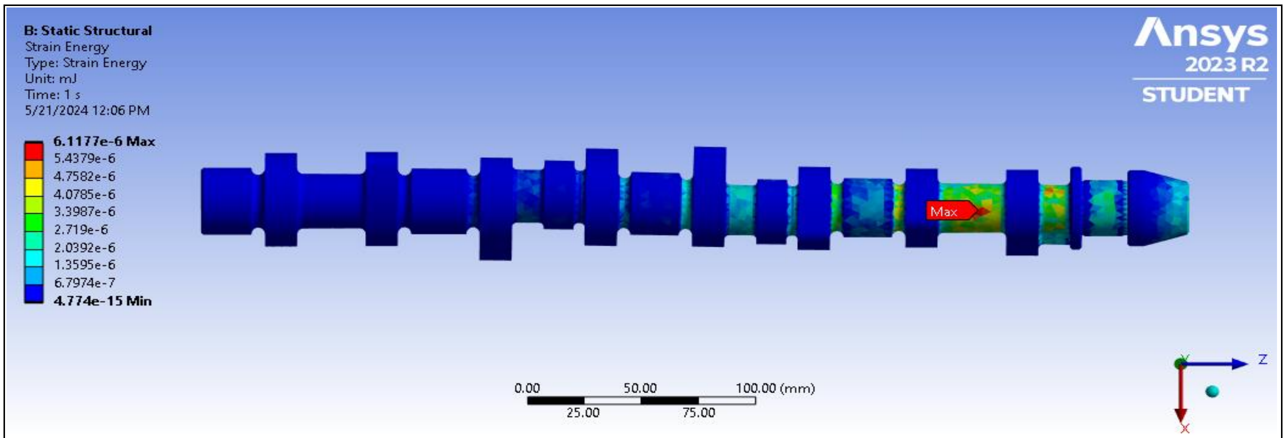

Figure IV.37: *The strain energy of the camshaft.*

Comments on the results obtained:

Based on the results obtained from ***Figure IV.37***, the maximum value of the strain energy reaches $6.111*10^{-6}$ mJ. This value is considered a very small value and indicates that the material has a small amount of energy as a result of deformation under loads. As we can see, the minimum value of the strain energy is estimated at $4.774*10^{-7}$ mJ and it indicates There are some areas in the material that weigh less energy than others. Also, the distribution of energy is homogeneous in the material and there are no areas of high energy storage that could lead to dangerous stress concentrations. All these results reinforce the idea that the camshaft operates safely under mechanical loads.

IV.4 Suggestions and improvements

We have allocated this section to suggest an improvement in the camshaft, whether in its design or in the material it is made of, in order to bring benefit to the research. The proposal that we propose in this section will be a change in the material of the camshaft from gray cast iron to **Cast Carbon Steel** while maintaining the same design of the camshaft. Our choice of this material came based on the comparison made in [64]. In order to prove the validity of our proposal, we will make a comparison between a camshaft made of **Gray Cast Iron** and **Cast Carbon Steel**.

Table IV.6: *Mechanical properties of Cast Carbon Steel and Gray Cast Iron.*

Properties	*Cast Carbon Steel*	*Gray Cast Iron*
Young's Modulus (GPa)	230	110
Poisson's Ratio	0.30	0.28
Density (kg/m^3)	7820	7200
Ultimate Tensile Strength (MPa)	585	240

We will compare based on four indicators, which are the natural frequencies of each material and also the total deformation, Equivalent Elastic Strain and Equivalent Von-Mises's stress

IV.4.1 according to the natural frequencies

It is important to compare natural frequencies to understand how different materials affect the dynamic performance of structures. ***Table IV.7*** shows the values of the natural frequencies and the total deformations obtained for Cast Carbon Steel and Gray Gast Iron in each position during the conditional analysis. As shown, the values of the natural frequencies in the six positions of Cast Carbon Steel are greater than the values of the natural frequencies of gray cast iron. Looking at the total distortion values, Gray Cast Iron has a total distortion value of Cast Carbon Steel, which is normal because it has smaller natural frequencies.

Table IV.7: *The values of frequencies and deformation of Cast Carbon Steel and Gray Gast Iron.*

Items	***Cast Carbon Steel***	***Gray Cast Iron***
$\boldsymbol{\delta_1}$	31.642 mm	32.973 mm
$\boldsymbol{f_1}$	550.4 *Hz*	395.8 *Hz*
$\boldsymbol{\delta_2}$	31.535 mm	32.864 mm
$\boldsymbol{f_2}$	557.49 *Hz*	400.96 *Hz*
$\boldsymbol{\delta_3}$	32.695 mm	33.971 mm
$\boldsymbol{f_3}$	1473.3 *Hz*	1060 *Hz*
$\boldsymbol{\delta_4}$	30.102 mm	31.363 mm
$\boldsymbol{f_4}$	1495.6 *Hz*	1075.7 *Hz*
$\boldsymbol{\delta_5}$	63.305 mm	66.096 mm
$\boldsymbol{f_5}$	2345.8 *Hz*	1703 *Hz*
$\boldsymbol{\delta_6}$	37.595 mm	39.321 mm
$\boldsymbol{f_6}$	2776.4 *Hz*	1998.2 *Hz*

In order to illustrate the difference between the values of natural frequencies between Cast Carbon Steel and Gray Cast Iron, we have drawn Bar graphs shown below in ***Figure IV.38***.

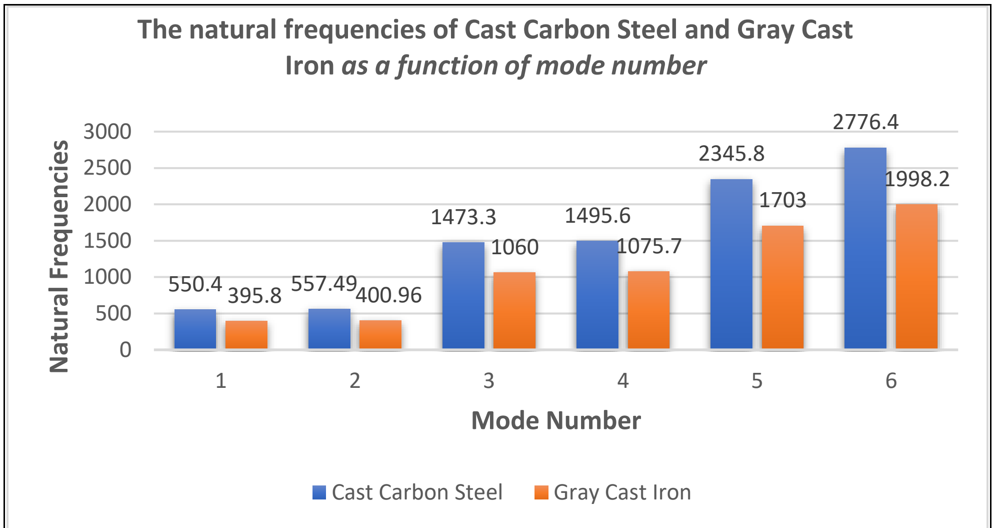

Figure IV.38: *Bar graphs showing the natural frequencies Cast Carbon Steel of and Gray Cast Iron as a function of the mode number.*

<u>Compare and analyze:</u>

<u>The first and second mode:</u>

As we can see in the first and second modes, the steel had a first frequency of 550.4 *Hz*, which is much higher than the first frequency of Cast Iron, whose first frequency was 395.8 *Hz*. As for the second situation, the frequency value for carbon steel, 557.49 *Hz*, is greater than the second frequency for Cast Iron, which was 400.96 *Hz*. In the first and second modes, the natural frequency values of the steel were significantly higher than those of the Gray Cast Iron. This indicates that the Steel has a higher hardness in these frequency ranges.

<u>The third and fourth mode:</u>

Between these two situations, as we notice, the third frequency of steel reaches 1473.3 *Hz*, which is much greater than the value obtained in Cast iron, which was 1060 *Hz*. Considering the fourth mode, the carbon steel still has higher values than the Cast iron, 1075.7 *Hz*, and this time its frequency value reaches 1495.6 *Hz*. Once again, we see that carbon steel has higher frequencies than gray cast iron. This reinforces the idea that cast carbon steel has higher hardness in these frequency ranges.

<u>The fifth and sixth:</u>

As we note, the value of the fifth and sixth frequencies of carbon steel (2345.8 *Hz* to 2776.4 *Hz*) is higher than that of gray cast iron (1703 *Hz* to 1998.2 *Hz*) again. This also indicates that carbon steel provides higher resistance to vibration distortions in these frequency ranges.

a summary and based on natural frequency analysis, we find that cast carbon steel provides better performance in terms of vibration resistance than gray cast iron.

IV.4.2 According to the total deformation

Total deformation is another indicator for comparison between Cast carbon steel and Gray cast iron, ***Figure IV.39*** shows the distribution of Total deformation for a cast carbon steel camshaft.

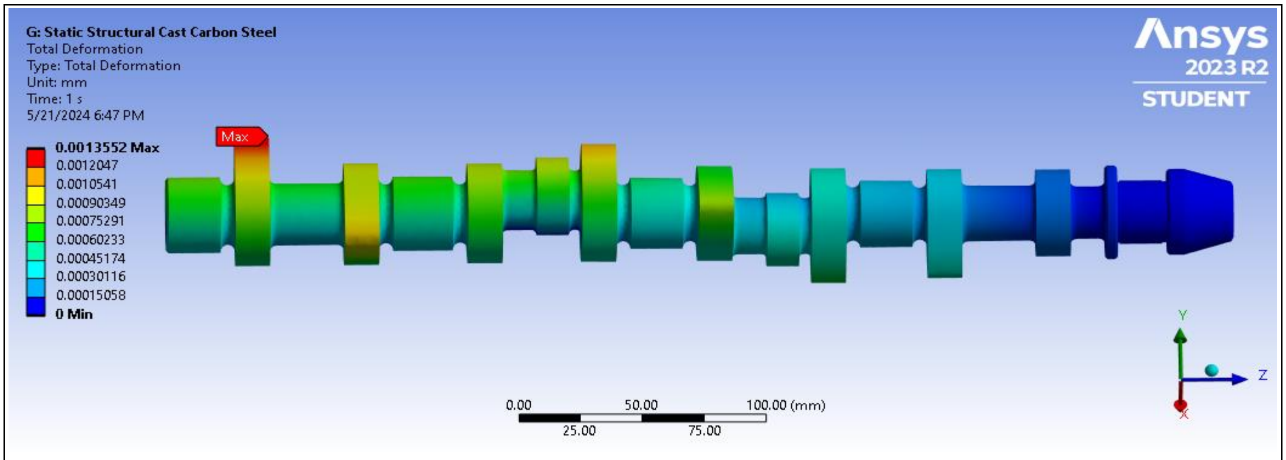

Figure IV.39: *The total deformation of cast carbon steel camshaft.*

In order to notice the difference in total deformation between the two materials, we drew a Bar graph shown below in ***Figure IV.40***.

<u>Compare and analyze:</u>

As we note, the maximum value of total deformation for Cast Carbon Steel is 0.0013552 mm, which is a very small value and indicates that it has high hardness compared to the maximum value of total deformation that we obtained for Gray Cast Iron, which was 0.0027993 mm, so it is less deformed by a respectable value. These results indicate that both Cast carbon steel and Gray Cast Iron have a very high minimum deformation value with a slight advantage over Cast carbon steel by a slight difference. In summary, the maximum deformations for both materials show that steel cast with carbon steel is more resistant to deformation under loads than solid cast iron.

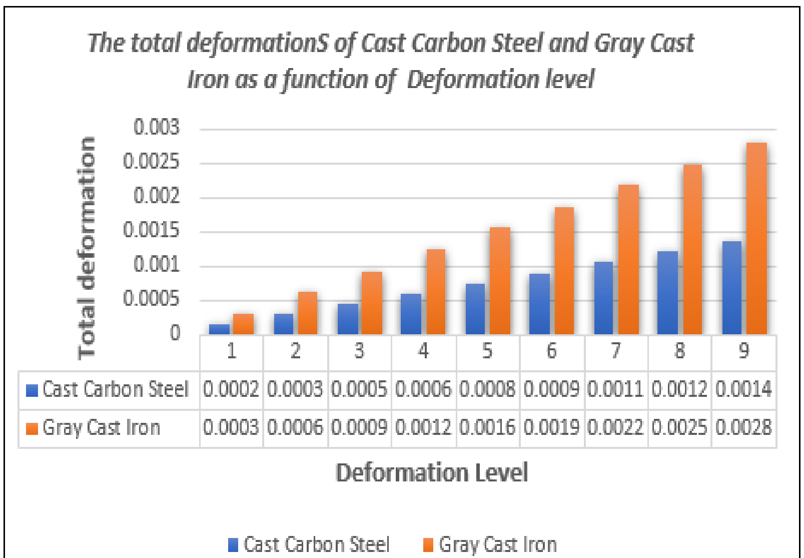

Figure IV.40: *Bar graphs showing the total deformations of Cast Carbon Steel and Gray Cast Iron as a function of Deformation level.*

IV.4.3 According to the Equivalent Elastic Strain

Figure IV.41 shows the equivalent elastic stress distribution for a cast carbon steel camshaft

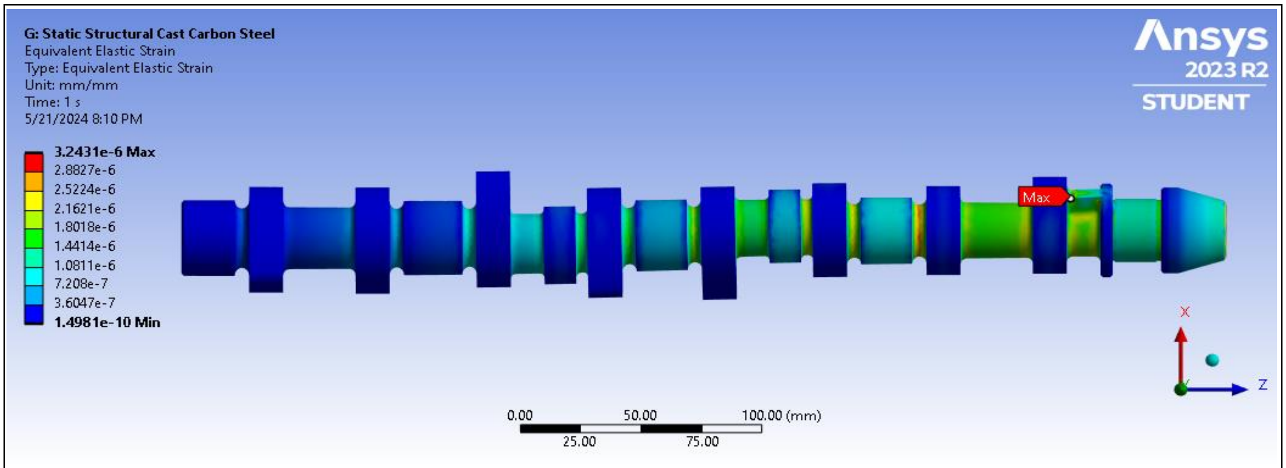

Figure IV.41: *Equivalent Elastic Strain Cast Carbon Steel of camshaft.*

Compare and analyze:

As we can see from ***Figure IV.42***, Gray Cast Iron has higher elastic stress values than Cast Carbon Steel, which increase with increasing levels. As we notice, the maximum elastic stress value for gray cast iron reached $6.73*10^{-6}$, which is a very small value, as we mentioned previously, and indicates that it has resistance to elastic stresses under loads. As for cast carbon steel, its highest elastic stress value reaches $3.241*10^{-6}$, which is a very small value and indicates that cast carbon steel is more resistant to elastic stresses than gray cast iron. This indicator also confirms that the two materials have a high resistance to stresses under loads, and compared to each other, it turns out once again that cast carbon steel is more resistant to elastic stresses.

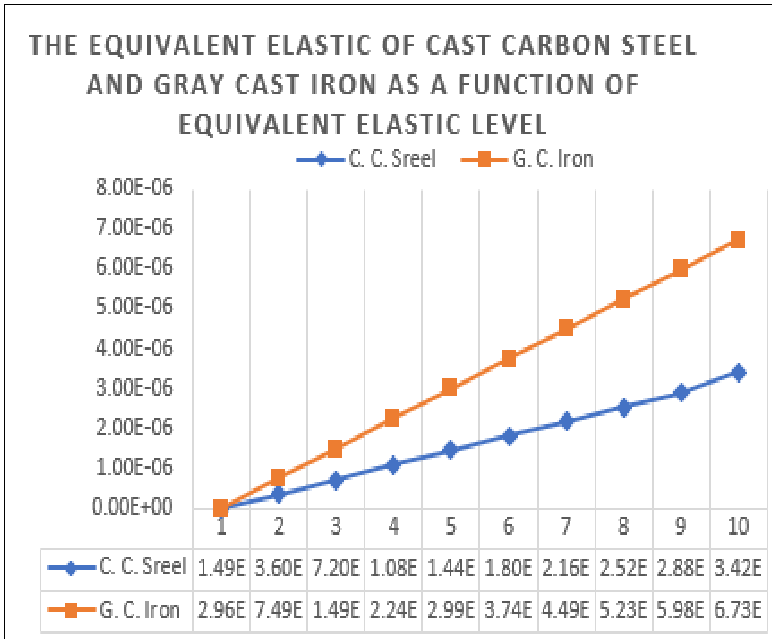

Figure IV.42: *Graphic curve showing Equivalent Elastic Strain of Cast Carbon Steel and Gray Cast Iron as a function of the level.*

IV.4.4 According to the Equivalent Von-Mises's stress

The Last indicator to compare cast Carbon steel and Gray cast iron is the Equivalent Von-Mises's stress. ***Figure IV.43*** shows the distribution of the Equivalent Von-Mises's stress on a cast carbon steel camshaft

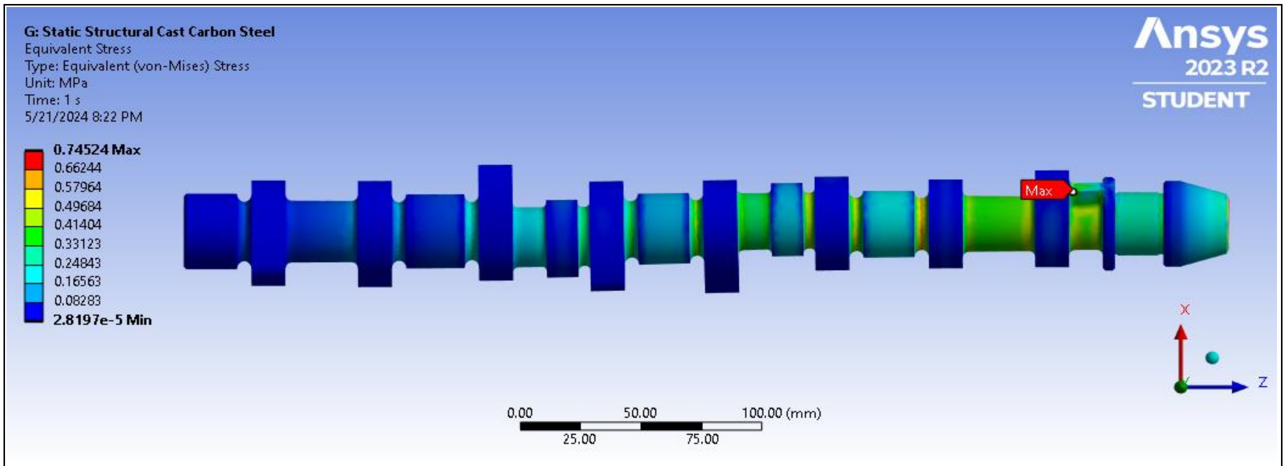

Figure IV.43: *Equivalent Von-Mises's stress of Cast Carbon Steel camshaft.*

Compare and analyze:

As we can see from ***Figure IV.44*** the results obtained for the equivalent von Mises's stress values for both materials are very close to each other. 0.7452 MPa represents the highest value of the von Mises's equivalent stress to which Cast Carbon Steel is subjected to mechanical loads and indicates that it can withstand stresses within safe limits for the material. As for 0.7404 MPa, it represents the highest von Mises equivalent stress to which Gray Cast Iron is exposed under the same mechanical loads. It is a value very close to that of Carbon Steel. This indicates that the two materials have similar behavior under the same loads in terms of equivalent stresses. Depending on the values of the von Mises's equivalent stress, it can be said. Cast Carbon Steel provides slightly better performance than Gray Cast Iron.

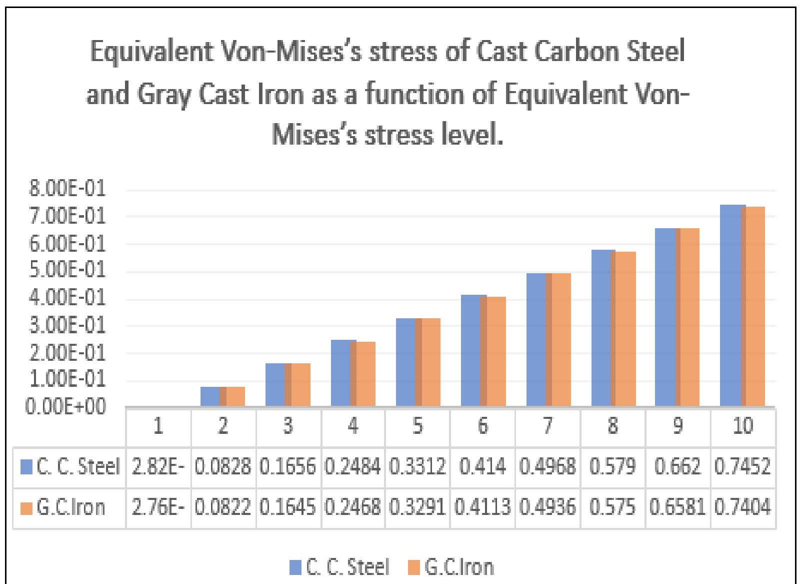

Figure IV.44: *Bar graphs of the Equivalent Von-Mises's stress of Cast Carbon Steel and Gray Cast Iron as a function of the level.*

IV.5 Conclusion

In this chapter, we modeled the distribution system of the diesel engine (13511-64071). This modeling was limited to the camshaft as it is the primary and direct component responsible for opening and closing the valves. To perform the modeling, we used applications SolidWorks and Ansys. We used SolidWorks for modeling the geometric shape of the camshaft, where we observed all the necessary steps for its modeling. We used Ansys for calculations and analysis, which was divided into two parts. The first part involved modal analysis; a technique used to determine the inherent dynamic characteristics of the camshaft in the form of natural frequencies. In this analysis, we fixed the camshaft at both ends as a boundary condition. The we obtained the natural frequency values as well as the deformations at these frequencies for six modes. These values were high, with the smallest frequency being 395.8 *Hz*, indicating that our camshaft has high stiffness and resistance to deformation. In the second part of this chapter, we conducted static structural analysis, which is a method used to evaluate the design and structure of systems by determining indicators such as deformations and stresses. In this analysis, we fixed the camshaft from one side and applied a moment force of 706.5 Nm as a boundary condition. Through this analysis, we found the deformation values in the three axes (X, Y, Z) as well as the total deformations. We also obtained the equivalent elastic strain and the equivalent Von Mises stress. All the results from this analysis were good and indicated that the camshaft has good structural integrity and operates safely under mechanical loads.

The last task we performed in this chapter was to propose Cast Carbon Steel as an alternative material to Gray Cast Iron for the camshaft. To validate this proposal, we made a comparison based on four indicators: the natural frequencies of the structure, total deformations, equivalent elastic strain, and the equivalent Von Mises stress. All these indicators ultimately suggested that we can substitute gray cast iron with Cast Carbon Steel as an alternative material for the camshaft.

General conclusion

General conclusion

The main objective of our study was to make a numerical simulation the camshaft of a diesel engine made of Gray cast iron (13511-64071) when subjected to mechanical loads in order to determine its efficiency and durability under harsh mechanical conditions. To achieve this, we used SolidWorks and Ansys applications. We modeled the geometric shape of the camshaft using SolidWorks. For the calculations and analysis, we used Ansys, where we performed two types of analyses: modal analysis and static structural analysis.

In the modal analysis, we obtained six natural frequencies and six mode shapes. The natural frequencies we obtained were relatively high, with the lowest natural frequency of the structure being 395.8 Hz for the first mode shape, and the highest natural frequency of the structure being 1998.2 Hz for the sixth mode shape. These high frequency values indicated that the camshaft structure can more effectively resist vibrations and has high resistance and stiffness to deformation under mechanical loads.

In the static structural analysis, after applying a moment of 706.5 Nm to the camshaft as a boundary condition, the first indicator we obtained was the total deformation, which also showed positive results. The maximum value of the total deformation was 0.0027993 mm, indicating that the camshaft is well-designed to withstand the applied loads and that gray cast iron is a suitable material for it. Subsequently, we obtained the values and distribution of the equivalent elastic stress and the maximum principal elastic strain. The maximum value of the equivalent elastic stress was 6.7368E-6, while the maximum principal elastic strain was 7368E-6. Both values indicated that the material operates within its elastic range, and the camshaft can withstand the loads without entering the "plastic deformation" range. Next, we obtained two other indicators to assess the camshaft's efficiency under mechanical loads: the Von Mises stress and the maximum principal stress. Their maximum values were 0.74047 MPa and 0.81866 MPa, respectively. These values indicated that Gray cast iron is not at risk of failure or permanent deformation under the loads, and that the material can handle the loads without approaching the yield limit. The final indicator we considered was the strain energy, whose maximum value was 6.111E-6 mJ. This suggested that the energy distribution within the material is uniform and that there are no regions with high energy storage that could lead to dangerous stress concentrations.

As a summary of all this and based on the results of the previous analyses conducted on the Gray cast iron camshaft for the diesel engine, which included the evaluation of natural frequencies, total deformations, and stresses under mechanical loads, we conclude that the distribution system of the diesel engine (13511-64071) possesses excellent structural properties, enabling it to handle the expected mechanical loads with high efficiency. Despite all these positive results obtained for the gray cast iron camshaft, the comparison we conducted revealed that Cast carbon steel has higher resistance to mechanical loads. This indicates that there is greater potential to improve the efficiency of the distribution system specifically, and the diesel engine in general.

References

References

[1] H. Bayrakceken, I. Ucun, and S. Tasgetiren, "Fracture analysis of a camshaft made from nodular cast iron," *Engineering Failure Analysis,* vol. 13, no. 8, pp. 1240-1245, 2006.

[2] K. K. D. Dave Marmik M, "Static Structure Analysis of Diesel Engine

Camshaft," *IJSR - INTERNATIONAL JOURNAL OF SCIENTIFIC RESEARCH,* vol. Volume : 2, no. ISSN No 2277 - 8179, pp. 208-209, 2013.

[3] A. Andoko, R. Prasetya, and F. Gapsari, "Stress and Fatigue Life Simulation of Camshaft with Structural Static ANSYS Approach," *Advances in Science and Technology,* vol. 125, pp. 61-65, 2023.

[4] L. Witek, "Failure and thermo-mechanical stress analysis of the exhaust valve of diesel engine," *Engineering Failure Analysis,* vol. 66, pp. 154-165, 2016.

[5] B. Fersaoui, M. Cerdoun, A. May, and C. Carcasci, "Thermo-mechanical stress analysis within a steel exhaust valve of an internal combustion engine," *Proceedings of the Institution of Mechanical Engineers, Part C: Journal of Mechanical Engineering Science,* vol. 236, no. 1, pp. 635-654, 2022.

[6] L. Witek and P. Zelek, "Stress and failure analysis of the connecting rod of diesel engine," *Engineering Failure Analysis,* vol. 97, pp. 374-382, 2019.

[7] X. Liu, Y. Wang, and W. Liu, "Finite element analysis of thermo-mechanical conditions inside the piston of a diesel engine," *Applied Thermal Engineering,* vol. 119, pp. 312-318, 2017.

[8] M. Tahar-Abbes, P. Maspeyrot, A. Bounif, and J. Frêne, "Effet thermomécanique sur la lubrification hydrodynamique d'un piston de moteur Diesel," in *CFM 2007-18ème Congrès Français de Mécanique*, 2007: AFM, Maison de la Mécanique, 39/41 rue Louis Blanc-92400 Courbevoie.

[9] Q. Zhang, Z. Zuo, and J. Liu, "Failure analysis of a diesel engine cylinder head based on finite element method," *Engineering Failure Analysis,* vol. 34, pp. 51-58, 2013.

[10] A. d. A. Cardoso and E. C. Andreatta, "Thermomechanical analysis of diesel engine exhaust manifold," SAE Technical Paper, 0148-7191, 2016.

[11] L. Witek, M. Sikora, F. Stachowicz, and T. Trzepiecinski, "Stress and failure analysis of the crankshaft of diesel engine," *Engineering Failure Analysis,* vol. 82, pp. 703-712, 2017.

[12] *https://mrcet.com/downloads/digital_notes/ME/III%20year/Internal%20Combustion%20Engines.pdf*.

[13] "https://dc-4one.blogspot.com/2014/09/mesin-dan-konfigurasinya.html." (accessed.

[14] J. Sabhadiya. "Invention Of The Internal Combustion Engine – A Brief History." https://www.engineeringchoice.com/who-invented-the-internal-combustion-engine/ (accessed.

[15] "https://www.q-files.com/technology/lets-explore-how-things-work/how-does-a-car-engine-work." (accessed.

[16] "https://www.bossgoo.com/product-detail/volvo-d3-1-d3-6d-diesel-22794711.html." (accessed.

[17] "https://articulo.mercadolibre.com.ve/MLV-718552506-empacadura-de-camara-ecosport-focus-mazda-3-ranger-23-_JM." (accessed.

[18] "https://autopartes-francesas.mercadoshops.com.mx/MLM-1463220619-carter-aceite-clio-sport-megane-ii-10-29-84-_JM." (accessed.

[19] "https://unevoc.unesco.org/up/UNIT_1__Introduction_to_tractors_LFM_Autosaved.pdf." (accessed.

[20] "https://www.bizoo.ro/produse/supapa-admisie/piese-de-schimb-cat-2839/start-0/10/," ed.

[21] "https://www.fdautoparts.com/post/5795." (accessed.

[22] "Carbon Cleaning, carbon-cleaning.com." (accessed.
[23] "https://www.gpgarage.it/product-category/motore/frizioni-volani/." (accessed.
[24] J. B. Heywood, *Internal combustion engine fundamentals*. McGraw-Hill Education, 2018.
[25] "https://www.eobdcode.com/mecanique/symptomes-de-soupape-de-moteur-pliee/." (accessed.
[26] "https://www.noahsgarage.com/how-diesel-engine-works/." (accessed.
[27] A. ALLALOU and S. TAIL, "Simulation numérique de la combustion dans un moteur à combustion interne," *Mémoire du Master, Université Akli Mohand Oulhadj de Bouira,* 2021.
[28] "https://www.autotoolexperts.com/common-gdi-engine-problems/." (accessed.
[29] "https://mypdh.engineer/lessons/timing-gears-camshaft-and-valve-mechanism/." (accessed.
[30] "Valve mechanism construction." https://www.newkidscar.com/engine/valve-mechanism-construction/ (accessed.
[31] "https://www.blogmecanicos.com/2020/07/." (accessed.
[32] "DISTRIBUTION, TOUT EST DANS LE TIMING." https://newsdanciennes.com/distribution-tout-est-dans-le-timing/ (accessed.
[33] "https://www.enricoparts.com." (accessed.
[34] G. Mhadhbi, "Étude et développement d'un simulateur numérique pour la distribution variable du moteur diesel," Université du Québec à Rimouski, 2021.
[35] "https://www.slideserve.com/flint/valve-and-seat-service." (accessed.
[36] S. Abderahmane, "Moteur à combustion interne."
[37] "https://www.piecesauto.fr/pieces-detachees/poussoir-hydraulique.html." (accessed.
[38] M. R. ASRI and I. E. K. BOUCEKKINE, "Étude d'un arbre à cames d'un moteur à combustion interne par analyses des éléments finis (FEM: Finite Element Method)," Université Ibn Khaldoun-Tiaret-, 2022.
[39] "https://www.thelittlecarshop.com/triumph-tr6-culasse-rampe-culbuteurs-7452." (accessed.
[40] "https://listado.mercadolibre.com.ve/construccion-electricidad/balancines-motor-diesel." (accessed.
[41] "https://www.howmechanismworks.com/2018/09/what-is-valve-timing-diagram-why-do-we.html." (accessed.
[42] "VALVE TIMING DIAGRAM OF TWO STROKE AND FOUR STROKE ENGINES: THEORETICAL AND ACTUAL." https://www.ingenieriaymecanicaautomotriz.com/valve-timing-diagram-of-two-stroke-and-four-stroke-engines-theoretical-and-actual/ (accessed.
[43] "Valve Timing Diagram - Learn for 2-Stroke, 4-Stroke Engines, Variable Valve Timing." https://testbook.com/mechanical-engineering/valve-timing-diagram (accessed.
[44] D. T. OUKSEL, *Cours Moteurs à Combustion Interne*.
[45] "https://mechanicalboost.com/engine-valve/#Function_of_Engine_Valves." (accessed.
[46] "The Inner Workings of Variable Valve Timing Technology." https://www.tomorrowstechnician.com/the-inner-workings-of-variable-valve-timing-technology/ (accessed.
[47] "1-MS-Module 1-Diesel Engine Fundamentals." https://sites.ntc.doe.gov/partners/tr/Training%20Textbooks/09-Mechanical%20Science/1-MS-Module%201-Diesel%20Engine%20Fundamentals.pdf (accessed.
[48] "https://mechanicalboost.com/camshaft/#Components_of_Camshaft." (accessed.
[49] "http://www.mstworkbooks.co.za/technology/gr8/gr8-technology-06.html." (accessed.
[50] R. Saddek, "Etude et fonctionnement géométrique d'un arbre â came."
[51] "https://www.ornikar.com/code/cours/mecanique-vehicule/moteur/arbre-cames." (accessed.
[52] *Vehicular Engine Design*
[53] G. Nikishkov, "Introduction to the finite element method," *University of Aizu,* pp. 1-70, 2004.

[54] "FEM Operations Toolbox." https://www.mathworks.com/products/connections/product_detail/fem-operations-toolbox.html (accessed.
[55] F. Z. Bhat, "Application of Finite Element Analysis," 2021.
[56] D. Samir, "METHODE DES ELEMENTS FINIS."
[57] B. K. BOURAS, "Etude et analyse des champs électriques DC et AC d'un isolateur silicone par la méthode des éléments finis," 2022.
[58] "https://www.researchgate.net/figure/Flowchart-for-FEA-analysis_fig1_320786408." (accessed.
[59] M. T. Gherbi, "Modélisation par éléments finis d'une pâle d'hélicoptère sous chargement aérodynamique," Boumerdes, 2010.
[60] P. E. Richard T. Morgan. "Analysis of Anchoring Attachments Using Finite Element Modeling." https://www.structuremag.org/?p=15443 (accessed.
[61] B. Bailey, "Investigation of a composite hingeless helicopter rotor blade with integral actuators," Carleton University, 2000.
[62] J.-L. Batoz and G. Dhatt, *Modélisation des structures par éléments finis*. Presses Université Laval, 1990.
[63] "https://forum.ansys.com/forums/topic/what-is-the-source-of-mesh-quality-spectrum/."
[64] M. Zamros and P. Ku, "Analysis of fatigue characteristics on camshaft using finite element analysis," in *Journal of Physics: Conference Series*, 2022, vol. 2222, no. 1: IOP Publishing, p. 012010.